

Solvent production by the
hyperthermophilic archaeon *Hyperthermus*
butylicus

by

Sarah Danielle Kim

A thesis
presented to the University of Waterloo
in fulfillment of the
thesis requirement for the degree of
Master of Science
in
Biology

Waterloo, Ontario, Canada, 2021

©Sarah Danielle Kim 2021

AUTHOR'S DECLARATION

I hereby declare that I am the sole author of this thesis. This is a true copy of the thesis, including any required final revisions, as accepted by my examiners.

I understand that my thesis may be made electronically available to the public.

Abstract

Hyperthermus butylicus is one of the few hyperthermophilic (organisms that thrive in temperatures 80°C and above) archaea that can produce 1-butanol as a major fermentation end-product. The reported end-products (acetone, isopropanol, acetate, and butyrate, in addition to 1-butanol) bare similarity to that of solvent producing clostridial species, and an alcohol dehydrogenase (ADH) (Hbut_0414) is found to be responsible for the production of 1-butanol in *H. butylicus*. It was not clear, however, if ethanol is produced and which pathway(s) and key enzymes are involved in the solvent production by *H. butylicus*. To gain a greater understanding of the metabolism of this microorganism, the aims of this thesis were to examine its growth and solvent production.

Through optimization experiments for *H. butylicus* growth conditions, it was determined that a pH of 7.0, sulfur concentration of 10.0 g/L, and H₂ pressure of 3.0 atm (over-pressurized) resulted in the highest growth (> 1.0 x 10⁸ cells/mL). It was found that precipitated sulfur from Sigma-Aldrich was strictly required. Using gas chromatography, the fermentation end-products ethanol, acetone, isopropanol, and 1-butanol in batch cultures of *H. butylicus* were detected. The synthesis of these solvents was found to be growth dependent where an increase in growth correspondingly resulted in an increase in solvent production, demonstrating significance between metabolic activity and growth in the microorganism. The addition of sodium acetate and sodium butyrate in the growth media affected both the growth and solvent production. In cultures supplemented with acetate, a decrease in growth was observed compared to cultures supplemented with butyrate and without any supplementation. Supplementing the growth medium with 5- and 15-mM of sodium acetate and sodium butyrate resulted in an increase in ethanol and 1-butanol, respectively, indicating that *H. butylicus* could utilize these organic acids for producing their corresponding alcohols.

Bioinformatic analyses (BLAST, HMM) showed no significant similarity for key solvent-producing enzymes was found in *H. butylicus* when searched against enzymes produced by other existing butanol producing organisms. It is concluded that *H. butylicus* is the first hyperthermophile capable of acetone-butanol-ethanol (ABE) fermentation, but the responsible pathway remains unknown. It is proposed that a novel butanol production pathway in *H. butylicus* exists, which may share similarities to the ABE pathway in *C. acetobutylicum*, keto-acid pathway in *Saccharomyces cerevisiae*, butyraldehyde dehydrogenase pathway in *C. saccharoperbutylacetonicum* N1-4, the two-

step PDC/ADH pathway in *Thermococcus guaymasensis*, and an organic acid reduction pathway involving an aldehyde:ferredoxin oxidoreductase.

Further investigation is required to enhance the understanding of *H. butylicus*' metabolism. Future studies for the biochemical determination of key enzymes, quantifying the amount of organic acids consumed, and the pH dependency of solvent production in the presence and absence of organic acids will provide insight into revealing pathways responsible for the solvent production in *H. butylicus*.

Acknowledgements

I would like to express my sincere appreciation to my supervisor, Dr. Kesen Ma, for his patience and guidance throughout my graduate studies. His constant encouragement and belief in my abilities have helped me feel more confident in them and has pushed me to constantly strive for the best. The skills I have learned from my years in the Ma lab, both technical and those applicable to life, I will carry with me always. I would like to thank my committee members, Dr. Bernard Glick and Dr. Andrew Doxey, for providing me with their expertise, unending willingness to provide feedback, and wonderful conversations.

An immense amount of gratitude is given to my family – to my parents Young-ran Kim and Soon-kil Kim, my siblings Sharon Kim and Andrew Kim, my grandparents Kyung-ok Lee and Chan-young Jeon, and my extended family. I would not be where I am without their unwavering support and love.

I thank my lab-mates Navin Asokumar, Faisal Alharbi, Can Wang, Ching Emily Tse, Thuy Nikki Nguyen, and colleagues Kate Sinclair, Sura Ali, Michael Mansfield, Jackson Tsuji, Hye Lee, and others. They have made my graduate studies such an enjoyable experience, and I cannot thank them enough.

Dedication

This thesis is dedicated to my grandmother (1940 – 2020), who meant the world to me. Halmoni, you were nothing short of extraordinary and I miss you dearly every day. Let us meet in our dreams.

Table of Contents

AUTHOR'S DECLARATION	ii
Abstract	iii
Acknowledgements	v
Dedication	vi
List of Figures	ix
List of Tables	xi
List of Abbreviations	xii
1.0 Introduction	1
1.0 Microbial production of alcohols.....	1
1.1 Alcohol fermentation.....	1
1.1.1 Alcohol fermentation for consumption.....	1
1.1.2 Biofuels.....	2
1.2 Metabolic pathways for butanol production and key enzymes involved.....	5
1.2.1 Acetone-butanol-ethanol (ABE) pathway in <i>Clostridium acetobutylicum</i>	7
1.2.2 Butanol and isobutanol pathway in <i>Saccharomyces cerevisiae</i>	9
1.2.3 Bioconversion of carboxylic acids to alcohols.....	10
1.2.4 Bioengineered metabolic pathways.....	14
1.3 Hyperthermophiles.....	16
1.4 <i>Hyperthermus butylicus</i>	19
1.5 Objectives.....	21
2.0 Materials and Methods	22
2.1 Microorganisms, chemicals, and materials.....	22
2.2 Anaerobic techniques.....	24
2.3 Growth of <i>H. butylicus</i>	26
2.3.1 Monitoring growth of <i>H. butylicus</i>	28
2.3.2 Optimization of growth.....	28
2.3.3 Addition of organic acids.....	29
2.4 Instruments and equipment.....	30
2.5 Detection of metabolic end-products.....	31
2.5.1 Determination of solvents using gas chromatography (GC).....	31
2.5.2 Preparation of GC samples.....	32

2.6 Integration of gas chromatography peak areas	33
2.6.1 Automatic integration by PeakSimple software	33
2.6.2 Manual Integration	34
2.6.3 PeakSimple Software parameters	34
2.6.4 Operation of PeakSimple with Shimadzu GC-14a	35
3.0 Results	36
3.1 Growth of <i>H. butylicus</i>	36
3.1.1 Optimization of growth conditions.....	36
3.1.2 Growth of <i>H. butylicus</i> in acetate and butyrate supplemented media	40
3.2 Solvent detection	42
3.2.1 Optimization of liquid-liquid extraction procedure.....	42
3.2.2 Optimization of the GC method	42
3.2.3 Standard curves	48
3.2 Solvent production of <i>H. butylicus</i>	59
3.3.1 Solvent production under optimized growth conditions.....	59
3.3.2 Solvent production in the presence of butyrate	61
3.3.3 Solvent production in the presence of acetate	63
4.0 Discussion	65
4.1 Optimal growth conditions for <i>H. butylicus</i>	66
4.2 Effect of acetate and butyrate on the growth of <i>H. butylicus</i>	68
4.3 Dependency of solvent production by <i>H. butylicus</i> on growth conditions.....	70
4.4 Stimulation of <i>H. butylicus</i> solvent production in the presence of acetate and butyrate	72
4.5 Proposed pathways and key enzymes involved in solvent production by <i>H. butylicus</i>	74
4.6 Conclusions	77
4.7 Future Prospects	78
References	79
Appendix A Gene Sequence Analysis	87
Appendix B GC Operation Procedure	94
Appendix C PeakSimple Operation Procedure	100
Appendix D GC Integrator Operation Procedure	106
Appendix E Standard Curve Raw Data	107
Appendix F Solvent Production Raw Data	118

List of Figures

Figure 1. Schematic diagram of three pathways for glycolysis: EMP pathway, PP pathway, and ED pathway.	6
Figure 2. Schematic diagram of ABE fermentation pathway for the production of butanol by <i>C. acetobutylicum</i>	8
Figure 3. Schematic diagram showing a proposed 1-butanol and isobutanol production pathway by <i>S. cerevisiae</i>	9
Figure 4. Schematic diagram showing two potential butanol production pathways within the bacterium <i>C. saccharoperbutylacetonicum</i> N1-4.....	11
Figure 5. Schematic diagram showing a proposed pathway for reduction of organic acid to its corresponding alcohol by an aldehyde:ferredoxin oxidoreductase.	13
Figure 6. Schematic diagram of engineered <i>Clostridium</i> ABE production pathway in <i>E. coli</i>	14
Figure 7. Schematic diagram of engineered keto-acid pathway in <i>E. coli</i> for 1-butanol production ...	15
Figure 8. Phylogenetic tree of life	16
Figure 9. Manifold system used to create anaerobic environments in sealed serum bottles	24
Figure 10. Schematic diagram of a GC sample.....	32
Figure 11. Chromatograph from PeakSimple (version 4.51) displaying the difference between automatic integration and manual integration	33
Figure 12. Chromatograph from PeakSimple (version 4.51) displaying height and time	34
Figure 13. Growth of <i>H. butylicus</i> at varying pHs.	36
Figure 14. Growth of <i>H. butylicus</i> under varying pressures of H ₂	37
Figure 15. Growth of <i>H. butylicus</i> under varying sulfur concentrations.....	38
Figure 16. <i>H. butylicus</i> growth under optimal conditions	39
Figure 17. Growth of <i>H. butylicus</i> in butyrate supplemented media.....	40
Figure 18. Growth of <i>H. butylicus</i> in acetate supplemented media.....	41
Figure 19. GC chromatograph of a control sample recorded using PeakSimple software (version 4.51)	48
Figure 20. GC chromatograph of a 3 mM 1-butanol standard sample recorded using PeakSimple software (version 4.51).....	49
Figure 21. GC chromatograph of a 3 mM mixed standard sample recorded using PeakSimple software (version 4.51).....	49

Figure 22. 1-Butanol standard curve from gas chromatography (peak ratio vs. concentration)	51
Figure 23. 1-Butanol standard curve from gas chromatography (area vs. concentration).....	52
Figure 24. Comparison of ethanol height and corresponding concentration.....	53
Figure 25. Comparison of acetone height and corresponding concentration	54
Figure 26. Comparison of isopropanol height and corresponding concentration.....	54
Figure 27. Ethanol standard curve from gas chromatography.....	55
Figure 28. Acetone standard curve from gas chromatography.....	56
Figure 29. Isopropanol standard curve from gas chromatography	57
Figure 30. Solvent production by <i>H. butylicus</i> under optimal growth conditions.....	60
Figure 31. Comparison of solvent production by <i>H. butylicus</i> in butyrate supplemented media.....	62
Figure 32. Comparison of solvent production by <i>H. butylicus</i> in acetate supplemented media.....	64
Figure 33. Proposed pathway for solvent production in <i>H. butylicus</i>	76

List of Tables

Table 1. Examples of industrial applications by commercially available enzymes from hyperthermophiles	18
Table 2. Chemicals used in this study	22
Table 3. Composition of <i>H. butylicus</i> medium.....	27
Table 4. Composition of trace mineral solution used for the growth of <i>H. butylicus</i>	27
Table 5. Instruments, equipment, and major laboratory supplies used in this study	30
Table 6. Optimization of GC method (Shimadzu GC-14a equipped with DB-5 and DB-624 combined GC column)	43
Table 7. Identification and calculation of solvents using unique peaks	50
Table 8. Comparison of ethanol, acetone, and isopropanol peak area	58
Table 9. Comparison of 1-butanol peak area.....	58
Table 10. Potential <i>P. furiosus</i> AOR homologs in <i>H. butylicus</i>	73

List of Abbreviations

ABE	Acetone-butanol-ethanol
ADH	Alcohol dehydrogenase
AEI	Acetone-ethanol-isopropanol
AOR	Aldehyde:ferredoxin oxidoreductase
BADH	Butyraldehyde dehydrogenase
BDH	Butanol dehydrogenase
ED	Entner-Doudoroff pathway
EMP	Embden-Meyerhof-Parnas pathway
GC	Gas chromatography
HPLC	High performance liquid chromatography
PDC	Pyruvate decarboxylase
POR	Pyruvate:ferredoxin oxidoreductase
PP	Pentose Phosphate pathway
TCA	Tricarboxylic acid cycle

1.0 Introduction

1.0 Microbial production of alcohols

1.1 Alcohol fermentation

Alcohol fermentation is a biological process that converts biomass into one or more different alcohols by a microorganism. Fermentation products are predominately produced from the metabolic intermediate pyruvate formed via central metabolic pathways involved in carbohydrate catabolism (Hoelzle et al. 2014) (see: **Section 1.2**). Depending on the substrate and fermentative organism in question, the type of alcohol fermentation can vary. The importance of alcohol fermentation spans from its applications in biofuel production and biotechnology to its major role in alcoholic beverages and fermented foods, which will be further discussed in the following sections.

1.1.1 Alcohol fermentation for consumption

Microbial solvent production is widely used in food fermentation and has long been practiced across cultures as a means of preserving, producing, or flavouring food, as well as producing beverages (Katz 2012). In recent years, fermented foods have gained particular attention due to their various health benefits in addition to extending the “shelf life” (Soni and Dey 2014). The first fermentation event is predicted to have occurred “by accident”, resulting in a natural phenomenon that human cultures have observed and subsequently learned from (Katz 2012). Biochemically, fermentation is a pathway where the NADH that is produced is re-oxidized by the intermediate that is produced in the pathway. Louis Pasteur, a French chemist, was the first to report the microbial nature of fermentation in 1857 (Durre 1998) and as a consequence of his observations, the scientific underpinnings of alcoholic fermentation were established. One of the earliest records showing evidence of alcohol fermentation comes from a study by McGovern et al. (2004) who identified residues of alcohol in pottery pieces dating back 9,000 years that originated from the early Neolithic village of Jiahu in China (McGovern et al. 2004). The fermented beverage was reported to be a mixture of rice, honey, and fruit suggesting the mixing of carbohydrates with yeast sources was done intentionally (McGovern et al. 2004; Katz 2012). The process of fermentation was likely influenced by the environment and varies depending on the region (i.e., the resources available and microbial communities present). For example, millet

and rice, which are naturally found growing in regions of China underwent alcohol fermentation by molds that digested the substrates into simple sugars (Katz 2012). Similarly, barley and wheat which are found in the Middle East uses a different method of germination called “malting”; a process that is used to digest sugars for alcohol fermentation (Tanno and Willcox 2012). The utilization of microorganisms for food fermentation is one example demonstrating the potentially multifaceted benefit of utilizing microorganisms for human well-being.

1.1.2 Biofuels

Depletion of the world’s petroleum supply has spurred increased interest in finding alternative and renewable sources of energy including the possibility of producing biofuels from microbial fermentation. Approximately 40% of the world’s total energy consumption is in the form of liquid fuels, making biofuels both an attractive and practical alternative to fossil fuels (Tan et al. 2008). With bioenergy predicted to be able to meet up to approximately one-third of the global energy demand by 2050 (Guo et al. 2015), a considerable amount of research focus on the microbial production of biofuels is expected.

Research efforts to develop alternative fuel sources have long focused on bioethanol as it is an established biotechnological process and due to its production feasibility (Jin et al. 2011; Aditiya et al. 2016). Alongside biodiesel, bioethanol is the most widely used alternatives to petrol-based fuels (Serrano-Ruiz et al. 2011). Bioethanol production has been steadily increasing every year, with global production reported at nearly 30 billion gallons in 2019 compared to approximately 20 billion gallons in 2009 (Karimi et al. 2021). Currently, the industrial production of bioethanol relies primarily on food sources as raw materials (Wang et al. 2021). This presents challenges as the source material for bioethanol can also be used for the production of food and feed thus, bringing direct competition for food production. This can furthermore have an impact on food supply and potentially increase food prices (Obergruber et al. 2021). With the challenges that exist in bioethanol production, there has been an increased desire for alternative bio-solvents from microbial fermentation with biobutanol in the forefront.

Butanol (C_4H_9OH), or butyl alcohol, is a four-carbon alcohol mixture, composed of four structural isomers (n-butanol/1-butanol, secondary-butanol/2-butanol, tert-butanol, and iso-

butanol) (Pan et al. 2020). It is commonly used as a solvent in cosmetic and pharmaceutical industries for the production of antibiotics, vitamins, and hormones. In addition, butanol is a chemical intermediate for the synthesis of methyl methacrylate and butyl acrylate (monomeric precursors of polymers) which are important compounds used for manufacturing a wide range of products including plastics (Lee et al. 2008; Garcia et al. 2011). Biobutanol is considered to be a more desirable biofuel than bioethanol because of its advantageous chemical properties: biobutanol has a higher energy content, is less explosive and volatile, has a higher flash point, and does not readily absorb moisture (Garcia et al. 2011; Ndaba et al. 2015), making biobutanol comparatively safer to handle than bioethanol. Additionally, butanol can be used in either pure or mixed concentrations with gasoline due to its higher energy density and lower polarity (Sarathy et al. 2012), while ethanol can only be mixed up to 85% with gasoline (Durre 2007). It is beneficial to mix or “blend” biofuels with gasoline because the alcohol acts as a fuel additive, allowing the fuels to burn cleaner and produce lower levels of CO₂ emissions (Varoil et al. 2014). Despite efforts to find alternatives to non-renewable fuel sources, fossil fuels continue to make up approximately 83% of the primary energy consumed globally (Pugazhendhi et al. 2019). Both bioethanol and biobutanol possess a major advantage over petroleum-based fuels which is that they “generate low net [greenhouse gas] emissions” when produced from lignocellulosic materials (Nigam and Singh 2011), and therefore have a lower environmental impact. Additionally, butanol can be produced from a variety of biomass feedstocks (including waste) reducing the competition for food production, unlike bioethanol (Abdehagh et al. 2014) (see: **Section 2.1**).

One difficulty in industrial biobutanol production is the severe toxicity of the solvent on the producing microorganism. Since butanol is toxic to microorganisms in high concentrations, the level of butanol tolerance of the producing microorganism directly impacts the total butanol production (Knoshaug and Zhang 2009). For example, *Clostridium acetobutylicum* D64 can produce up to 13 g/L of butanol, however, is only able to tolerate a maximum of 2% (i.e., 20 g/L) of butanol (v/v) (Liu et al. 2012). Biobutanol also has a low production rate (approximately 30 times lower) relative to bioethanol (Anitha et al. 2020), with reports showing < 0.3 g/L/h production rate for biobutanol by Clostridial species compared to 3.46 g/L/h for bioethanol by *S. cerevisiae* (Wang et al. 2017; Azhar et al. 2017). Research is directed to overcoming these

challenges through methods such as finding an efficient separation technique to recover butanol, enhancing butanol tolerance and yield in genetically altered strains, and genetic engineering to increase butanol production, among others (Liu et al. 2012; Gonzalez-Ramos et al. 2013).

1.2 Metabolic pathways for butanol production and key enzymes involved

Industrial solvent production by microorganisms is largely dominated by mesophilic microorganisms. For example, the gram-negative bacterium *Clostridium acetobutylicum* is a well-known industrial acetone-butanol-ethanol (ABE) producer (Lee et al. 2008; Gheshlaghi et al. 2009), while strains of *Saccharomyces cerevisiae* (yeast) and *Zymomonas mobilis* (gram-negative) are commonly used to produce ethanol from sugar- and starch-based feedstocks (Doran-Peterson et al. 2008; Xia et al. 2019). Solvent production in mesophiles generally begins with simple sugars, such as glucose, which is then converted into pyruvate via either the Embden-Meyerhof-Parnas (EMP) pathway, the Pentose Phosphate (PP) pathway or, the Entner-Doudoroff (ED) pathway (**Fig. 1**) (Xia et al. 2019). These three pathways aid in the breakdown of glucose for energy and carbon metabolism in a process called glycolysis, which is central to all domains of life. The EMP pathway has modified forms especially within anaerobes, where the pathway is used to synthesize ethanol and CO₂, as opposed to in aerobes where the pathway is used to produce pyruvate for the tricarboxylic acid cycle (TCA). The PP pathway oxidizes the glucose-6-phosphate intermediate from the EMP pathway to produce NADPH and pentose phosphates. These two pathways function to produce ATP, NAD(P)H, and the biosynthetic precursors for amino acids, nucleotides, and fatty acids (Chen et al. 2016). The ED pathway is similar to the EMP pathway, however, utilizes two key enzymes that are unique to this pathway (6-phosphogluconate dehydrates and 2-keto-3-deoxygluconate-6-phosphate aldolase). Solvent production in *Z. mobilis*, a facultative anaerobe, is unique in that it exclusively uses the ED pathway for ethanol fermentation (Conway 1992; Xia et al. 2019).

While industrial microbial solvent production is currently largely dominated by mesophilic microorganisms, there are several hyperthermophiles that possess the ability to produce solvents as their major metabolic end-products. In fact, three hyperthermophiles are known to produce butanol naturally, *Thermococcus* ES-1, *Pyrodicticum abyssi* sp. nov., and *Hyperthermus butylicus*, however, the pathways for butanol production in these organisms are currently unknown (Ma et al. 1995; Pley et al. 1991; Zillig et al. 1990).

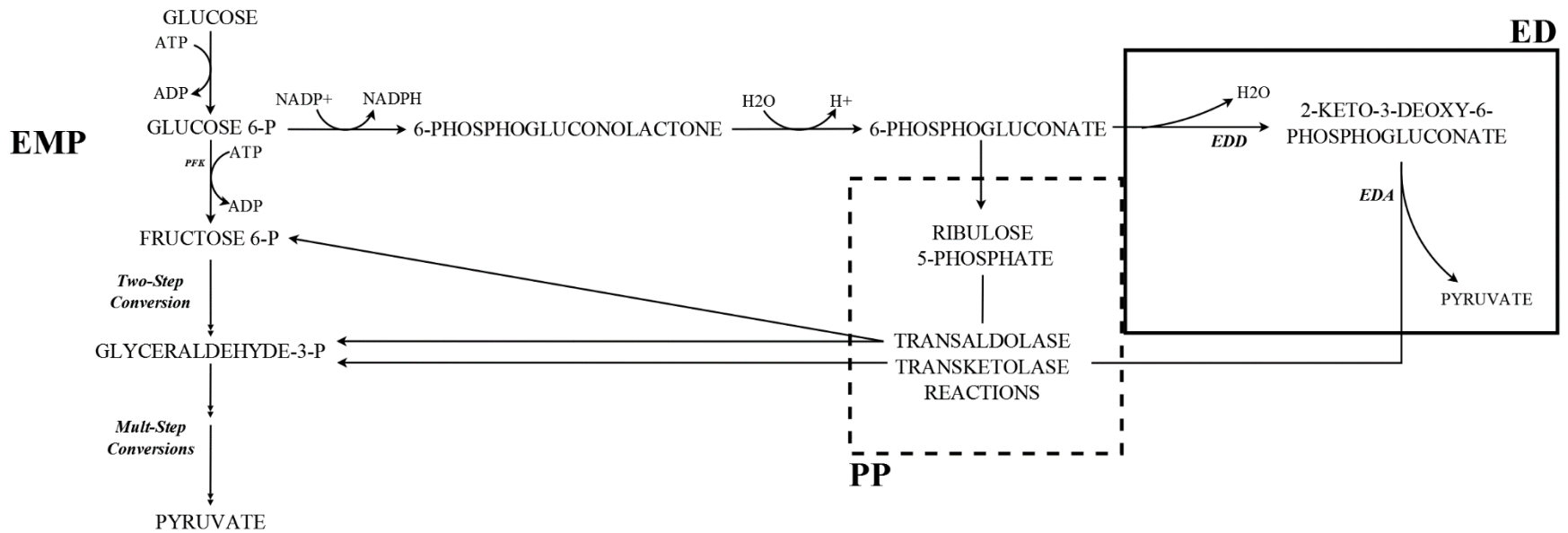


Figure 1. Schematic diagram of three pathways for glycolysis: EMP pathway, PP pathway (dotted lines), and the ED pathway (solid line). PFK: 6-phosphofructokinase; EDD: 6-phosphogluconate dehydratase; EDA: aldolase. (Modified from Wolfe 2015).

1.2.1 Acetone-butanol-ethanol (ABE) pathway in *Clostridium acetobutylicum*

C. acetobutylicum is a well-known industrial producer of biobutanol and the most extensively studied solventogenic bacterial species (Lee et al. 2008). Its pathway for solvent production (ABE pathway) involves a two-stage process, the acidogenesis phase and the solventogenic phase, and begins with the conversion of a simple sugar (glucose) into pyruvate (**Fig. 2**).

Pyruvate is converted into acetyl-CoA by the concurrent reduction of ferredoxin by pyruvate-ferredoxin:oxidoreductase (POR) then, following the condensation of two acetyl-CoA molecules, acetoacetyl-CoA is produced via the action of the enzyme acetyl-CoA-acetyltransferase. The accumulation of organic acids (acetic acid and butyric acid from acetyl-CoA) causes the pH of the culture to become more acidic, resulting in the metabolism entering the solventogenic phase. The conversion of organic acids (acetate and butyrate) into their corresponding solvents (ethanol and butanol, respectively) stops the production of acid, resulting in a decrease in cell growth and an increase in pH (Lee et al. 2008).

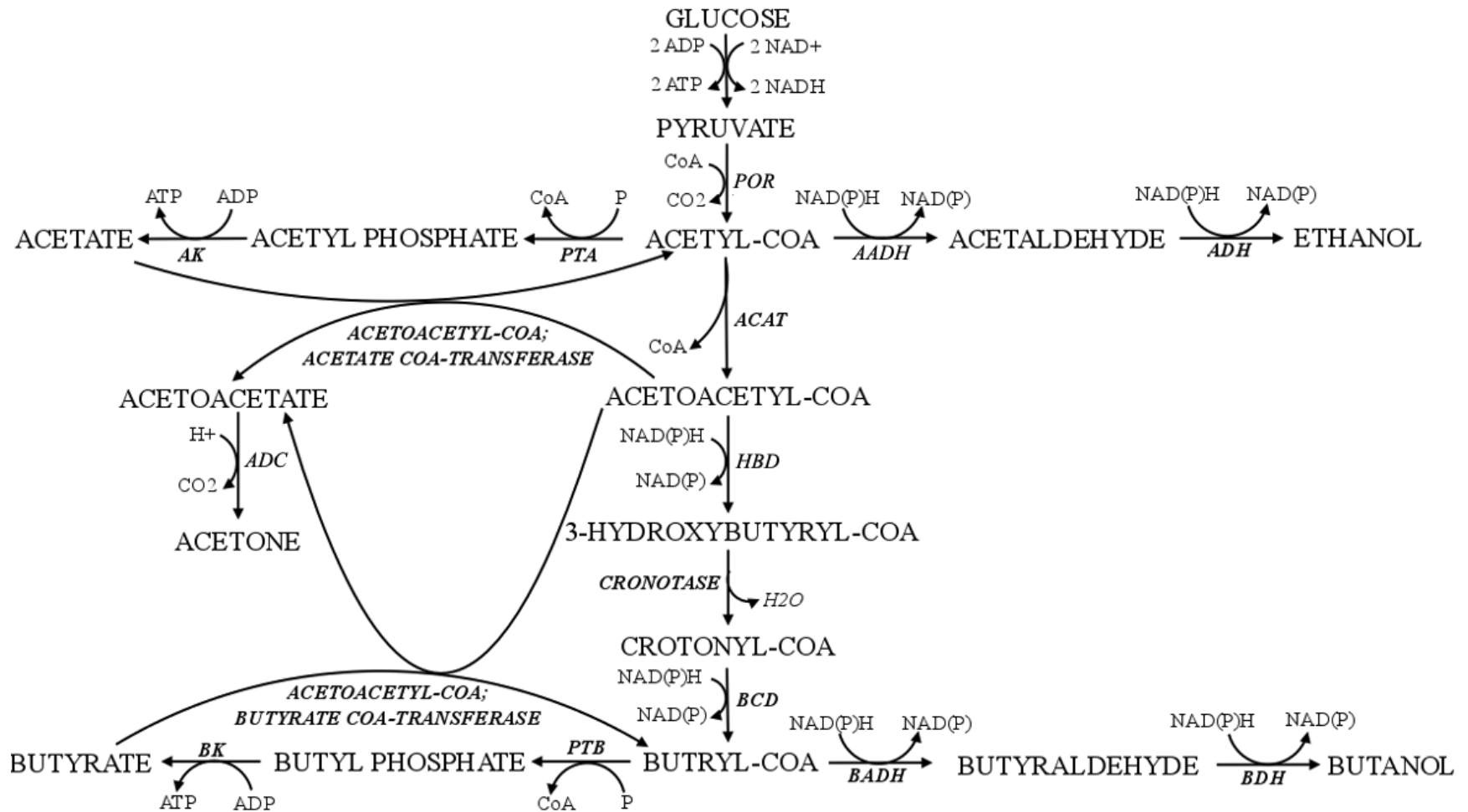


Figure 2. Schematic diagram of ABE fermentation pathway for the production of butanol by *C. acetobutylicum*. POR: pyruvate:ferredoxin oxireductase; AK: acetate kinase; PTA: phosphotrans-acetylase; AADH: acetaldehyde dehydrogenase; ADH: alcohol dehydrogenase; ACAT: acetyl-coenzyme A acetyltransferase/Thiolase; ADC: acetoacetate decarboxylase; HBD: beta-hydroxybutyryl-CoA dehydrogenase; BK: butyrate kinase; PTB: phosphotrans-butyrylase; BDH: butyryl-CoA dehydrogenase; BADH: butyryldehyde dehydrogenase; BDH: butanol dehydrogenase. (Modified from Garcia et al. 2011).

1.2.2 Butanol and isobutanol pathway in *Saccharomyces cerevisiae*

A pathway for 1-butanol production has been found to occur naturally in a strain of *S. cerevisiae*, called the “glycine degradation” pathway (Branduardi et al. 2013; Swidah et al. 2018). This pathway utilizes intermediates from amino acid biosynthesis (glycine) as a substrate for the production of 1-butanol, and additionally, can use serine for the production of iso-butanol in a similar way. Both pathways involve the deamination of the amino acid (glycine and serine) to ultimately produce alpha-keto valerate and alpha-isoketovalerate, respectively, then finally into their corresponding alcohols (1-butanol and isobutanol, respectively) via the Elrich pathway (catabolism of amino acids to alcohols) (Branduardi et al. 2013). (**Fig. 3**). The “glycine-butanol” pathway is alternatively referred to as the “keto-acid” pathway (or “2-keto acid pathway”) (Jambunathan & Zhang 2014; Si et al. 2014) as the key intermediates for the amino acid biosynthetic pathways are alpha-keto-acids (see: **Section 1.2.4**).

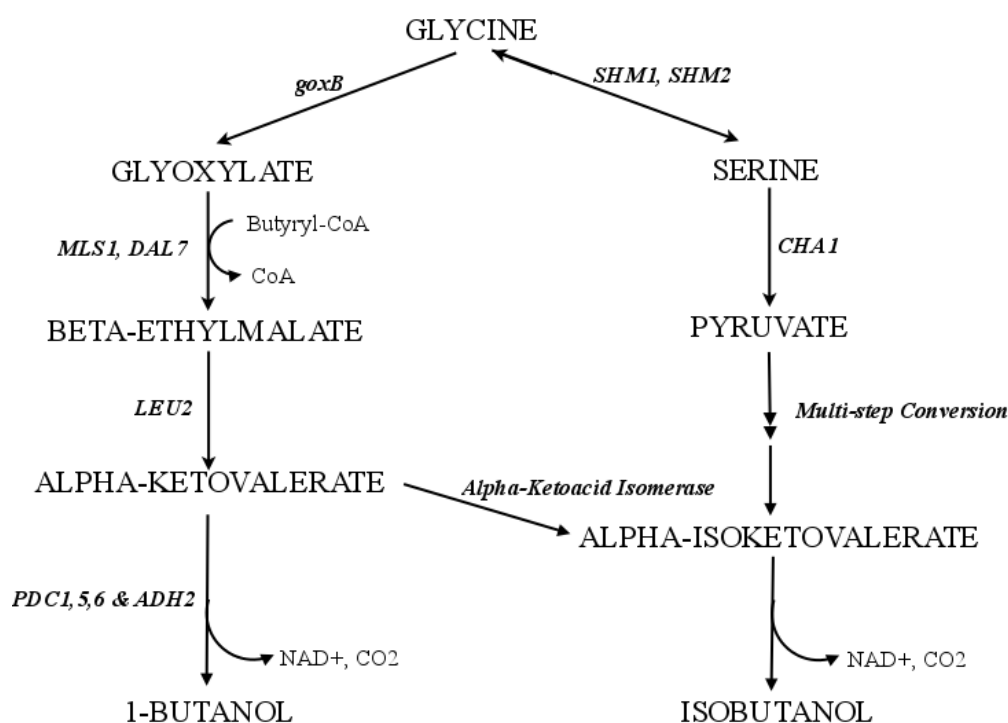


Figure 3. Schematic diagram showing a proposed 1-butanol and isobutanol production pathway by *S. cerevisiae*. Reduction of butanal to butanol is shown as a single step. *goxB*: glycine oxidase; *SHM1*, *SHM2*: serine hydroxymethyl-transferase; *MLS1*, *DAL7*: malate synthase; *CHA1*: serine deaminase; *LEU2*: beta-isopropylmalate dehydrogenase; *PDC1,5,6*: pyruvate decarboxylase; *ADH2*: alcohol dehydrogenase. (Modified from Branduardi et al. 2013).

1.2.3 Bioconversion of carboxylic acids to alcohols

ABE producing Clostridia are known to produce butyrate and/or 1-butanol through the intermediate butyryl-CoA, however, researchers have found an alternative mechanism for 1-butanol production by a *Clostridium* spp. that can convert a carboxylic acid, specifically butyric acid, directly to 1-butanol (Al-Shorgani et al. 2012). Known as a “hyper-butanol-producing-strain”, *C. saccharoperbutylacetonicum* N1-4 that was isolated and used for industrial butanol production has been recently sequenced (Wang et al. 2017). This bacterium is unique in that it possesses the ability to utilize butyric acid as a substrate to produce 1-butanol. Typically, butyric acid inhibits cell growth thus limiting solvent production, however, in combination with glucose, butanol production was enhanced more than 40-fold in *C. saccharoperbutylacetonicum* N1-4 (Al-Shorgani et al. 2012). Without glucose addition, butanol production still increased when at least 1 g/L of butyric acid was added (0.28 g/L to 0.80 g/L). However, when 5 g/L of glucose and 1 g/L butyric acid were added butanol production increased two-fold (1.61 g/L) (Al-Shorgani et al. 2012). This suggests that the presence of butyric acid triggered the solventogenic pathway in this bacterium resulting in an increased butanol production. Researchers also reported that presence of butyric acid inhibited cell growth through enhanced butanol production (Al-Shorgani et al. 2012).

There are two proposed CoA-transferase pathways for butanol production by *C. saccharoperbutylacetonicum* N1-4 from the bioconversion of butyrate (**Fig. 4**). The first is the reverse pathway of butyrate production where butyrate is converted to the butyryl-CoA intermediate by the butyrate-CoA-transferase enzyme. Butyryl-CoA is then converted to butyraldehyde and subsequently butanol through the enzymes butyraldehyde dehydrogenase (BADH) and butanol dehydrogenase (BDH) (**Fig. 4A**), respectively, which is similar to butanol production in *C. acetobutylicum* (**Fig. 2**). The second pathway involves the conversion of butyrate to butyryl-phosphate and then to the intermediate butyryl-CoA through the action of the enzyme butyrate kinase and subsequently phosphotransbutyrylase (Al-Shorgani et al. 2012). For butanol production, butyryl-CoA is converted the same way as the first hypothesized pathway – butyraldehyde then butanol by BADH and BDH (**Fig. 4B**).

A



B



Figure 4. Schematic diagram showing two potential butanol production pathways (A and B) within the bacterium *C. saccharoperbutylacetonicum* N1-4. CoAT: CoA transferase, BADH: butylaldehyde dehydrogenase, BDH: butanol dehydrogenase, BK: butyrate kinase, PTB: phosphotransbutyrylase. (Modified from Al-Shorgani et al. 2012).

The reduction of organic acids was first observed in the solventogenic bacterium *Clostridium thermoaceticum*, where it was found that *C. thermoaceticum* possessed the ability to reduce a variety of tested carboxylic acids (i.e., acetate, propionate, butyrate) into their corresponding aldehydes (i.e., ethanol, 1-propanol, 1-butanol) (White et al. 1989). The enzyme that catalyzed these reactions was reported to be what was termed a “carboxylic acid reductase (aldehyde dehydrogenase)” (White et al. 1989; Strobl et al. 1992). Another Clostridial *spp.* was found more recently to possess the ability to reduce organic acids, however, via an “aldehyde oxidoreductase-like” enzyme (Isom et al. 2015). Researchers found that *C. ragsdalei* could convert propionic, butyric, pentanoic, and hexanoic acids to the corresponding alcohols, 1-propanol, 1-butanol, 1-pentanol, and 1-hexanol, respectively (Isom et al. 2015).

Aldehyde:ferredoxin oxidoreductases (AORs) are a family of molybdenum or tungsten oxidoreductases isolated from strictly anaerobic microorganisms. They are involved in the reduction of an organic acid, that is either externally added or intermediately produced, to its corresponding alcohol *in vivo* (Huber et al. 1995; Nissen and Basen 2019). Most solvent producing microorganisms commonly convert pyruvate into acetaldehyde by a pyruvate decarboxylase or into the intermediate acetyl-CoA, with pyruvate dehydrogenase or pyruvate:ferredoxin oxidoreductase (see: **Section 2.3.1**) (Olson et al. 2015). Microorganisms that possess the AOR enzyme, however, may have this pathway in which the direct reduction of acetate to acetaldehyde is required (Nissen and Basen 2019) (**Fig 5**).

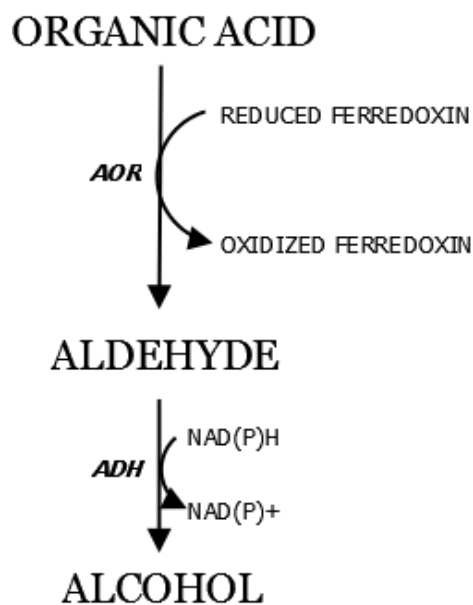


Figure 5. Schematic diagram showing a proposed pathway for reduction of organic acid to its corresponding alcohol by an aldehyde:ferredoxin oxidoreductase. AOR: aldehyde:ferredoxin oxidoreductase, ADH: alcohol dehydrogenase. (Modified from Nissen and Basen 2019).

The first evidence of an AOR in a hyperthermophile was in *Pyrococcus furiosus*, however, the proposed role of the AOR was as a “glyceraldehyde-oxidizing enzyme” (Mukund and Adams 1991). In another study, a synthetic route (“AOR pathway”) was successfully engineered into *P. furiosus* which allowed the organism to produce the corresponding alcohols when organic acids (acetate, butyrate, propionate, isobutyrate, valerate, isovalerate, caproate, phenylacetate) were exogenously supplemented into culture media (Basen et al. 2014). This was achieved by the insertion of the gene for bacterial ADH into *P. furiosus* (Basen et al. 2014).

1.2.4 Bioengineered metabolic pathways

Metabolic engineering is the intentional manipulation/modification of genetic processes and pathways to maximize the yield of a compound of interest. It involves the manipulation of enzymatic, transport, and regulatory functions of the cell thus, requires organism(s) that will be modified to be fully sequenced and characterized (Koffas et al. 1999; Garcia-Granados et al. 2019). This practice is commonly employed in industry to maximize the yield of a desired solvent. *E. coli* is a model organism for industrial solvent production as it is well-characterized with a wealth of genetic and physiological information, making the microbe a suitable host for making modifications (Atsumi et al. 2008). *E. coli* does not naturally produce 1-butanol as a fermentation product, however, this bacterium is often used as a host to clone and express genes for 1-butanol production (Atsumi et al. 2008; Branduardi et al. 2013) (**Fig. 6**).

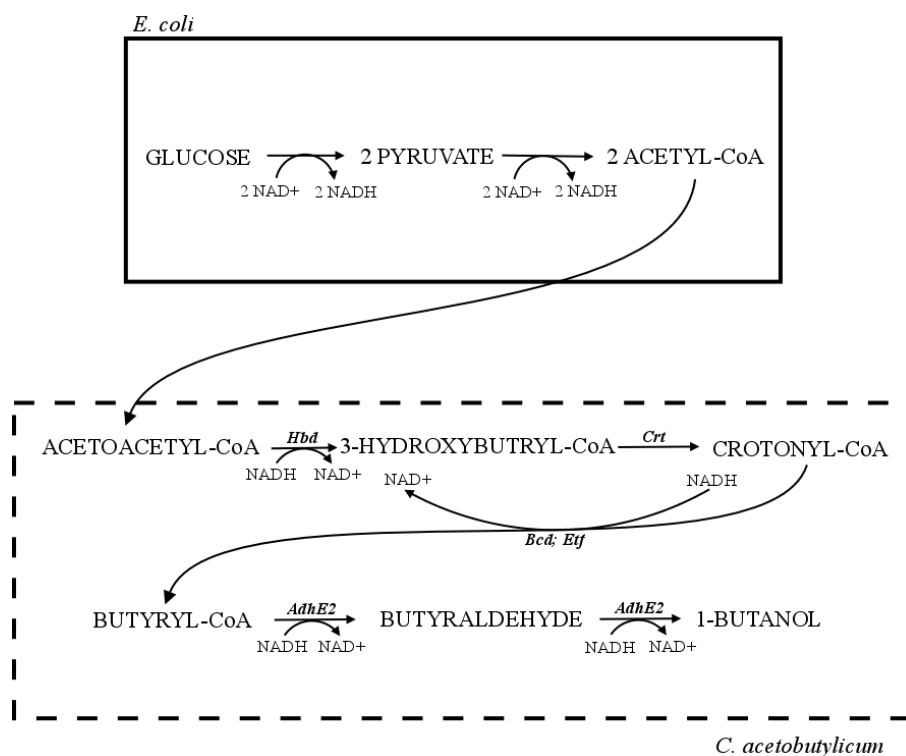


Figure 6. Schematic diagram of engineered *Clostridium* ABE production pathway in *E. coli*. *E. coli* metabolism (solid line), *Clostridium* (dotted line). Thl: acetoacetyl-CoA thiolase; Hbd: 3-hydroxybutyryl-CoA dehydrogenase; Crt: crotonase; Bcd: butyryl-CoA dehydrogenase; Etf: electron transfer flavoprotein; AdhE2: aldehyde/alcohol dehydrogenase. (Modified from Atsumi et al. 2008)

The pathway for the metabolism of glucose to acetyl-CoA was maintained in *E. coli*, and the conversion from acetoacetyl-CoA to 1-butanol in *C. acetobutylicum* was introduced. Reports have shown that solvent yields in *E. coli* were similar to those obtained in Clostridia when engineered with the Clostridia butanol pathway (Atsumi et al. 2008). The keto-acid pathway (refer to: **Section 1.2.2**), another known pathway for 1-butanol production, has been successfully engineered into *E. coli* (**Fig. 7**), and is similar to the novel pathway found to be naturally occurring in *S. cerevisiae* (refer to: **Fig. 3**)

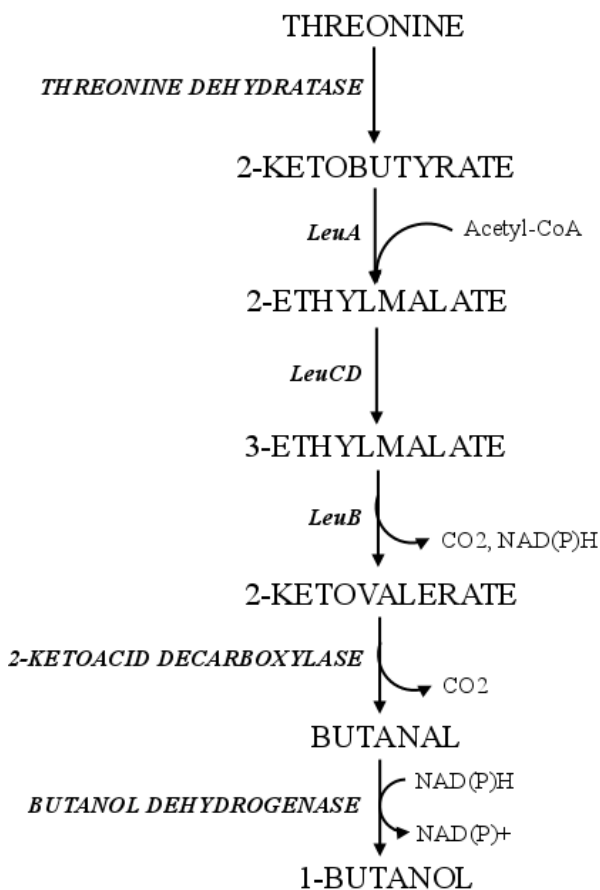


Figure 7. Schematic diagram of engineered keto-acid pathway in *E. coli* for 1-butanol production. LeuA: 2-isopropylmalate synthase; LeuCD: 2-isopropylmalate isomerase; LeuB: 2-isopropylmalate dehydrogenase. (Modified from Branduardi et al. 2013).

1.3 Hyperthermophiles

Hyperthermophiles are a group of unique microorganisms that grow optimally and thrive in temperatures above 80°C (Schonheit and Schafer 1995; van Wolferen et al. 2013). This group of mainly anaerobic, chemolithoautotrophic and heterotrophic microorganisms are the primary producers in these extremely hot environments, typically utilizing polypeptides as their main carbon and energy source (Huber and Stetter 1998). Most sulfate-reducing microorganisms are also primarily hyperthermophilic, with sulfate reduction considered to be one of the most ancient energetic pathways, and many organisms belonging to the archaeal phylum *Crenarchaeota* (Wagner et al. 2004). Hyperthermophiles can be found in both terrestrial and marine thermal environments including (but not limited to) hot springs, solfataric fields, and hydrothermal vents, with extreme pH, salinity, and atmospheric conditions (Stetter 2006). Although the majority of hyperthermophiles belong to the archaeal domain, bacterial hyperthermophiles also exist. More than 90 species of hyperthermophilic archaea and bacteria have been identified thus far (van Wolferen et al. 2013; Giulio 2003; Setter 2006). Hyperthermophiles represent the most ancient forms of life and may be the closest genetic relative to the last common ancestor of all present-day microorganisms (**Fig. 8**) (Stetter 2006).

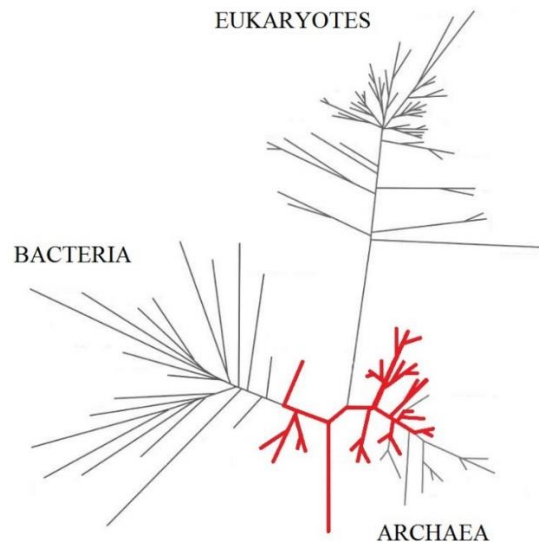


Figure 8. Phylogenetic tree of life. Hyperthermophilic lineages shown by thick red lines. (Modified from Stetter 2006).

The research interest in studying hyperthermophiles is a consequence of their extreme physiological adaptations and their potential applications in biotechnology. In particular, their unique thermostable enzymes are of key interest (Huber and Stetter 1998; Atomi et al. 2011). Hyperthermophilic enzymes function most optimally at extremely high temperatures (above 70°C, with some displaying peak activity at 110°C) and are inactive at moderate temperatures (below 40°C) (Vielle and Ziekus 2001; Unsworth et al. 2007). Being active under conditions of extreme pH, high substrate concentrations, and high pressure, the utilization of hyperthermophilic enzymes could provide potentially important advantages in industrial processes compared to their mesophilic counterparts (i.e., enzymes which are optimally active between 25 – 50°C) as most industrial processes are performed under harsh conditions (Vielle and Ziekus 2001; Sarmiento et al. 2015).

Notwithstanding these advantages, it is difficult to cultivate and obtain pure enzymes from hyperthermophiles due to the unique metabolic requirements for growing these organisms (Huber et al. 1995; Vielle and Ziekus 2001). Additionally, growing hyperthermophiles on a large scale often produces low yields of the desired product (Sarmiento et al. 2015). Thus, for technical reasons, hyperthermophilic enzymes are often genetically engineered and expressed in mesophilic microbial hosts before they are purified and used to enhance industrial processes. Currently, more than 3,000 extremophilic enzymes have been identified for industrial applications (Dumorne et al. 2017). **Table 1** displays examples of some hyperthermophilic enzymes that are industrially produced following genetic introduction to mesophiles.

There are several advantages to performing industrial processes at high temperatures including reducing the risk of foreign microbial contamination, improving substrate transfer rates and reaction rates, decreasing the viscosity of the medium, and increasing the solubility of substrates (Vielle and Ziekus 2001; Unsworth et al. 2007). Studying hyperthermophiles offers the possibility of developing an enhanced understanding of thermostable enzyme evolution, their unique metabolic pathways, and biochemical reactions, all of which may be used to facilitate a variety of biotechnical processes.

Table 1. Examples of industrial applications by commercially available enzymes from hyperthermophiles. (Adapted from Vielle and Zeikus 2001; de Miguel Bouzas et al. 2006; Ebaid et al. 2019; Atalah et al. 2019).

Enzyme	Temp (°C)	Commercial Product	Manufacturer	Application
Amylase	90	AlphaStar PLUS Termamyl®	Dyadic Novozymes	Starch hydrolysis for glucose syrup production
Glucose (xylose) isomerase	90	Sweetzyme®	Novozymes Genecor	Conversion of glucose to fructose
Glutamate Dehydrogenase	Up to 60	Glutamate Dehydrogenase (NAD(P)) (by Roche)	Roche	Diagnostic tests
Laccase	65-70	Denilite® IIS (by Novozymes)	Novozymes	Textile production
Ligases (<i>Pfu</i> from <i>Pyrococcus furiosus</i>)	Up to 85	Various	Stratagene	Molecular biology
Lipases	Up to 90	Resinanse® HT	Novozymes	Kraft pulp treatment
Polymerases (<i>Pfu</i> from <i>P. furiosus</i> , <i>Vent</i> from <i>Thermococcus litoralis</i> , <i>Pwo</i> from <i>P. woesei</i> , <i>Deep Vent</i> from <i>Pyrococcus</i> strain <i>GB-D</i> , <i>DNA</i> from <i>Thermococcus sp. strain 9N-7</i>)	Up to 80	Various	Various	Molecular biology
Protease S	85 – 90	<i>Pfu</i> Protease S	TaKaRa Biomedicals	Protein fragmentation for sequencing
Xylanase	Up to 60	Xylanase (by ProFood)	ProFood	Feed and foods, biofuel production, pharmaceutical industry, papermaking

1.4 *Hyperthermus butylicus*

H. butylicus is a hyperthermophilic archaeon that was originally isolated from the seafloor of a solfataric (volcanic vents emitting water vapour and sulfuric gas) habitat on the coast of the island of São Miguel, Azores, Portugal (Zillig et al. 1990). The Azores are an archipelago consisting of nine volcanic islands in the north Atlantic Ocean located more than 1000 km to the west of mainland Portugal. This strictly anaerobic microbe has a relatively broad optimal temperature range between 95°C – 106°C and metabolizes peptides as its primary energy and nitrogen source (Zillig et al. 1990). When the genome of *H. butylicus* was sequenced, it was found to consist of a single circular chromosome of 1,667,163 bp with 53.7% G-C content (Brugger et al. 2007). Moreover, the genome of *H. butylicus* was found to share many genes that code for proteins in other hyperthermophiles such as *Aeropyrum pernix* and *Pyrobaculum aerophilum*. *H. butylicus* contains a high percentage of codons that specify charged amino acids. This is consistent with the observation that this organism's proteins contain a lot of charged residues on its surface (Brugger et al. 2007). Growth of *H. butylicus* is strongly stimulated by the presence of elemental sulfur (S⁰) and hydrogen gas (H₂), with the reduction of sulfur and the absence of oxygen resulting in the generation of hydrogen sulfide (H₂S). To conserve energy, this organism may use a sulfur reducing complex that was identified using genome sequence analysis and located in the cell membrane (Brugger et al. 2007). Similar complexes were studied from other organisms to reduce elemental sulfur to H₂S, however, no experimental data was cited in *H. butylicus*. The protein components associated with the sulfur reducing complex are sulfur reductase, hydrogenases, and electron transfer activities bound to the surface of membranes which catalyze sulfur reduction to H₂S (Brugger et al. 2007). In addition to 1-butanol (67 mmol at a 2.2 x 10⁸ cells/mL density), trace amounts of acetic acid, propionic acid, phenylacetic acid, hydroxyphenylacetic acid, propylbenzene, acetophenone, and hydroxyacetophenone have been found in the spent growth medium of *H. butylicus* when supplied with tryptone, using gas chromatography-mass spectroscopy (Zillig et al. 1990). The presence of these metabolic end-products is a possible indication of amino acid catabolism (i.e., acetic acid is the product of alanine and glycine metabolism, and phenylacetic acid is the product of the metabolism of phenylalanine) (Kinoshita et al. 1957; Christensen 1990). Using high performance liquid chromatography to assess the organic contents of the spent growth medium, acetone, isopropanol, and butyrate were found in addition to 1-butanol (Tse 2016); this is similar to the

end-products that has been found in the spent growth medium of *Clostridium* species. Additionally, the gene encoding the enzyme (Hbut_0414) which catalyzes the reaction for butanol production in *H. butylicus* has been found (Tse 2016). Despite this, the solvent production pathway for this microorganism is still unknown as well as the optimum conditions for its growth and solvent production.

1.5 Objectives

A better understanding of the growth and solvent production of *H. butylicus* is expected to provide valuable insight for future biotechnology research directed toward using hyperthermophiles for biofuel production and other potential applications. Past studies (Tse 2016) have shown that an alcohol dehydrogenase (Hbut_0414) is responsible for the production of 1-butanol in *H. butylicus*, however, the pathway for butanol production in this organism is currently unknown. Additionally, using high performance liquid chromatography, *H. butylicus* has been found to produce acetone, ethanol, and isopropanol, in addition to 1-butanol. Thus, the aims of this research are as follows:

- 1) To optimize and study the growth of *H. butylicus* under different growth conditions.
- 2) To confirm and quantify the presence of solvents (acetone, ethanol, isopropanol, and 1-butanol) using gas chromatography (GC) following the optimal growth of *H. butylicus*.
- 3) To determine the effect of organic acid addition (acetate and butyrate) in growth media on *H. butylicus*' growth and solvent production.

2.0 Materials and Methods

2.1 Microorganisms, chemicals, and materials

Hyperthermus butylicus (DSM 5456) was obtained from Deutsche Sammlung von Mikroorganismen und Zellkulturen, Germany (DSMZ). All chemicals and laboratory supplies such as Eppendorf tubes and disposable syringes used in this study are from commercially available sources (**Table 2**).

Table 2. Chemicals used in this study.

Chemical	Company
1-Butanol (GC Grade)	Sigma-Aldrich
(4-(2-hydroxyethyl)-1-piperazineethanesulfonic acid (HEPES))	Bio Basic Inc.
Acetone (GC Grade)	Sigma-Aldrich
Ammonium chloride (NH ₄ Cl)	Sigma-Aldrich
Ammonium sulfate ((NH ₄) ₂ SO ₄)	J.T. Baker
Boric acid (H ₃ BO ₃)	Sigma-Aldrich
Calcium Chloride, Dihydrate (CaCl ₂ ·2H ₂ O)	Sigma-Aldrich
Citric acid (HOC(CH ₂ CO ₂ H) ₂)	J.T. Baker
Cobalt(II) chloride hexahydrate (CoCl ₂ ·6H ₂ O)	J.T. Baker
Cupric(II) sulfate pentahydrate (CuSO ₄ ·5H ₂ O)	J.T. Baker
Elemental sulfur	Sigma-Aldrich
Ethanol (GC Grade)	Sigma-Aldrich
Ethyl acetate (GC Grade)	Sigma-Aldrich
Hydrochloric acid (HCl)	Fischer Scientific
Iron(II) sulfate (FeSO ₄)	Sigma-Aldrich
Isobutanol (GC Grade)	Alfa Aesar
Isopropanol (GC Grade)	Sigma-Aldrich
Magnesium chloride hexahydrate (MgCl ₂ ·6H ₂ O)	J.T. Baker
Magnesium sulfate (MgSO ₄)	Fischer Scientific
Magnesium sulfate heptahydrate (MgSO ₄ ·7H ₂ O)	EM Science
Manganese sulfate monohydrate (MnSO ₄ ·H ₂ O)	J.T. Baker
Monopotassium phosphate (KH ₂ PO ₄)	B.D.H. Chemicals
Nickel(II) chloride (NiCl ₂ ·6H ₂ O)	Sigma-Aldrich
Nitrilotriacetic acid (N(CH ₂ CO ₂ H) ₃)	Eastman Chemicals
Potassium aluminum sulfate dodecahydrate (AlK(SO ₄) ₂ ·12H ₂ O)	B.T. Baker
Potassium chloride (KCl)	B.D.H. Chemicals
Potassium iodide (KI)	Sigma-Aldrich
Resazurin	Sigma-Aldrich
Sodium acetate (NaCH ₃ COO)	Fischer Scientific
Sodium bromide (NaBr)	Fischer Scientific
Sodium butyrate (Na(C ₃ H ₇ COO))	Sigma-Aldrich
Sodium chloride (NaCl)	Bio Basic Inc.
Sodium hydroxide (NaOH)	Fischer Scientific

Sodium molybdate dihydrate ($\text{Na}_2\text{MoO}_4 \cdot 2\text{H}_2\text{O}$)	Fischer Scientific
Strontium chloride hexahydrate ($\text{SrCl}_2 \cdot 6\text{H}_2\text{O}$)	Sigma-Aldrich
Tryptone	Bio Basic Inc.
Zinc sulfate heptahydrate ($\text{ZnSO}_4 \cdot 7\text{H}_2\text{O}$)	B.D.H. Chemicals

2.2 Anaerobic techniques

A manifold (**Fig. 9**) system allows for the alternate transfer of vacuum and gas (either N₂ or H₂) following a method developed previously (Tse 2016). Using aseptic techniques, sterile 25G needles were attached to the manifold by which a sealed container (such as a serum bottle with a rubber stopper) can be made anaerobic. Sterile 25G needles punctured through the stoppers allow for the exchange of gases within the sealed container. The gases are deoxygenated when they pass through a heated catalyst. Sealed bottles were degassed for 40 min followed by 3 cycles of gassing (with N₂)/degassing (by vacuum) for 3 min each. In the gas position (at ~2 psi N₂) a second needle (25G) was used to puncture the stopper and ethanol was added to the needle to show some bubbling, indicating the flushing out of the N₂ ensuring that the bottles have an oxygen-free headspace (bottles are flushed for 2 min). Lastly, needles were removed and pressurized with N₂ to have a positive pressure headspace (0.14 atm over-pressurized).

Syringes were made anaerobic by rinsing with degassed sterilized water or an anaerobic buffer. To ensure microbubbles of air in the syringe are completely removed/absorbed, ~1 mL of anaerobic buffer was drawn into the syringe, then left aside for ~5 min; the same was done with the desired solution (~1 mL of solution, left for ~5 min).

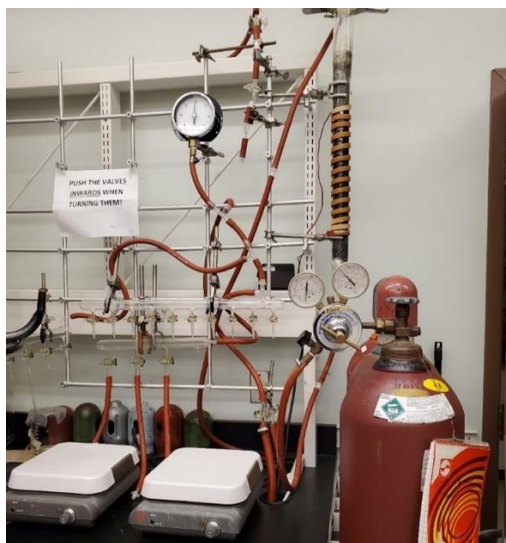


Figure 9. Manifold system used to create anaerobic environments in sealed serum bottles.

The use of H₂ was required to be performed in the fume hood where another manifold is installed for safety. The procedure is principally the same as described above for the use of N₂. However, for adding pressurized H₂ (> ~0.2 atm, but up to 3 atm over-pressure) to a sealed container, there was no use of any manifold. A red vacuum rubber tubing (Inner diameter: 1/4", Outer diameter: 5/8") connected to a sterile syringe, a sterile syringe filter, and a 25G needle attached to the regulator on the H₂ tank was used to add H₂ directly to a desired (sealed) container such as a serum bottle in a fume hood. The H₂ tank was slowly opened to 44 psi, and gas was allowed to flow for ~10 seconds to remove any oxygen from the tubing. The needle was used to puncture the rubber stopper on the bottle and gas was allowed to flow into the bottle for ~20 seconds. After ~20 seconds, the needle was removed from the bottle (a visible bump in the stopper will appear indicating the presence of added H₂). The bottle was held tightly during the entire procedure for safety.

2.3 Growth of *H. butylicus*

H. butylicus was grown in medium supplemented with trace minerals and vitamin solutions, described previously by DSMZ and modified by Tse (2016). *H. butylicus* was routinely cultured anaerobically at 95°C in 60 mL glass serum bottles.

The medium composition is based on Medium 491 provided by DSMZ (Deutsche Sammlung von Mikroorganismen und Zellkulturen, Germany), with modifications. All chemicals were added sequentially in the order listed and mixed on a stir plate until completely dissolved with the exception of elemental sulfur and sodium sulfide, which were added separately from the rest of the components (**Table 3**). Trace mineral solution (**Table 4**) is from DSMZ (Medium 141), with modifications (Balch et al. 1979). The medium pH was adjusted to 6.6 and was stored in 4°C until needed.

Table 3. Composition of *H. butylicus* medium.

Chemical	g/L
NaCl	17.0
MgSO ₄ ·7H ₂ O	3.5
MgCl ₂ ·6H ₂ O	2.75
KCl	0.325
NaBr	0.05
H ₃ BO ₃	0.0015
SrCl ₂ ·6H ₂ O	0.0075
Citric acid	0.005
KI	0.0025
CaCl ₂ ·2H ₂ O	0.2
KH ₂ PO ₄	0.5
NiCl ₂ ·6H ₂ O	0.002
(NH ₄) ₂ SO ₄	0.01
Elemental sulfur (from Sigma-Aldrich)	10.0
NH ₄ Cl	0.5
Tryptone	6.0
100x Trace minerals	10.0 mL (Table 3)
Resazurin	1.0
(4-(2-hydroxyethyl)-1-piperazineethanesulfonic acid (HEPES)	5.2
Na ₂ S·9H ₂ O (3% w/v)	10.0 mL
Deionized Water (DI H ₂ O)	Fill to 1.0 L

Table 4. Composition of trace mineral solution used for the growth of *H. butylicus*.

Chemical	g/L
Nitrilotriacetic acid	1.500
MgSO ₄	1.460
MnSO ₄ ·H ₂ O	0.450
NaCl	1.000
FeSO ₄	0.055
CoCl ₂ ·6H ₂ O	0.200
CaCl ₂ ·2H ₂ O	0.100
ZnSO ₄ ·7H ₂ O	0.180
CuSO ₄ ·5H ₂ O	0.010
AlK(SO ₄) ₂ ·12H ₂ O	0.018
H ₃ BO ₃	0.010
Na ₂ MoO ₄ ·2H ₂ O	0.010
Deionized Water (DI H ₂ O)	Fill to 1L

The volume of medium (from the prepared stock) needed for culturing varies depending on the number and size of the culture bottles used. The standard medium volume for a 60 mL serum bottle is 20 mL of *H. butylicus* medium. Elemental sulfur of 0.2 g was added to autoclaved 60 mL serum bottles (6 g/L), then pH-adjusted medium was added to the bottles (20 mL of medium each). After the medium was dispensed, the bottles were capped with grey butyl stoppers and aluminum seals, and a hand crimper was used to attach seals to bottles. The prepared bottles were then placed in a sonicator (VWR) filled 1/2 of the way with DI water for 3 min to dissolve the sulfur in the bottles. Under aseptic conditions, culture bottles were made anaerobic using a manifold (see: **Section 2.2**). Once anaerobic, bottles were placed in a water bath heated to 90°C and sterilized for 1 hour and then removed from the water bath. Bottles containing the medium were sterilized at 90°C for 1 hour each day, for a total of 3 days. Following the third day of sterilization, the medium was reduced with 0.2 mL of Na₂S (3% w/v) using a sterile anaerobic 1 mL syringe equipped with a sterile 25G needle (see: **Section 2.2**). Bottles were then placed in a heated 95°C water bath, and incubated for 15 min. The bottles were ready for inoculation once they were cooled to room temperature. The gas phase in the bottles was exchanged from N₂ to H₂ at ~2 psi (see: **Section 2.2**), then 10% of the total medium volume (v/v) of fresh late-log phase culture (cell density > 1.0 x 10⁸ cells/mL) was inoculated into each bottle, using an anaerobic syringe. Three atm of H₂ (over-pressurized) was added directly to each bottle (see: **Section 2.2**), then the bottles were incubated in a 95°C water bath, with growth monitored via direct microscopic cell counts (see: **Section 2.3.1**).

2.3.1 Monitoring growth of *H. butylicus*

Growth (cell density in cells/mL) of *H. butylicus* was monitored using a Nikon Eclipse E600 phase-contrast light microscope and a Petroff-Hausser counting chamber (1/400 mm², 0.02 mm deep). Growth curves were plotted on a semi-logarithmic scale for cell density (cells/mL) against time (hours).

2.3.2 Optimization of growth

H. butylicus cells were grown using elemental sulfur from different manufacturers (Fisher Scientific, VWR, Sigma-Aldrich) to determine which provided the maximum cell growth (cells/mL). The amount of sulfur was the same for all cultures (6 g/L) and growth was observed over 50 hours for each type of elemental sulfur.

Varying pH growth conditions (pH 6.0, 6.5, 7.0, and 8.0), H₂ pressures (0, 1, 2.5, 3 atm over-pressurized), and sulfur concentrations (0, 1, 5, 6, and 10 g/L), all in duplicates, were tested for cell growth (cells/mL) throughout each growth phase. The growth medium pH was adjusted to the desired pH prior to sterilization and pH was periodically checked using a pH meter with a pH electrode (Cole-Parmer) and pH paper (J.T. Baker).

2.3.3 Addition of organic acids

A 1 M stock solution of sodium acetate (MW: 82.03 g/mol) and sodium butyrate (MW: 110.1 g/mol) was prepared fresh each time (2 mL each). For 1 M sodium acetate stock, 0.16 g was weighed out then dissolved in 2 mL of deionized water. For 1 M sodium butyrate stock, 0.22 g was weighed out then dissolved in 2 mL of deionized water. Sodium acetate and sodium butyrate were added to 20 mL of *H. butylicus* media after all other components were added and dissolved but before the pH of the medium was adjusted (see: **Section 2.2**). The final concentrations of sodium acetate and sodium butyrate were 5 mM and 15 mM, respectively. For a final concentration of 5 mM, 0.1 mL of sodium acetate was added to 20 mL of *H. butylicus* medium; the same was done for 5 mM of sodium butyrate. For 15 mM, 0.3 mL of sodium acetate was added to 20 mL of *H. butylicus* medium; the same was done for 5 mM of sodium butyrate. The pH of the entire mixture was adjusted to pH 6.6, then dispensed into culture bottles. The remaining procedure was followed for preparing culture bottles for growth (see: **Section 2.2**).

2.4 Instruments and equipment

All instruments and equipment used in this study are commercially available (with the exception of the manifold system) (**Table 5**).

Table 5. Instruments, equipment, and major laboratory supplies used in this study.

Instruments and equipment	Company (Country)
Aluminum seal (20 mm CS/M)	Fisher Scientific (Canada)
Balance:	
Analytical (Fisher Scientific Accu-64)	Fisher Scientific (Canada)
Top-loading (Acculab AL-1502)	Acculab (USA)
Butyl grey stopper (20 mm)	Fisher Scientific (Canada)
Centrifuge (Heraeus Biofuge Pico)	Thermo Fisher Scientific (Canada)
Eppendorf tubes (1.5 mL)	Fisher Scientific (Canada)
Gas chromatography (Model 910)	Buck Scientific (USA)
Gas chromatography (Shimadzu GC-14a)	Shimadzu (Japan)
Gas chromatography vial (2 mL 9 mm Amber glass and screw top cap with PTFE septum)	Thermo Fisher Scientific (Canada)
Glass syringe (10 μ L)	Thermo Fisher Scientific (Canada)
Gas tanks (Air, Helium, Hydrogen, and Nitrogen)	Praxair (Canada)
Hand Crimper	Wheaton (USA)
Manifold system	Made by Ma's lab at University of Waterloo (Canada)
Microscope (Nikon Eclipse E600 phase-contrast light microscope)	Nikon (Japan)
Needles (25 G)	Thermo Fisher Scientific (Canada)
Rotary shaker	New Brunswick Scientific (Canada)
Petroff-Hauser counting chamber (1/400 mm ² , 0.02 mm deep)	Hausser Scientific (USA)
pH electrode	Cole Parmer (Canada)
pH meter (accumet Basic, AB15)	Fisher Scientific (Canada)
pH paper (BAKER-pHIX ¹ pH Papers with Color Scale)	J.T. Baker (USA)
Serum bottles (60 mL glass bottle)	Wheaton (USA)
Sonicator (Ultrasonic cleaner, 50-D)	VWR (Canada)
Stir plate (Corning PC-610)	Corning (USA)
Syringe (1 mL – Slip Tip)	VWR (USA)
Syringe filter (0.45 μ m)	Sarstedt (USA)
Vortex mixer	Fisher Scientific (Canada)
Waterbath (ISO Temp 215)	Fisher Scientific (Canada)

2.5 Detection of metabolic end-products

2.5.1 Determination of solvents using gas chromatography (GC)

A Shimadzu GC-14a equipped with an FID detector and a combined column, a DB-5 (Agilent J&W DB-5 GC Column, 30 m, 0.32 mm, 0.25 μm , 7-inch cage) and DB-624 (Agilent J&W DB-624 GC Column, 30 m, 0.32 mm, 1.80 μm , 7-inch cage), was used for the detection of solvents. GC conditions used were as follows: injector temperature: 250°C; flame ionizer detector (FID) temperature: 250°C; FID sensitivity range: 10^1 for 11.6 min, 10^2 for 8.4 min, 10^1 for 10 min; carrier gas: helium (pressure: 1 kg/cm²); H₂ (pressure: 1 kg/cm²); Air (pressure: 0.4 kg/cm²). The temperature program used was as follows: initial isotherm at 35°C held for 10 mins; ramp rate: 1°C/min to 40°C held for 2 mins, 45°C/min to 150°C; final isotherm: 150°C held for 1 min; Range: 1 for the first 11.6 mins, 2 for 8.4 min (to 20 min), 1 for the remainder for the run (10 min). One μL of sample was injected into the GC for analyses.

GC data was recorded using PeakSimple software (version 4.51, SRI Instruments). To allow for the electronic recording of GC samples the Shimadzu GC-14a was connected to a secondary GC (GC Buck) using electrical wiring, as the PeakSimple program is installed on a computer that is connected to the GC Buck. A low constant flow of N₂ (pressure: 20 psi) is required to be running while the GC Buck is on to avoid damaging the column. Both the GC Buck and Shimadzu GC-14a need to be on for PeakSimple to record the data.

Standard curves for acetone, ethanol, isopropanol, and 1-butanol were prepared at concentrations of 0.25, 0.5, 1, 3, and 5 mM, as well as mixed solvent standards (composed of acetone, ethanol, isopropanol, and 1-butanol) at the same concentrations. *H. butylicus* cultures supplemented with 5- and 15-mM of sodium butyrate and sodium acetate were analyzed for solvent production 3 atm H₂ (over-pressurized) and compared against solvent production under the absence of butyrate and/or acetate. A control containing uninoculated *H. butylicus* media was run in duplicate at each time point acting as a control. Sample preparation for culture samples and standard solutions were prepared as described in Section 2.3.2.

2.5.2 Preparation of GC samples

The extraction solution (composed of ethyl acetate and 2 g/L of isobutanol) was vortexed for 3 seconds, then 200 μ l of this solution was immediately dispensed into new 1.5 mL eppendorf polyethylene tubes. In the same tube, 1 mL of sample/standard was dispensed, and the cap was closed immediately. Tube(s) were vortexed for 3 seconds then put onto a shaker (New Brunswick Scientific Gyrotory G76 shaker) for 15 min at 200 rpm. Tube(s) were then centrifuged (Heraeus Biofuge Pico) for 2 min at 952 x g (10,000 rpm). Once the sample(s) were centrifuged, the supernatant (\sim 180 μ L) was obtained and dispensed into a clean 2 mL GC vial with a screw top cap and PTFE septum (Thermo Fisher Scientific) (**Fig. 10**).

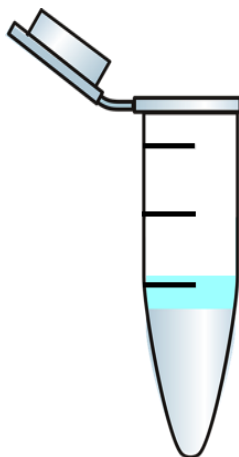


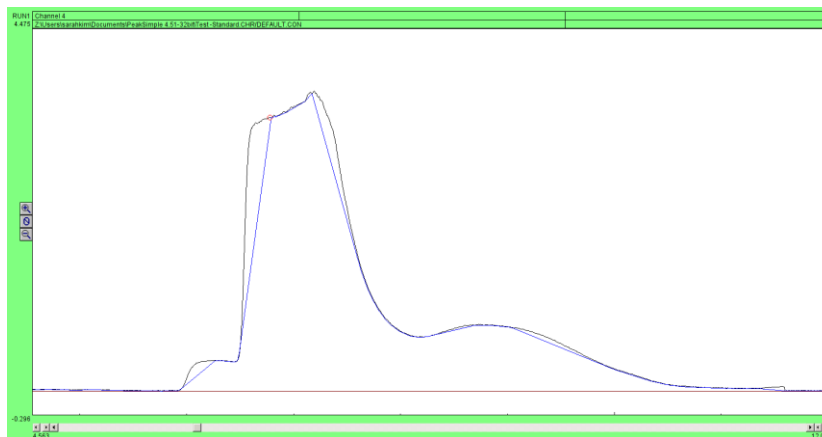
Figure 10. Schematic diagram of a GC sample. The top (“blue”) layer represents the solvent layer that is obtained and run on the GC; the bottom layer (the supernatant) represents the debris/other components of *H. butylicus* medium that will be discarded.

2.6 Integration of gas chromatography peak areas

2.6.1 Automatic integration by PeakSimple software

PeakSimple automatically integrates detected peaks however, as the solvent peaks in *H. butylicus* samples do not have a typical Gaussian shape, the default baseline does not include the entire area of the peak. As can be seen in **Fig. 11(a)**, the automatic integration created a baseline that follows the shape of the peaks rather than underneath the peak, as in **Fig. 11(b)**. This means that only a portion of the peak is integrated when using the automatic integration. To ensure the entire area of the peak is included when integrating standards and samples, a manual integration is required.

(a)



(b)

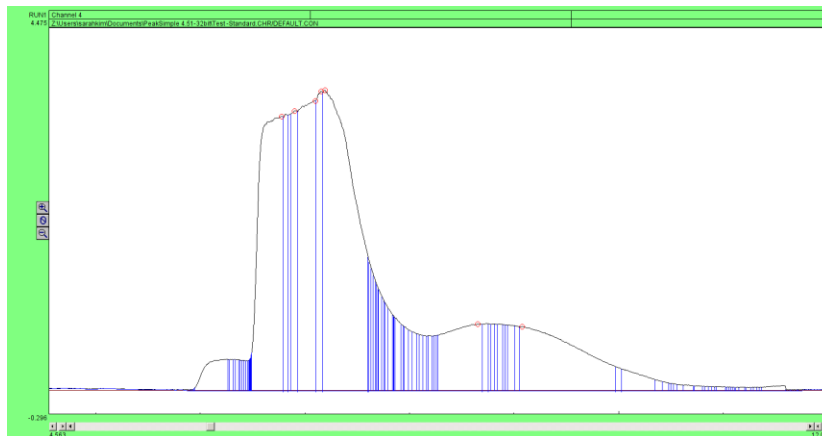


Figure 11. Chromatogram from PeakSimple (version 4.51) displaying the difference between (a) automatic integration and (b) manual integration. Blue lines indicate area of peak detected by the software.

2.6.2 Manual Integration

Using PeakSimple software (see: **Section: 2.5.1**) for recording and integration of GC chromatographic peaks, a combination of height (mV) and area is utilized to determine concentration (mM) of standards and *H. butylicus* samples. When determining the height of the peak, the cursor is simply placed on top of the peak and a value in the right-hand corner of the software will indicate the height (mV); the value to the left of the height is the corresponding time point (**Fig. 12**).

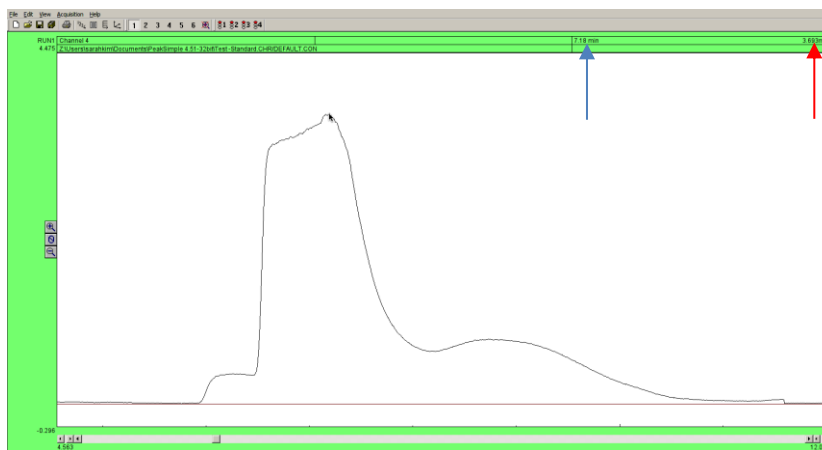


Figure 12. Chromatograph from PeakSimple (version 4.51) displaying height (mV) and time (min).

The height (mV) of a given peak is shown in the upper right-hand corner of the chromatograph; this is indicated by the red arrow. The corresponding time point is indicated by the blue arrow.

As briefly mentioned in Section 2.6.1, the solvent peaks in *H. butylicus* samples do not have a typical Gaussian shape and sample peaks often do not sit flush on the baseline. To account for this, a manual baseline must be created to include the entire area under a peak (**Appendix C: PeakSimple Operation Procedure**).

2.6.3 PeakSimple Software parameters

For integration of a GC peak area the area reject value is set to 0.001 to allow for the detection of smaller peaks (**Appendix C: PeakSimple Operation Procedure**).

2.6.4 Operation of PeakSimple with Shimadzu GC-14a

The voltage of the baseline (mV) must be equalized when the GC Buck is turned on (**Appendix C: PeakSimple Operation Procedure**). As mentioned in Section 2.5.1, the PeakSimple recording software is installed on a computer which is connected to the GC Buck. This means that when running a sample, PeakSimple will not automatically begin recording with the injection of a sample on the Shimadzu GC-14a, so the user must manually perform this step.

3.0 Results

3.1 Growth of *H. butylicus*

3.1.1 Optimization of growth conditions

H. butylicus was grown in 60 mL bottles at 95°C. Its growth was monitored by cell counts measured in duplicate using a Petroff Hauser counting chamber and a contrast phase microscope. Optimal growth conditions of *H. butylicus* are required to obtain maximum fermentation products. For the optimization of pH, *H. butylicus* was grown using the media described in Section 2.3 to determine the effect of pH on growth; the pH of the medium was adjusted to 6.0, 6.5, 7.0, and 8.0 with no other changes to the medium. pH was measured at room temperature before and after inoculation as well as throughout growth; measurements were conducted in duplicate using pH paper (Millipore, CA) that was also calibrated using a pH meter. Minimal difference was seen in *H. butylicus* grown in mediums with varying pHs however, the highest growth was observed at pH 7.0 (2.14×10^8 cells/mL) and the least favourable growth at pH 6.0 (9.13×10^7 cells/mL). Growth was progressively more favourable for 6.5 and 8.0 (Fig. 13).

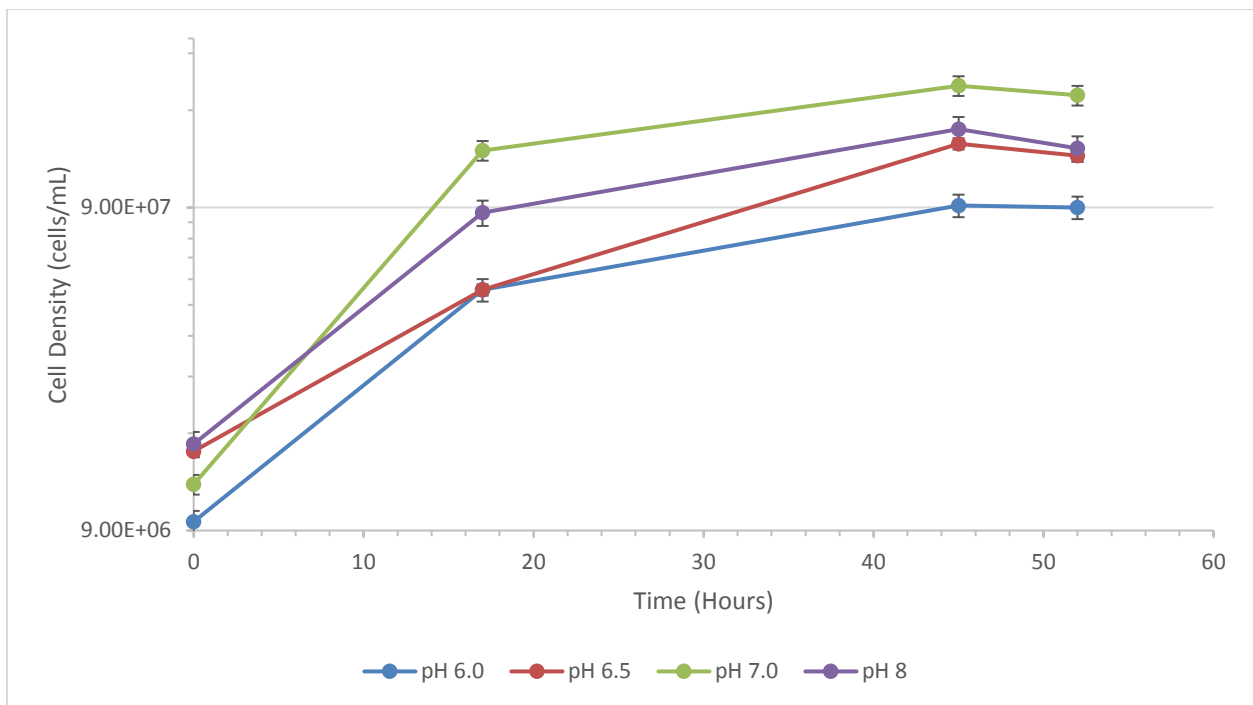


Figure 13. Growth of *H. butylicus* at varying pHs. Cell counts were from two biological replicates, each an average of duplicate counts. Error bars shown as \pm standard deviation.

Growth of *H. butylicus* is stimulated by the presence of H₂. To determine the magnitude of the effect, pressures of H₂ ranging from 3 psi, 1.0, 2.5, to 3.0 atm (over-pressurized) in culture bottles were tested. For the optimization of H₂, *H. butylicus* was grown using the medium described in Section 2.3. Cultures grown in 3 psi H₂ (or 0 atm over-pressurized) resulted in a lower cell density and longer log phase while only a minimal difference was observed for cultures grown in 2.5 and 3.0 atm H₂ (**Fig. 14**).

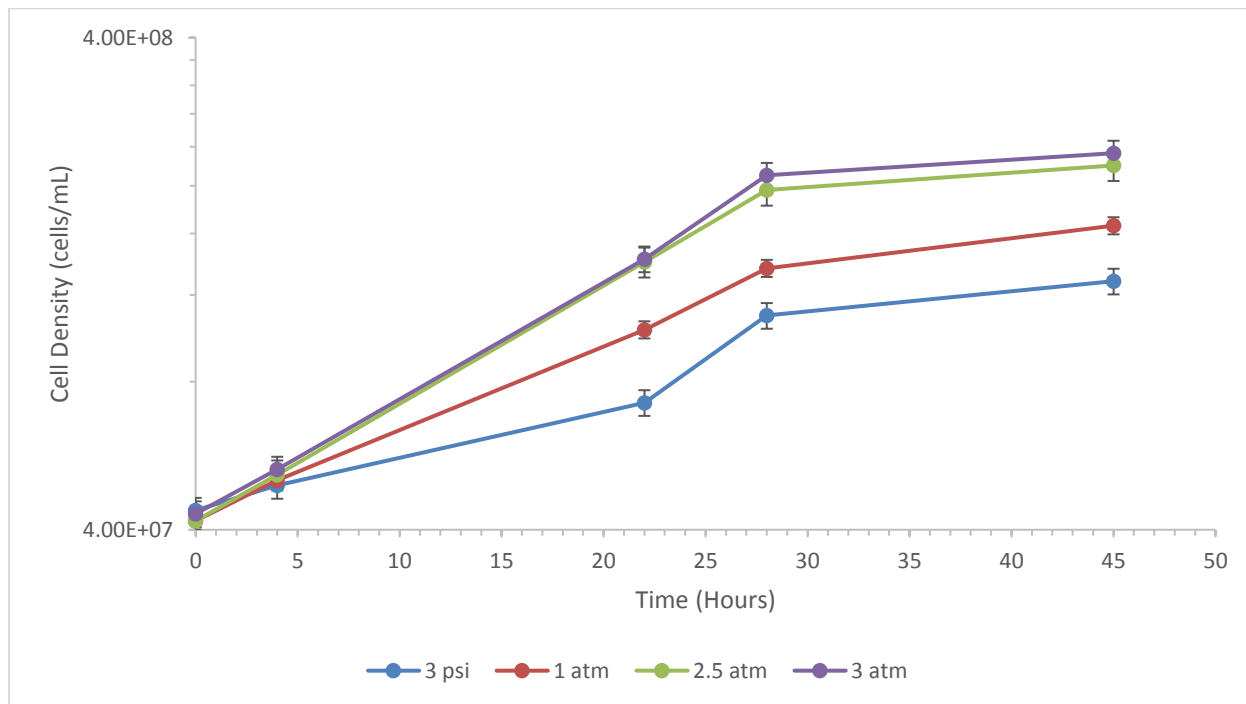


Figure 14. Growth of *H. butylicus* under varying pressures of H₂. Cell counts are from two biological replicates, each an average of duplicate counts. Error bars shown as \pm standard deviation.

In addition to H₂, growth of *H. butylicus* is also stimulated by the presence of sulfur. To determine how effectively *H. butylicus* can utilize varying concentration of sulfur, the medium was prepared in the presence of sulfur ranging from 0, 1.0, 5.0, to 10.0 g/L. The pH of the medium was kept constant at 7.0 and H₂ at 3.0 atm (over-pressurized) for each test. When comparing the different concentrations of sulfur, higher concentrations positively correlated with higher growth. A concentration of 10.0 g/L resulted in the highest growth while cultures grown without any sulfur displayed approximately half of the maximum cell density (1.17×10^8 cells/mL) (Fig. 15).

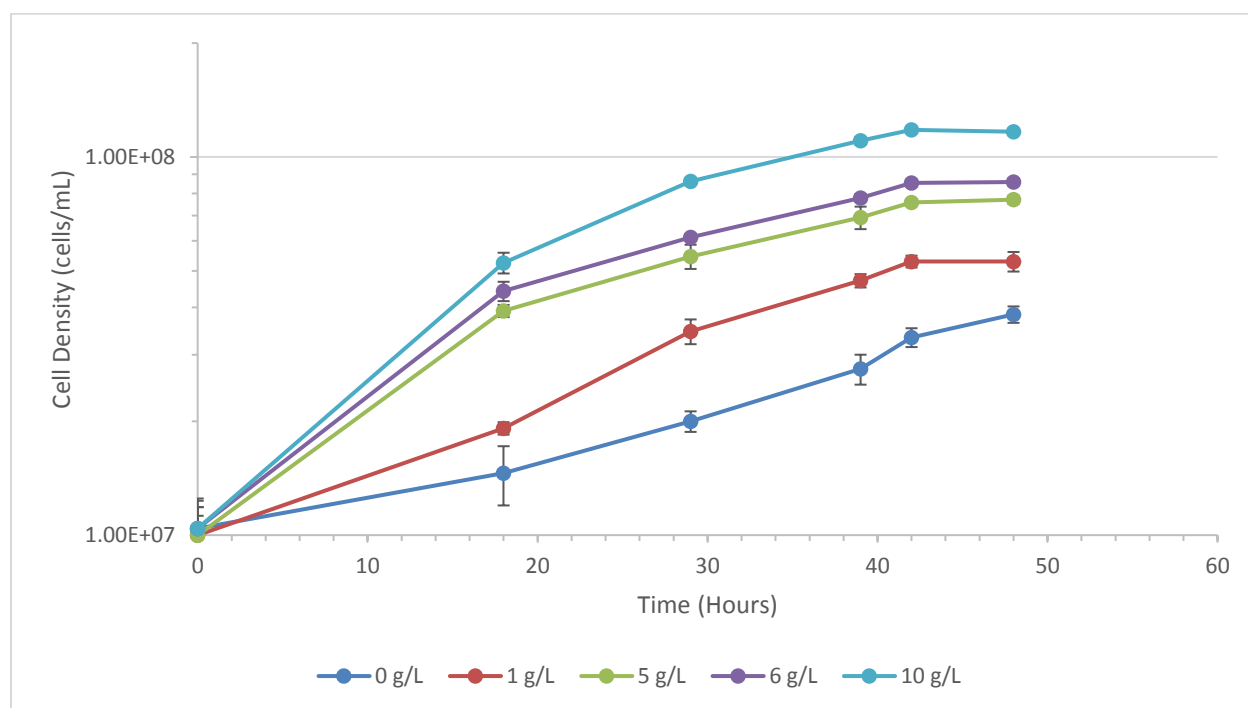


Figure 15. Growth of *H. butylicus* under varying sulfur concentrations. Cells were grown under the same medium composition and 3.0 atm of H₂ (over-pressurized). Cell counts are from two biological replicates, each an average of duplicate counts. Error bars shown as \pm standard deviation.

Following optimization, the following growth conditions were obtained: pH 7.0, 3.0 atm H₂ (over-pressurized), and 10.0 g/L of sulfur at 95°C. Growth under these optimal conditions was successfully achieved in the laboratory for cultures of *H. butylicus* grown in 20 mL of medium in 60 mL glass serum bottles. A final cell density of above 1.0 x 10⁸ cells/mL was achieved (**Fig. 16**).

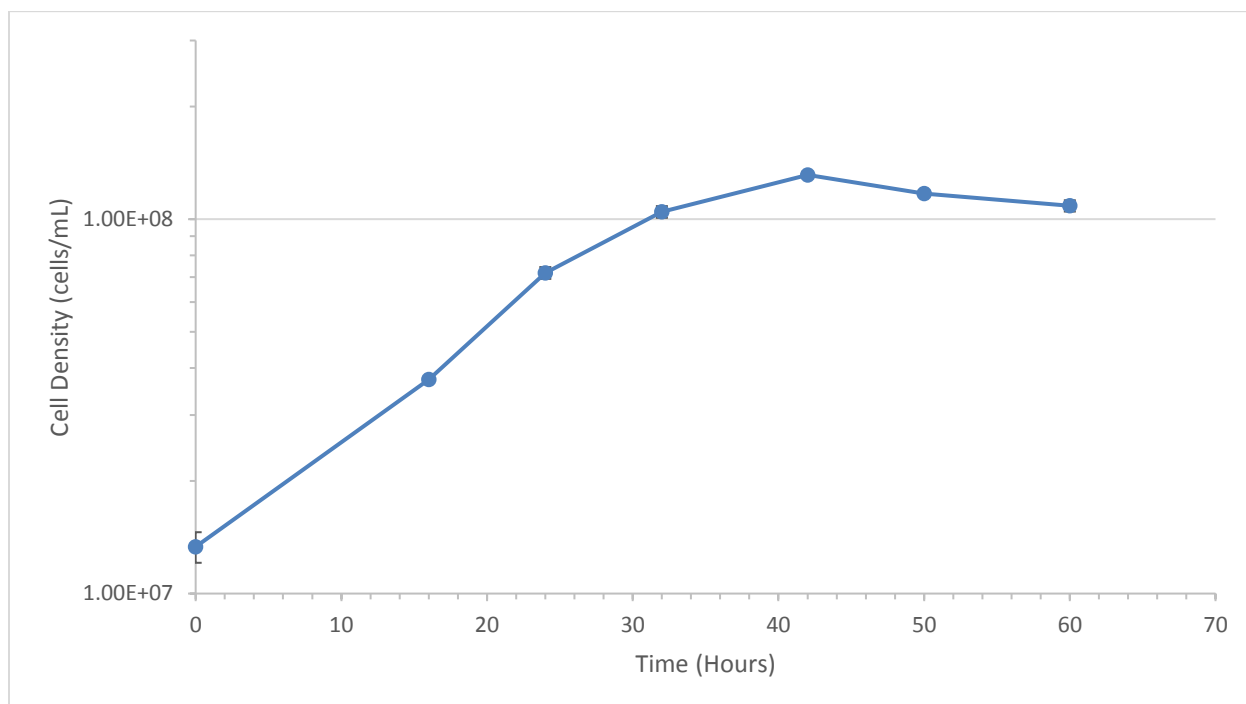


Figure 16. *H. butylicus* growth under optimal conditions. Cells were grown under the same composition of medium (10.0 g/L of sulfur), pH of 7.0, and 3.0 atm of H₂ (over-pressurized). Cell counts are from two biological replicates, each an average of duplicate counts. Error bars shown as ± standard deviation.

3.1.2 Growth of *H. butylicus* in acetate and butyrate supplemented media

The cell growth response of *H. butylicus* in the presence and absence of supplemented sodium butyrate and sodium acetate was tested. The cell culture in the medium containing supplemented butyrate showed no significant difference compared to the cell culture grown in un-supplemented medium. Both butyrate supplemented and un-supplemented cultures grew to a similar final maximum cell density of $> 1.0 \times 10^8$ cells/mL (**Fig. 17**). Cell cultures grown in medium supplemented with acetate grew slower with an extended log phase followed by a lower final cell density $< 1.0 \times 10^8$ cells/mL. Cultures with the addition of 15 mM acetate in the growth medium had the lowest growth (5.9×10^7 cells/mL) (**Fig. 18**).

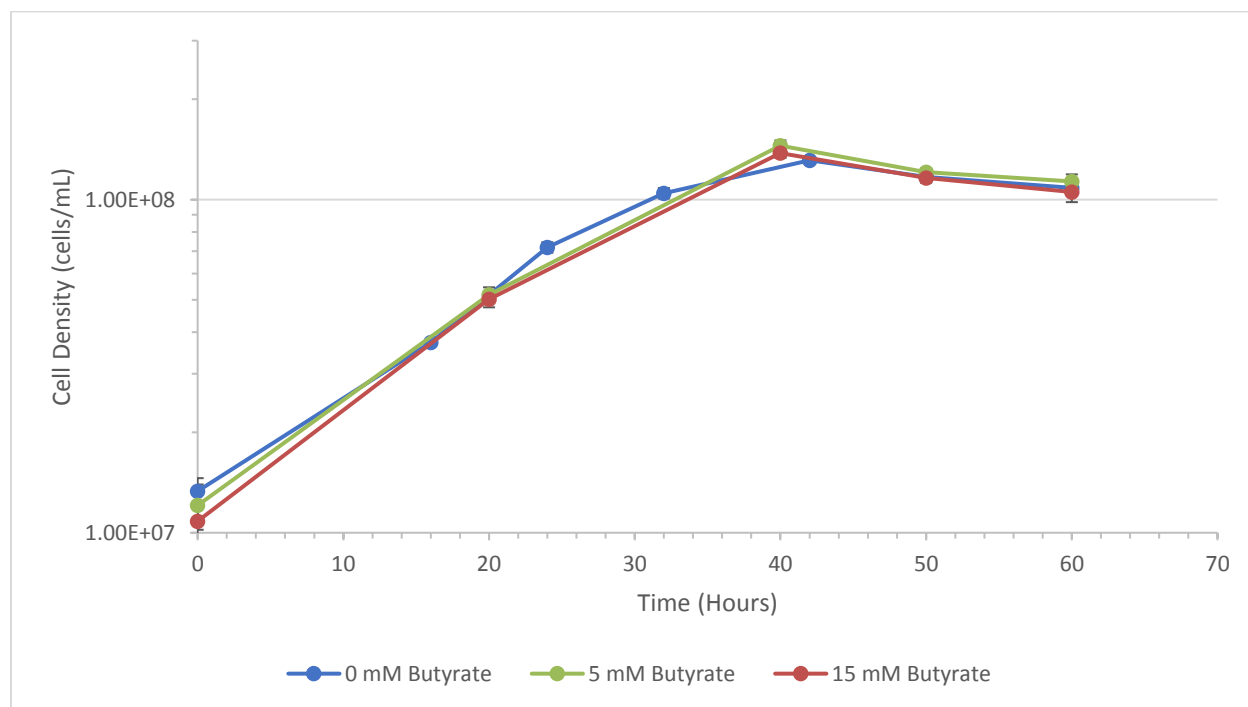


Figure 17. Growth of *H. butylicus* in butyrate supplemented media. Cells were grown under the same composition of medium (10.0 g/L of sulfur), pH of 7.0, and 3.0 atm of H₂ (over-pressurized). Cell counts are from two biological replicates, each an average of duplicate counts. Error bars shown as \pm standard deviation.

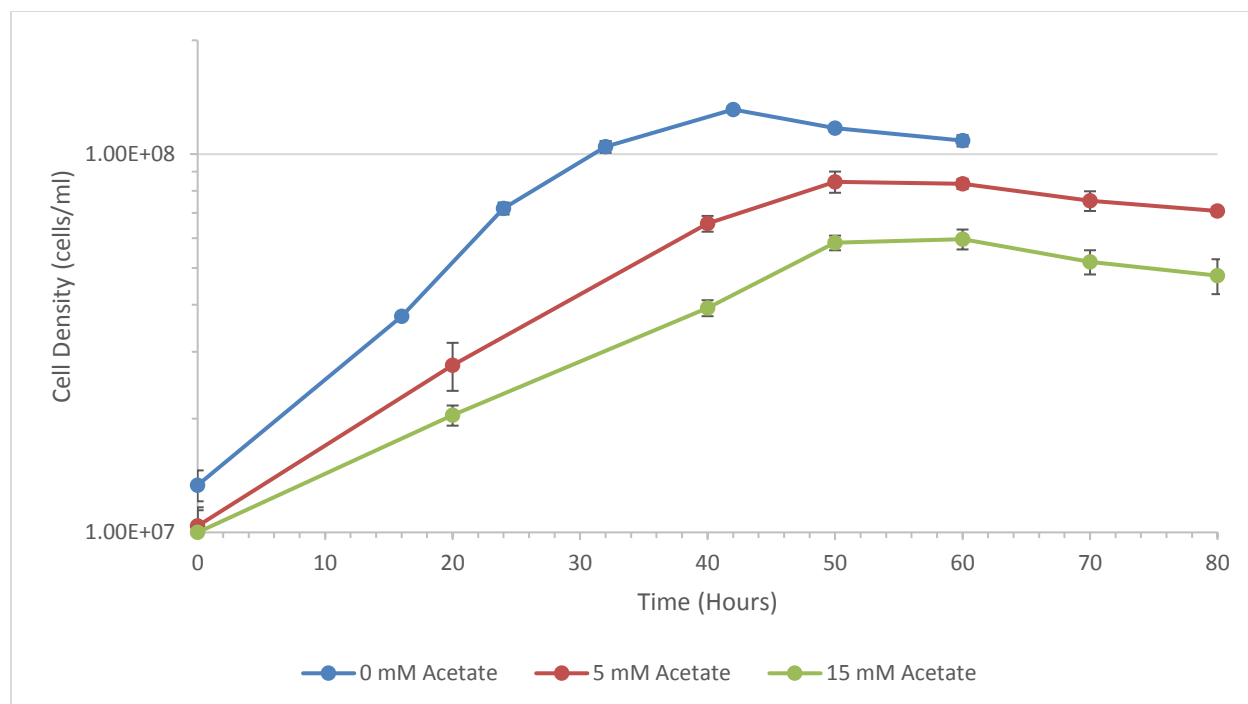


Figure 18. Growth of *H. butylicus* in acetate supplemented media. Cells were grown under the same composition of medium (10.0 g/L of sulfur), pH of 7.0, and 3.0 atm of H₂ (over-pressurized). Cell counts are from two biological replicates, each an average of duplicate counts. Error bars shown as \pm standard deviation.

3.2 Solvent detection

3.2.1 Optimization of liquid-liquid extraction procedure

When preparing samples for analysis using GC, an internal standard is commonly used to aid in quantifying unknown samples. The internal standard was 2.0 g/L of isobutanol in ethyl acetate, which was used as the extraction solution in a liquid-liquid extraction method to separate the desired solvents from other impurities in *H. butylicus* medium. To determine the sample volume and corresponding extraction solution (or internal standard) volume, varying ratios of 5 mM mixed (ethanol, acetone, isopropanol, and 1-butanol) standard to extraction solution was tested. A lower volume and equal ratio of 200 μ L:200 μ L (sample:extraction solution) resulted in more interfering peaks compared to 200 μ L:600 μ L. One mL to 200 μ L of sample to extraction solution resulted in the best resolution and highest peak areas. Shaking times for prepared GC samples were also optimized. Fifteen minutes of shaking provided the best separation of solvents and the maximum area of solvents when analyzed on the GC (data not shown).

3.2.2 Optimization of the GC method

Optimizing the GC method was a crucial step in detecting and quantifying the fermentation products of *H. butylicus*. All parameters were constantly considered when selecting the most optimal conditions for the GC run including the column that was used, injection and detector temperatures ($^{\circ}$ C), initial temperature ($^{\circ}$ C) and holding time (min), flow rate of carrier gas, ramp rate ($^{\circ}$ C/min), and final temperature ($^{\circ}$ C). The Shimadzu GC-14a equipped with a DB-5 and DB-624 combined column was ultimately used for detecting solvents from *H. butylicus*. Although acetone, ethanol, and isopropanol peaks could not be separated completely, a series of optimizations led to the final method (**Table 6**) which provided the best resolution and separation of peaks with the columns that were used: Injection temp.: 200 $^{\circ}$ C, Detector temp.: 300 $^{\circ}$ C, Initial temp.: 35 $^{\circ}$ C (hold for 10 min), Program rate: 3 $^{\circ}$ C/min to 40 $^{\circ}$ C, 45 $^{\circ}$ C/min to 150 $^{\circ}$ C, Final temp.: 150 $^{\circ}$ C (hold for 1 min), Range: 1 (for 10 min), 2 (for remainder of run).

Table 6. Optimization of GC method (Shimadzu GC-14a equipped with DB-5 and DB-624 combined GC column).

Test	Column	Method	Difference	Outcome
1	DB-5 (Cat No.: 123-5032)	Injection temp.: 200°C Detector temp.: 300°C Initial temp.: 35°C Program rate: 1°C/min to 45°C, 40°C/min to 150°C Final temp.: 150°C (hold for 1 min) Range: 4	None.	Column damaged from conditioning.
2	DB-624 UI (Cat No.: 123-1334)	Injection temp.: 200°C Detector temp.: 300°C Initial temp.: 35°C Program rate: 1°C/min to 45°C, 40°C/min to 150°C Final temp.: 150°C (hold for 1 min) Range: 4	Column changed.	1-Butanol not detected.
3	DB-624 UI (Cat No.: 123-1334)	Injection temp.: 200°C Detector temp.: 240°C Initial temp.: 80°C Program rate: 10°C/min to 90°C (hold for 1 min), 30°C/min to 150°C Final temp.: 150°C (hold for 1 min) Range: 4	New method according to parameters recommended by Agilent for new column.	No peaks detected.
4	DB-624 (Cat No.: 123-134)	Injection temp.: 250°C Detector temp.: 300°C Initial temp.: 40°C (hold for 5 min) Program rate: 2°C/min to 90°C, 40°C/min to 180°C Final temp.: 180°C (hold for 1 min) Range: 4	Column changed. New method according to parameters recommended by Restek.	No peak detected.
5	DB-624 (Cat No.: 123-134)	Injection temp.: 250°C Detector temp.: 300°C Initial temp.: 40°C (hold for 5 min) Program rate: 10°C/min to 240°C Final temp.: 240°C (hold for 3 min) Range: 4	Program rate and final temperature changed.	Too much peak splitting.

6	DB-624 (Cat No.: 123-134)	Injection temp.: 250°C Detector temp.: 300°C Initial temp.: 35°C (hold for 5 min) Program rate: 10°C/min to 100°C, 15°C to 220°C, 25°C to 240°C Final temp.: 240°C (hold for 1 min) Range: 4	Initial time and program rate changed.	Too much peak splitting (too many individual peaks)
7	DB-624 (Cat No.: 123-134)	Injection temp.: 200°C Detector temp.: 300°C Initial temp.: 35°C Program rate: 1°C/min to 45°C, 40°C/min to 150°C Final temp.: 150°C (hold for 1 min) Range: 4	Initial hold time, program rate, and final temperature changed.	Insufficient separation of peaks
8	DB-624 (Cat No.: 123-134)	Injection temp.: 200°C Detector temp.: 300°C Initial temp.: 35°C Program rate: 2°C/min to 45°C, 40°C/min to 150°C Final temp.: 150°C (hold for 1 min) Range: 4	Program rate changed.	Insufficient separation of peaks
9	DB-624 (Cat No.: 123-134)	Injection temp.: 200°C Detector temp.: 300°C Initial temp.: 35°C Program rate: 1.5°C/min to 45°C, 40°C/min to 150°C Final temp.: 150°C (hold for 1 min) Range: 4	Program rate changed.	Insufficient separation of peaks
10	DB-624 (Cat No.: 123-134)	Injection temp.: 200°C Detector temp.: 300°C Initial temp.: 35°C Program rate: 1.7°C/min to 45°C, 40°C/min to 150 degrees C Final temp.: 150°C (hold for 1 min) Range: 4	Program rate changed.	Acetone, ethanol, and isopropanol peaks are too small

11	DB-624 (Cat No.: 123-134)	Injection temp.: 200°C Detector temp.: 300°C Initial temp.: 35°C Program rate: 1.7°C/min to 45°C, 40°C/min to 150 degrees C Final temp.: 150°C (hold for 1 min) Range: 2	Range changed.	Poor separation of ethyl acetate, isobutanol, and 1-butanol. Poor separation of acetone, ethanol, and isopropanol.
12	DB-624 (Cat No.: 123-134)	Injection temp.: 200°C Detector temp.: 300°C Initial temp.: 35°C (hold for 5 min) Program rate: 1.7°C/min to 45°C, 40°C/min to 150°C Final temp.: 150°C (hold for 1 min) Range: 2	Initial temperature hold time changed.	Better separation of acetone, ethanol, and isopropanol from ethyl acetate, isobutanol, and 1-butanol. Poor separation within acetone, ethanol, and isopropanol.
13	Rt-U- BOND (Cat No.: 19772)	Injection temp.: 200°C Detector temp.: 300°C Initial temp.: 35°C (hold for 10 min) Program rate: 30°C/min to 175°C Final temp.: 175°C Range: 4	Column changed. New method according to parameters recommended by Restek for new column.	Column changed due to poor separation of acetone, ethanol, and isopropanol. Method changed according to recommended parameters from Restek. No peaks detected.
14	DB-5 (Cat No.: 123- 5032) + DB-624 (Cat No.: 123-134) Combined	Injection temp.: 200°C Detector temp.: 300°C Initial temp.: 35°C (hold for 5 min) Program rate: 3°C/min to 45°C, 40°C/min to 150°C Final temp.: 150°C (hold for 1 min) Range: 2	Two columns combined. Only program rate changed from the previous method (12).	Better separation of acetone, ethanol, and isopropanol from ethyl acetate, isobutanol, and 1-butanol. Poor separation within acetone, ethanol, and isopropanol. Better resolution of acetone, ethanol, and isopropanol.

15	DB-5 (Cat No.: 123-5032) + DB-624 (Cat No.: 123-134) Combined	Injection temp.: 200°C Detector temp.: 300°C Initial temp.: 35°C (hold for 10 min) Program rate: 3°C/min to 45°C, 40°C/min to 150°C Final temp.: 150°C (hold for 1 min) Range: 2	Initial temperature hold time changed.	Good separation of acetone, ethanol, and isopropanol from ethyl acetate, isobutanol, and 1-butanol. Poor separation within acetone, ethanol, and isopropanol. Better resolution of acetone, ethanol, and isopropanol.
16	DB-5 (Cat No.: 123-5032) + DB-624 (Cat No.: 123-134) Combined	Injection temp.: 200°C Detector temp.: 300°C Initial temp.: 35°C (hold for 10 min) Program rate: 3°C/min to 45°C, 40°C/min to 150°C Final temp.: 150°C (hold for 1 min) Range: 2	Column changed back to combined column. Previous method used (14).	Good separation of acetone, ethanol, and isopropanol from ethyl acetate and isobutanol. Poor separation within acetone, ethanol, and isopropanol. 1-Butanol not detected.
17	DB-5 (Cat No.: 123-5032) + DB-624 (Cat No.: 123-134) Combined	Injection temp.: 200°C Detector temp.: 300°C Initial temp.: 35°C (hold for 10 min) Program rate: 3°C/min to 60°C (hold for 2 min), 40°C/min to 150°C Final temp.: 150°C (hold for 1 min) Range: 2	Program rate changed.	Isobutanol peak blended with impurity.
18	DB-5 (Cat No.: 123-5032) + DB-624 (Cat No.: 123-134) Combined	Injection temp.: 200°C Detector temp.: 300°C Initial temp.: 35°C (hold for 10 min) Program rate: 3°C/min to 60°C, 40°C/min to 150°C Final temp.: 150°C (hold for 1 min) Range: 2	Program rate changed.	Isobutanol peak tails into 1-butanol. Good separation of acetone, ethanol, and isopropanol from ethyl acetate, isobutanol, and 1-butanol. Poor separation within acetone, ethanol, and isopropanol. Acetone, ethanol, and isopropanol are difficult to see at low concentrations (peaks

too small compared to other solvents).

19	DB-5 (Cat No.: 123-5032) + DB-624 (Cat No.: 123-134) Combined	Injection temp.: 200°C Detector temp.: 300°C Initial temp.: 35°C (hold for 10 min) Program rate: 3°C/min to 60°C, 40°C/min to 150°C Final temp.: 150°C (hold for 1 min) Range: 1 (for 10 min), 2 (for remainder of run)	Range changed.	Isobutanol peak tails into 1-butanol. Acetone, ethanol, and isopropanol can be seen at low concentrations.
20	DB-5 (Cat No.: 123-5032) + DB-624 (Cat No.: 123-134) Combined	Injection temp.: 200°C Detector temp.: 300°C Initial temp.: 35°C (hold for 10 min) Program rate: 3°C/min to 40°C, 45°C/min to 150°C Final temp.: 150°C (hold for 1 min) Range: 1 (for 11.6 min), 2 (for 8.4 min – to 20 min), 1 (for remainder of run)	Program rate changed. Range hold time changed.	Isobutanol no longer tails into 1-butanol. Acetone, ethanol, and isopropanol peaks still have poor separation but can be identified distinguishably. No issues with ethyl acetate, isobutanol, or 1-butanol. Final method (20) provided the best separation for all solvents.

3.2.3 Standard curves

Standard concentrations of 0, 0.25, 0.5, 1, 3, and 5 mM were separately prepared for 1-butanol, acetone, ethanol, and isopropanol. One mL standard samples were mixed with 200 uL of extraction solution (2 g/L isobutanol in ethyl acetate) and run on the GC. Using isobutanol as the internal standard, a peak ratio was obtained with the peak area of the known standard solvent and corresponding peak area of isobutanol. From the extraction solution there exists two impurity peaks that interfere with the peak areas of the target solvents (**Fig. 19**).

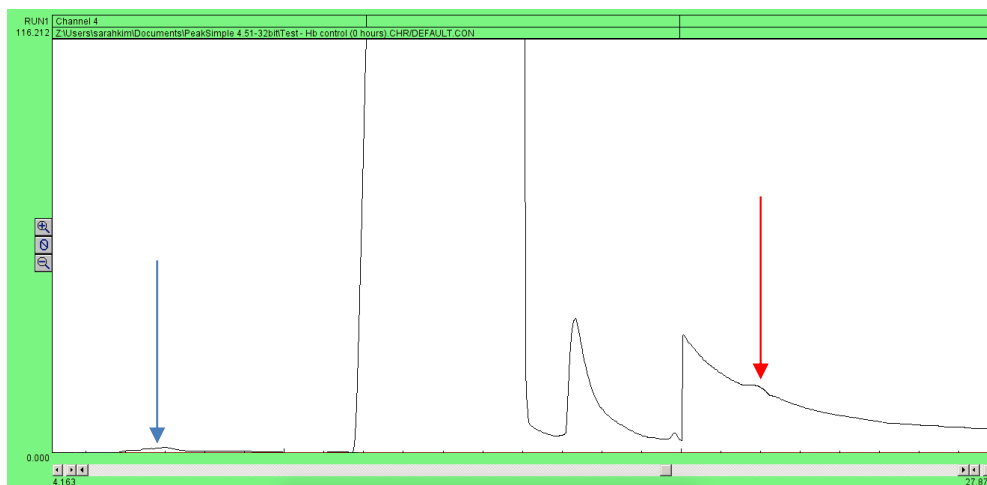


Figure 19. GC chromatograph of a control sample (0 mM) recorded using PeakSimple software (version 4.51). Control sample contains *H. butylicus* uninoculated media. Blue arrow indicates interference with peaks of acetone, ethanol, and isopropanol (6.25 – 6.40 min). Red arrow indicates interference with 1-butanol (20.75 – 21.85 min).

Each individual standard sample of 1-butanol, ethanol, acetone, and isopropanol showed a characteristic peak allowing it to be identifiable (**Fig. 20, Fig. 21**). Only 1-butanol was separated completely while the peaks of ethanol, acetone, and isopropanol were overlapping and could not be separated entirely. However, as mentioned, there were signature (or uniquely characteristic) peaks for ethanol, acetone, and isopropanol, respectively (**Fig. 21, Table 7**).

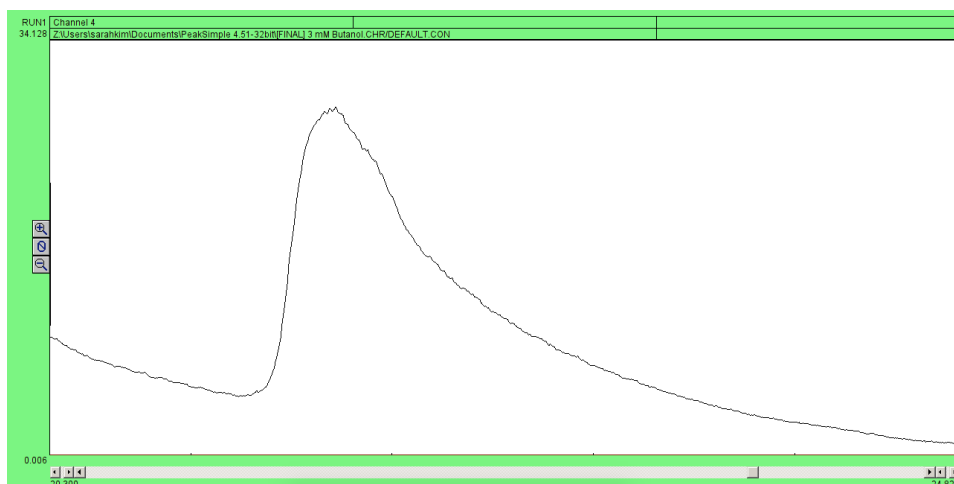


Figure 20. GC chromatogram of a 3 mM 1-butanol standard sample recorded using PeakSimple software (version 4.51). Retention time of peak is 20.75 – 21.85 min.

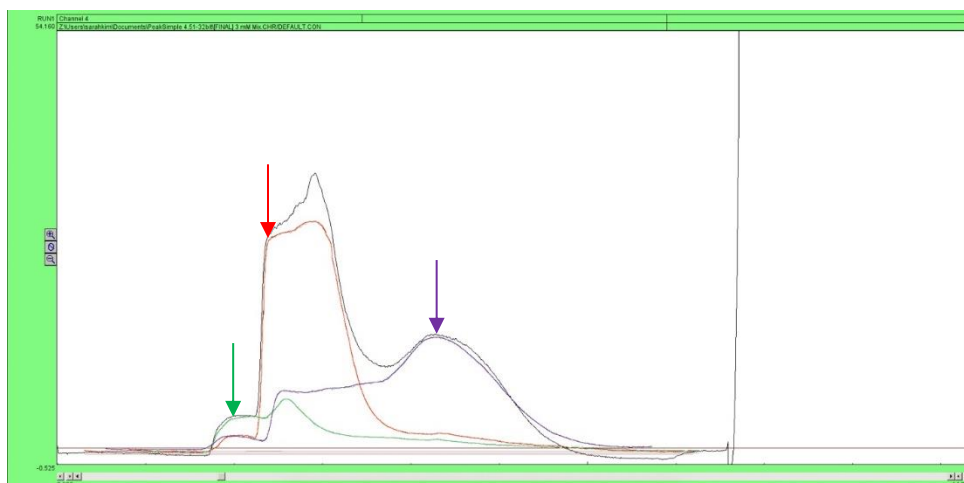


Figure 21. GC chromatogram of a 3 mM mixed standard sample recorded using PeakSimple software (version 4.51). Black – 3 mM mixed (acetone + ethanol + isopropanol), red – 3 mM acetone, green – 3 mM ethanol, purple – 3 mM isopropanol. Green arrow – 3 mM ethanol unique peak, red arrow – 3 mM acetone unique peak, purple arrow – 3 mM isopropanol unique peak.

Table 7. Identification and calculation of solvents using unique peaks.

Product	Unique Peak Retention Time (min)	How to determine presence of product	How to calculate concentration (mM) of product
1-Butanol	20.75 – 21.85	Overlap with a small extraction solution interference. If peak area is higher than the extraction solution interference (area > 3), it is considered to be 1-butanol.	Use PeakSimple software to integrate the area of 1-butanol peak. Use the standard curve and peak area to calculate concentration.
Ethanol	5.75 – 6.25	Overlap by a small extraction solution interference. Similar to 1-butanol, if peak is higher than the interference (area > 2) the peak is considered to be ethanol.	Use PeakSimple to measure height (mV) of the unique peak between 5.75 – 6.25 min. Use the standard curve to calculate its peak area, from which a ratio (to the area of corresponding isobutanol) is obtained. The ratio is then used to calculate its concentration using the ethanol standard curve.
Acetone	6.65 – 7.05	If there is a “bump” at 6.65- 7.05 min, acetone is indicated to be present.	Obtain height of peak (mV) at ~6.35 min using PeakSimple. Account for isopropanol impurity height interference (0.007 mV) and ethanol height. Multiply the area per mV value of acetone to get the area. Use the mix isobutanol peak area to obtain peak ratio value. Concentration can be calculated using the acetone standard curve.
Isopropanol	8.35 – 8.40	If there is a peak at 8.35 – 8.40 min, isopropanol is indicated to be present.	Use PeakSimple to measure the height (mV) of the unique peak between 8.35 – 8.40 min. Use the standard curve to calculate its peak area, from which a ratio (to

the area of corresponding isobutanol) is obtained. The ratio is then used to calculate its concentration using the isopropanol standard curve.

The standard curve for 1-butanol was obtained (Fig. 22), and its concentrations in both individual and mixed samples were proportional to their corresponding areas (Fig. 23).

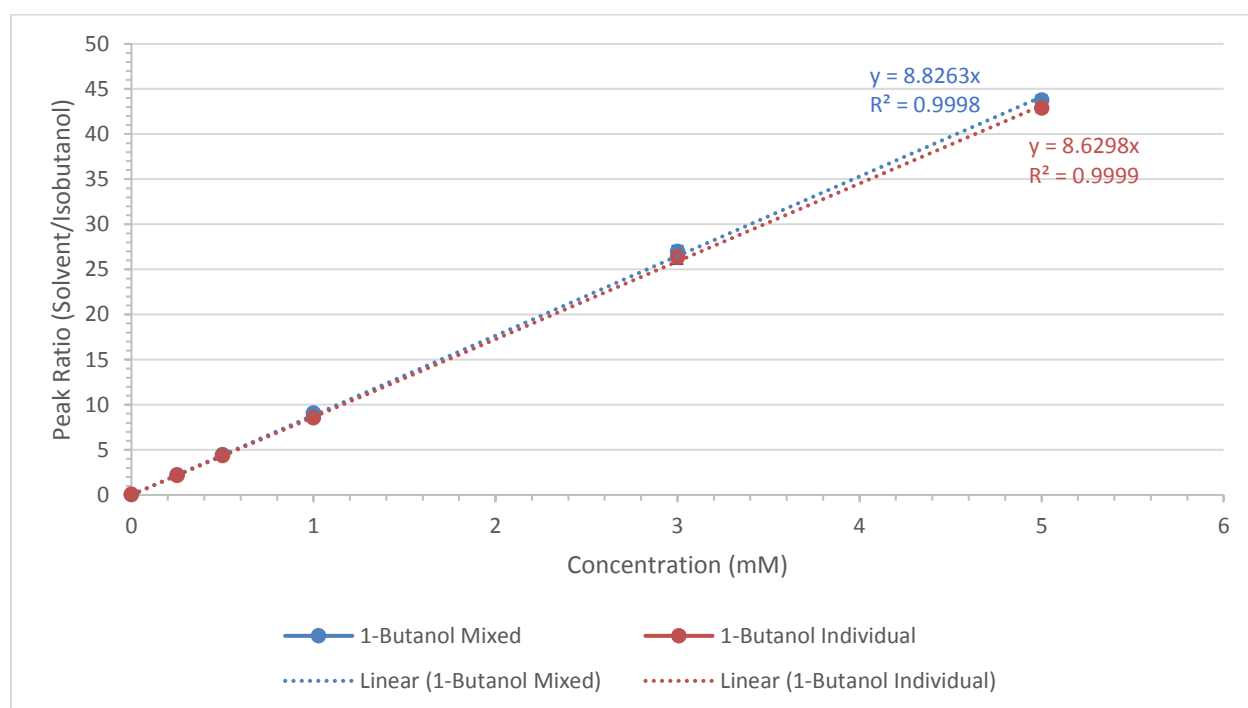


Figure 22. 1-Butanol standard curve from gas chromatography (peak ratio vs. concentration). Individual and mixed 1-butanol standard samples compared. GC sample points an average of duplicates. Error bars shown as \pm standard deviation.

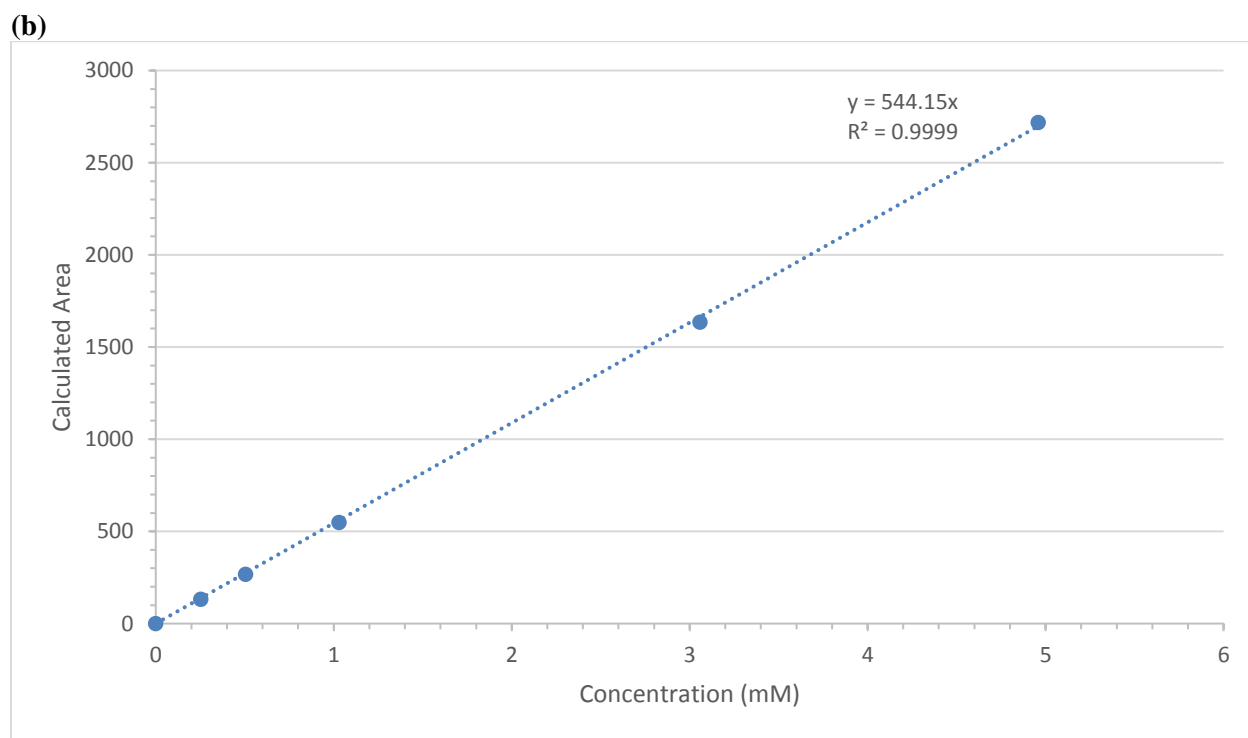
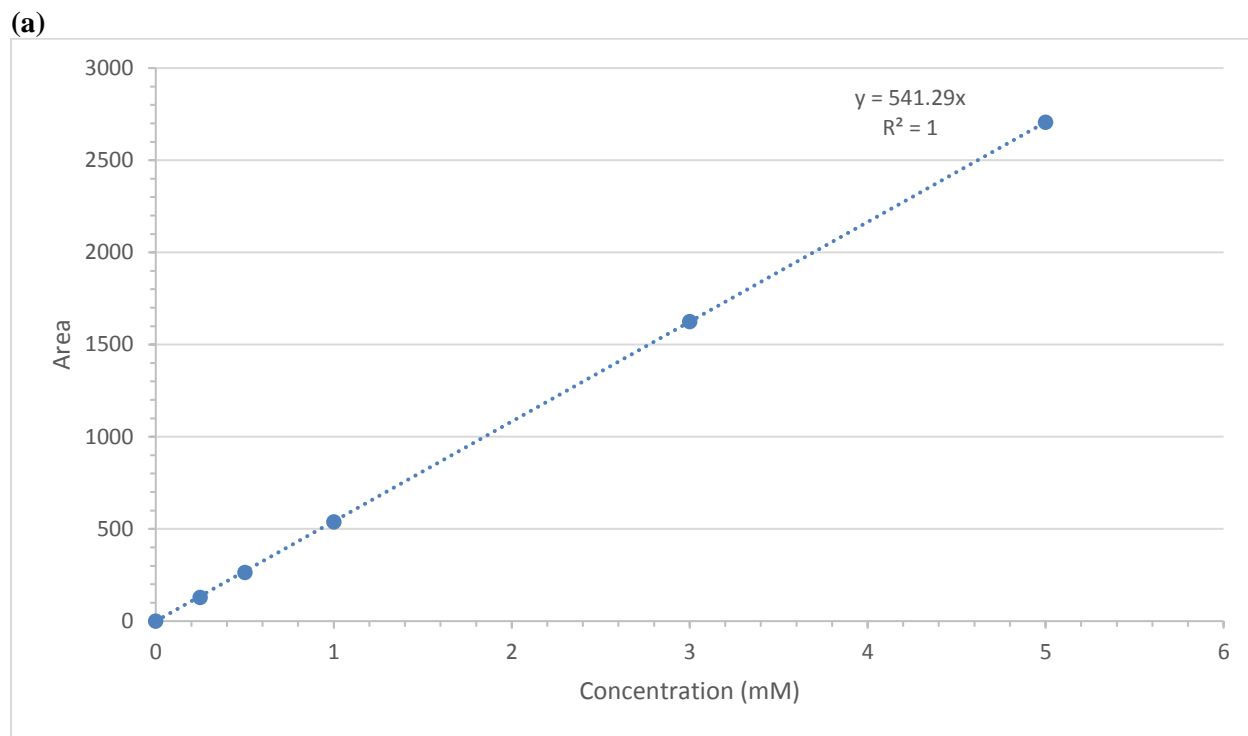


Figure 23. 1-Butanol standard curve from gas chromatography (area vs. concentration). (a) 1-Butanol area of an individual (containing just 1-butanol) standard sample and corresponding concentration (mM), (b) 1-Butanol calculated area in a mixed (containing the same concentration of acetone, ethanol, isopropanol, and 1-butanol) standard sample and corresponding calculated concentration (mM). GC sample points are an average of duplicates. Error bars shown as \pm standard deviation.

A height (mV) of each signature peak was found to be proportional to its corresponding peak area, which was also proportional to its corresponding concentration (**Fig 24 - 26**). Such signature peaks were used for identifying the presence of each solvent in the mix peak. The sum of the calculated peak area of each component from the mix peak was found to be approximately the same as the total peak area of the mix peak that was obtained by integration using the PeakSimple software (**Table 8**), with a less than 10% difference for all values. Therefore, the same approach was applied to analyzing the *H. butylicus* samples. Standard curves for ethanol, isopropanol, and acetone were prepared accordingly (**Fig. 27 – 29**).

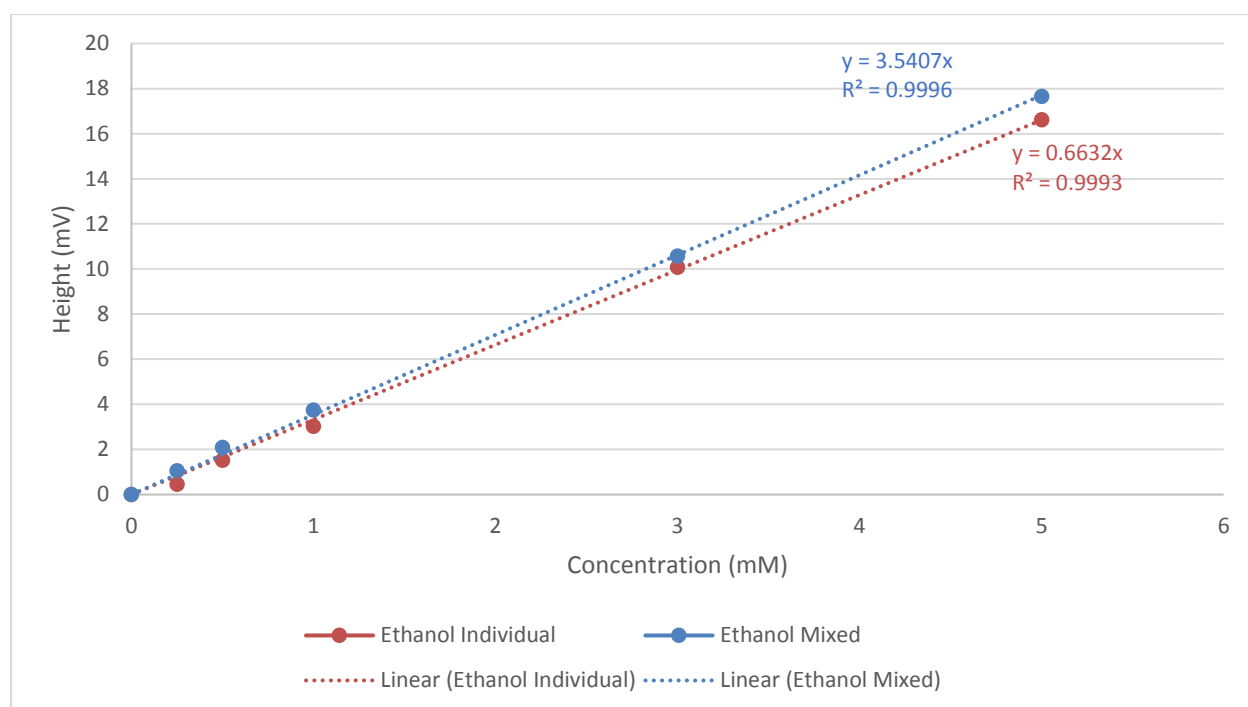


Figure 24. Comparison of ethanol height (mV) and corresponding concentration (mM). Individual and mixed ethanol (containing the same concentration of acetone, ethanol, isopropanol, and 1-butanol) standard samples compared. GC sample points an average of duplicates. Error bars shown as \pm standard deviation.

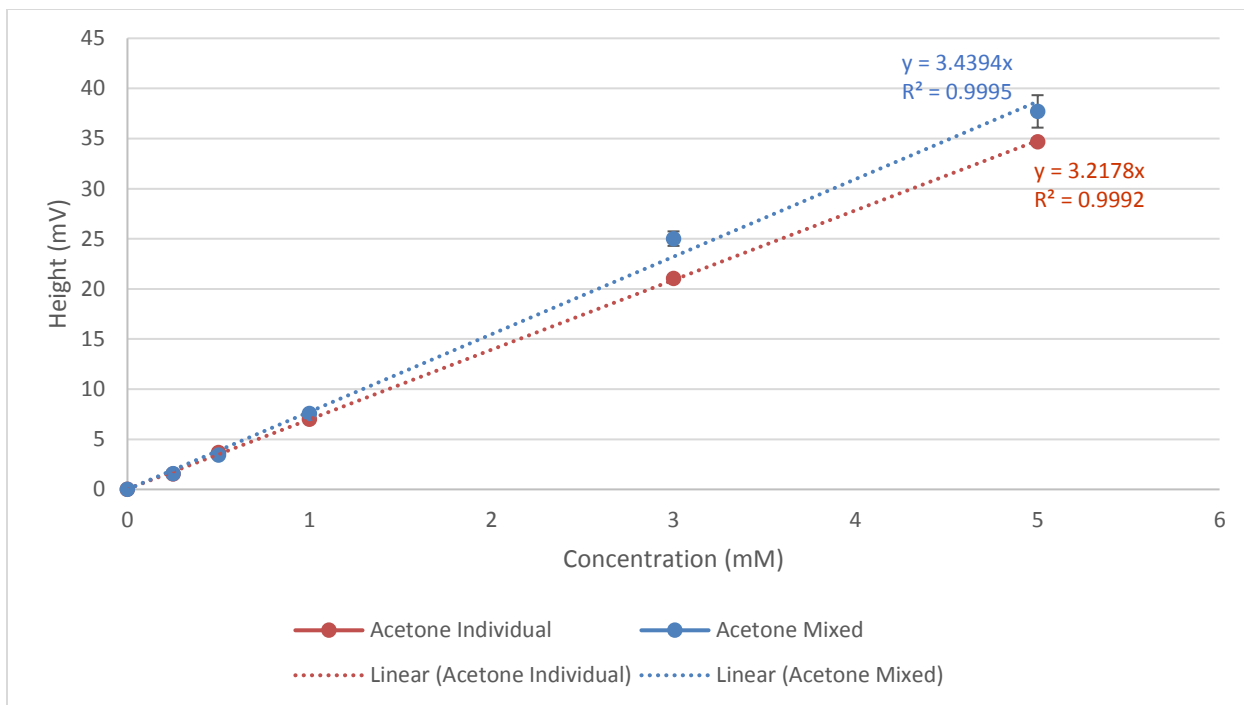


Figure 25. Comparison of acetone height (mV) and corresponding concentration (mM). Individual and mixed acetone (containing the same concentration of acetone, ethanol, isopropanol, and 1-butanol) standard samples compared. GC sample points are an average of duplicates. Error bars shown as \pm standard deviation.

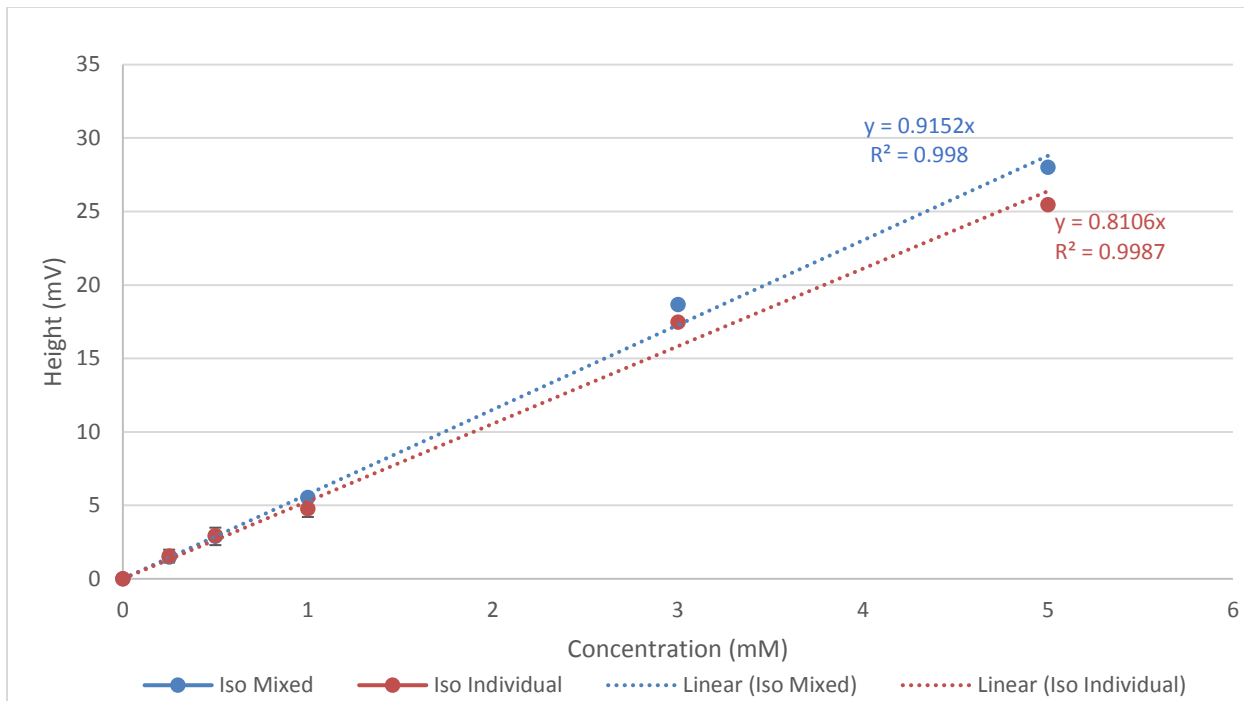
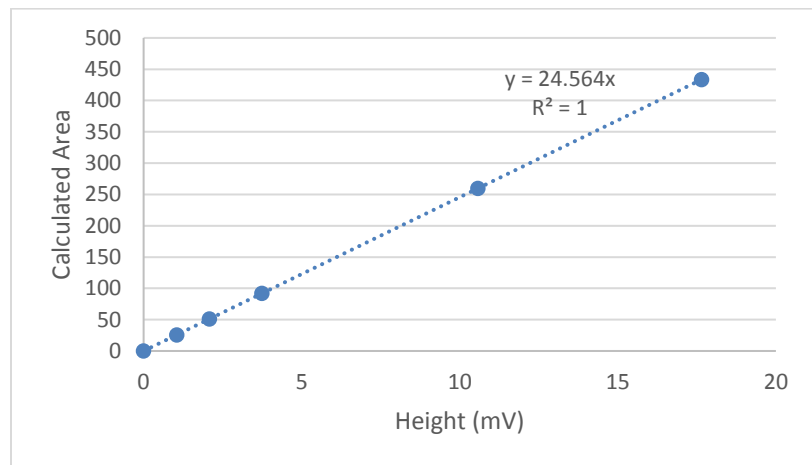
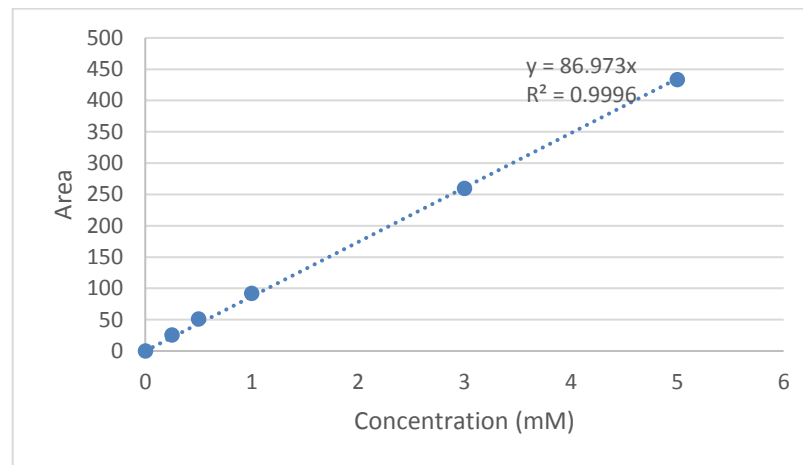


Figure 26. Comparison of isopropanol height (mV) and corresponding concentration (mM). Individual and mixed isopropanol (containing the same concentration of acetone, ethanol, isopropanol, and 1-butanol) standard samples compared. GC sample points are an average of duplicates. Error bars shown as \pm standard deviation.

(a)



(b)



(c)

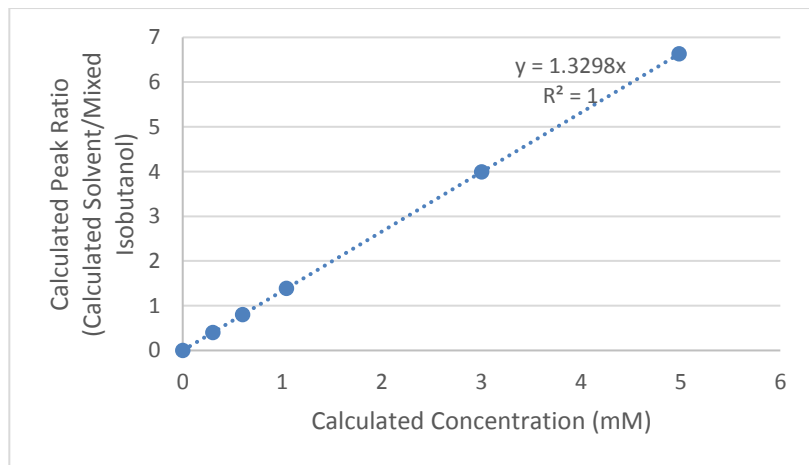
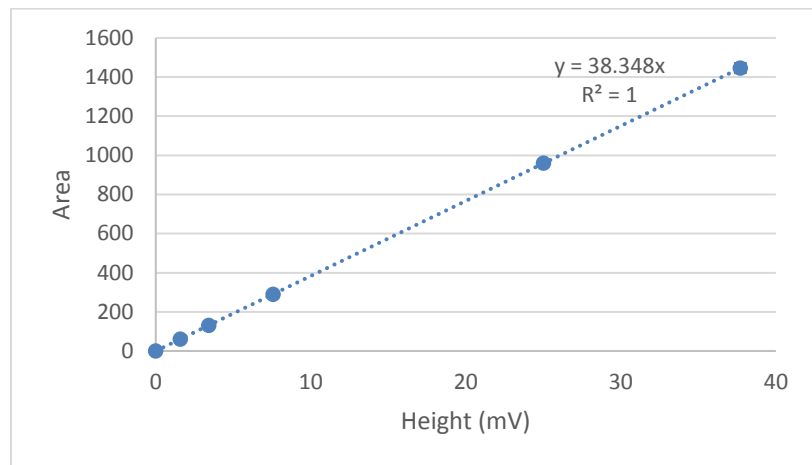
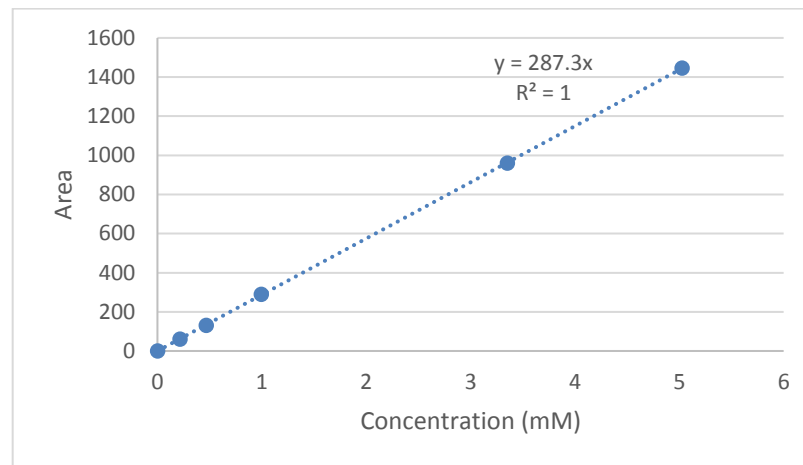


Figure 27. Ethanol standard curve from gas chromatography. (a) Ethanol area of a mixed (containing the same concentration of acetone, ethanol, isopropanol, and 1-butanol) standard sample and corresponding height (mV), (b) Mixed ethanol calculated area in a mixed (containing the same concentration of acetone, ethanol, isopropanol, and 1-butanol) standard sample and corresponding calculated concentration (mM), (c) Ethanol calculated peak ratio to calculated concentration (mM). GC sample points are an average of duplicates. Error bars shown as \pm standard deviation.

(a)



(b)



(c)

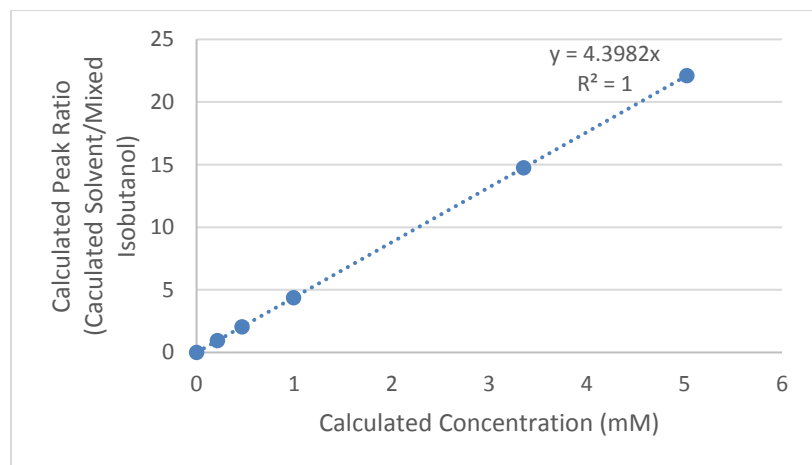
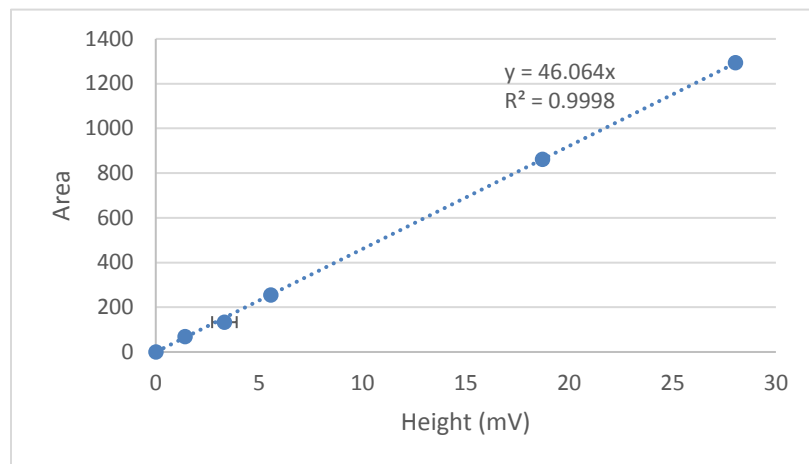
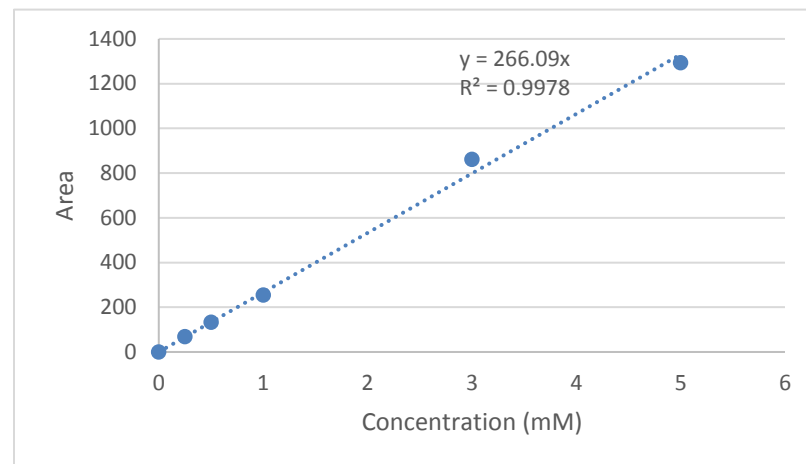


Figure 28. Acetone standard curve from gas chromatography. (a) Acetone area of a mixed (containing the same concentration of acetone, ethanol, isopropanol, and 1-butanol) standard sample and corresponding height (mV), (b) Mixed acetone calculated area in a mixed (containing the same concentration of acetone, ethanol, isopropanol, and 1-butanol) standard sample and corresponding calculated concentration (mM), (c) Acetone calculated peak ratio to calculated concentration (mM). GC sample points are an average of duplicates. Error bars shown as \pm standard deviation.

(a)



(b)



(c)

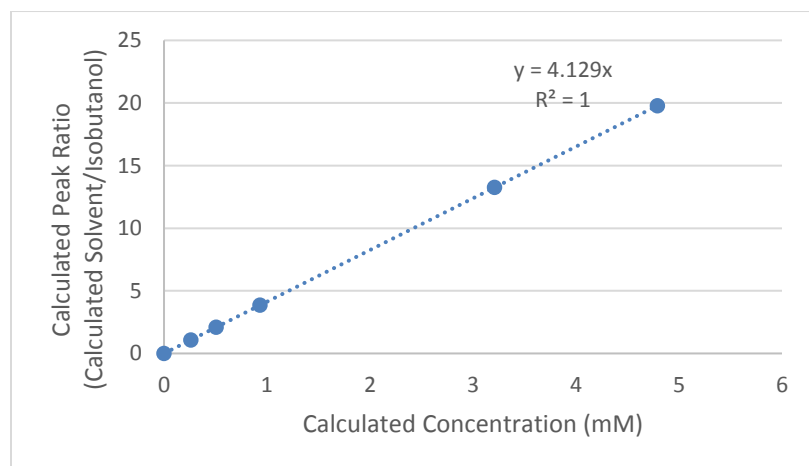


Figure 29. Isopropanol standard curve from gas chromatography. (a) Isopropanol area of a mixed (containing the same concentration of acetone, ethanol, isopropanol, and 1-butanol) standard sample and corresponding height (mV), (b) Mixed isopropanol calculated area in a mixed (containing the same concentration of acetone, ethanol, isopropanol, and 1-butanol) standard sample and corresponding calculated concentration (mM), (c) Isopropanol calculated peak ratio to calculated concentration (mM). GC sample points are an average of duplicates. Error bars shown as \pm standard deviation.

Table 8. Comparison of ethanol, acetone, and isopropanol peak area. Values are an average of duplicates.

Individual Acetone Peak Area	Individual Ethanol Peak Area	Individual Isopropanol Peak Area	Sum of Individual AEI Peak Area	Mixed AEI Peak Area	Difference (%)
0	0	0	0	0	0
66.25 ± 5.89	18.26 ± 0.09	58.57 ± 3.14	143.07 ± 2.76	146.45 ± 5.05	2.33
130.20 ± 3.52	37.98 ± 0.62	119.95 ± 1.49	288.14 ± 5.64	290.47 ± 1.68	0.81
264.83 ± 4.80	82.96 ± 1.05	245.43 ± 3.45	1186.02 ± 2.40	1298.52 ± 4.44	9.06
808.86 ± 2.47	245.49 ± 3.45	729.11 ± 3.78	1783.45 ± 2.81	1800.56 ± 8.45	0.95
1331.26 ± 2.46	411.76 ± 1.29	1228.02 ± 8.37	2971.03 ± 7.21	3115.83 ± 8.01	4.76

Table 9. Comparison of 1-butanol peak area. Values are an average of duplicates.

Individual Butanol Peak Area	Mixed Butanol Peak Area	Difference (%)
0	0	0
128.25 ± 1.22	132.51 ± 0.88	3.27
263.98 ± 3.38	267.74 ± 0.36	1.41
539.08 ± 0.88	549.67 ± 4.91	1.95
1625.61 ± 4.06	1635.06 ± 3.68	0.58
2706.90 ± 4.32	2719.30 ± 3.25	0.46

3.2 Solvent production of *H. butylicus*

3.3.1 Solvent production under optimized growth conditions

Production of solvents by *H. butylicus* under optimal growth conditions was observed using gas chromatography. Concentrations for each solvent was calculated using the standard curves shown in Section 3.2.3. The different time points tested corresponds to the different growth phases of *H. butylicus*. Production of ethanol and 1-butanol began at the early-log phase of growth (before 16 hours) and began to plateau shortly after the stationary late-log phase (after 40 hours). Production of isopropanol appeared to be linked to the production of acetone, where solvent production began during the mid-log phase (after 16 hours) for isopropanol and acetone production significantly decreased during the late-log phase (after 40 hours) (**Fig. 30**).

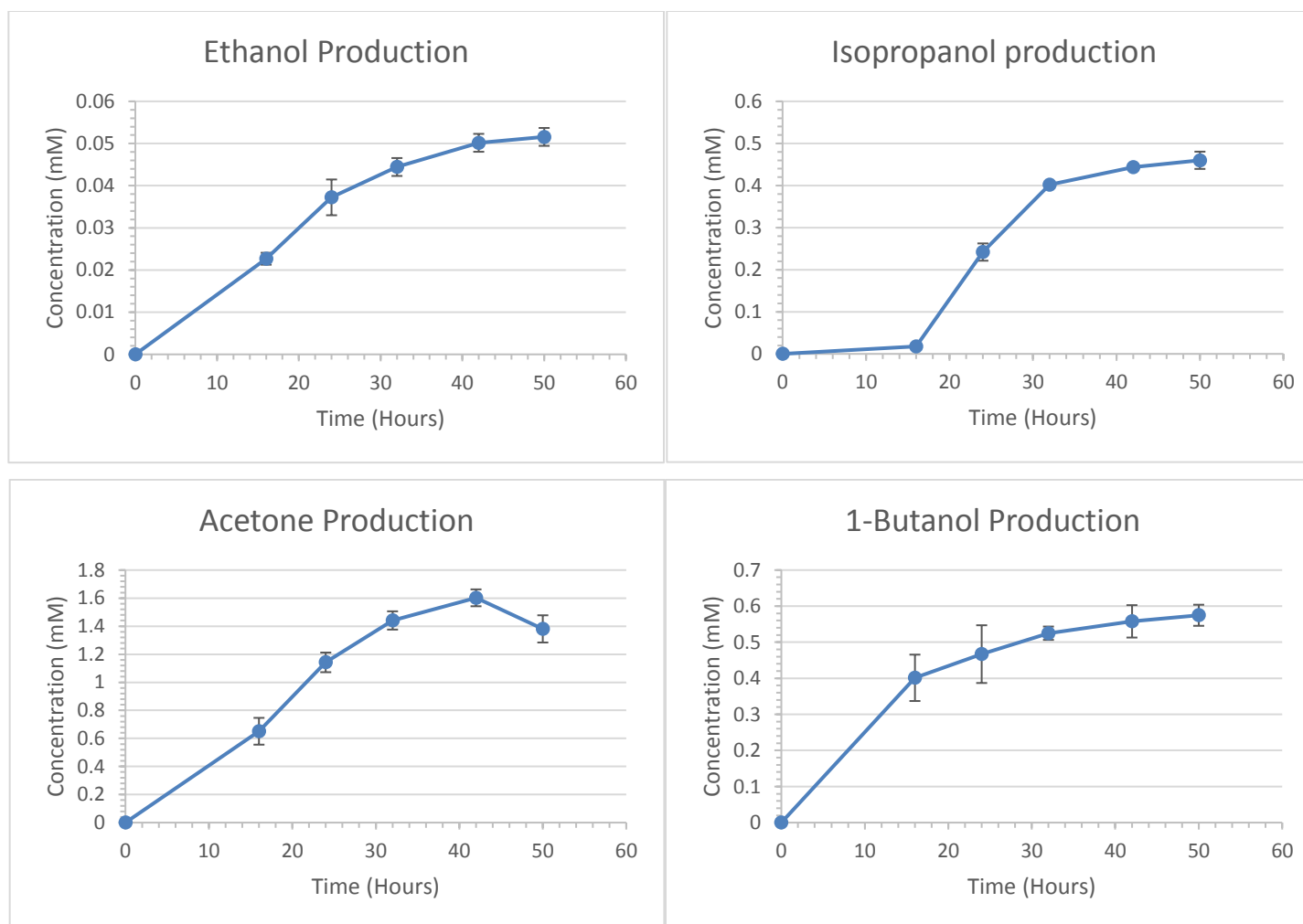


Figure 30. Solvent production by *H. butylicus* under optimal growth conditions. Cells were grown under the same composition of media and 3.0 atm of H₂ (over-pressurized). GC sample points are from two biological replicates, each an average of duplicate GC samples. Error bars shown as \pm standard deviation.

3.3.2 Solvent production in the presence of butyrate

The effect of butyrate supplemented medium on solvent production in *H. butylicus* was examined. Five- and 15-mM of butyrate were added to the medium described in Section 2.3 prior to inoculation. Production of solvents was detected using GC, and concentrations were determined using the standard curves described in Section 3.2.3. Relative to the solvent production under normal growth conditions (in the absence of butyrate), all solvents except for 1-butanol showed a similar rate of solvent production (**Fig. 31**). In the case of 1-butanol, the addition of butyrate appeared to cause a significant increase in 1-butanol production (**Fig. 31**). Solvent production in *H. butylicus* supplemented with 15 mM of butyrate resulted in the highest 1-butanol production which was approximately 6 times greater than under normal conditions. Although the addition of butyrate appeared to enhance the production of 1-butanol, the concentration of butyrate did not result in a corresponding equivalent production of 1-butanol (i.e., 5 mM butyrate does not equal an additional 5 mM production of 1-butanol) (**Fig. 31**).

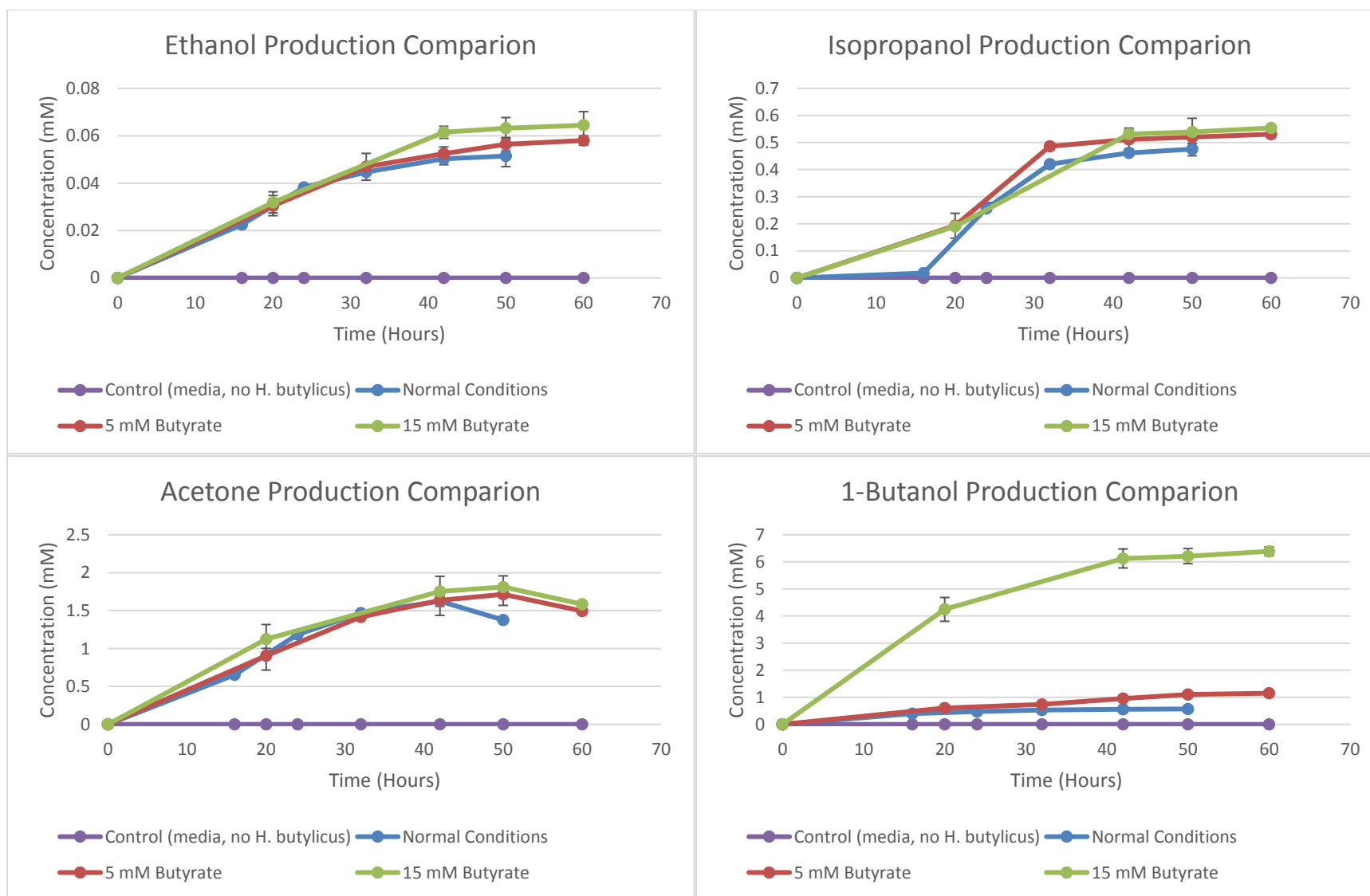


Figure 31. Comparison of solvent production by *H. butylicus* in butyrate supplemented media. Cells were grown under the same composition of media and 3.0 atm of H_2 (over-pressurized). GC sample points are from two biological replicates, each an average of duplicate GC samples. Error bars shown as \pm standard deviation.

3.3.3 Solvent production in the presence of acetate

The effect of acetate supplemented medium on solvent production in *H. butylicus* was examined. Five- and 15-mM of acetate were added into the medium described in Section 2.3 prior to inoculation. Production of solvents was detected using GC, and their concentrations was determined using the standard curves described in Section 3.2.3. Due to the less growth observed in the presence of acetate (see: **Section 3.1.3**), all solvents except ethanol showed lower production of solvents under the normal growth condition (in the absence of acetate). Similar to the addition of butyrate, the addition of acetate did not appear to result in a corresponding equivalent production of ethanol (i.e., 5 mM acetate does not equal an additional 5 mM production of ethanol) (**Fig. 32**).

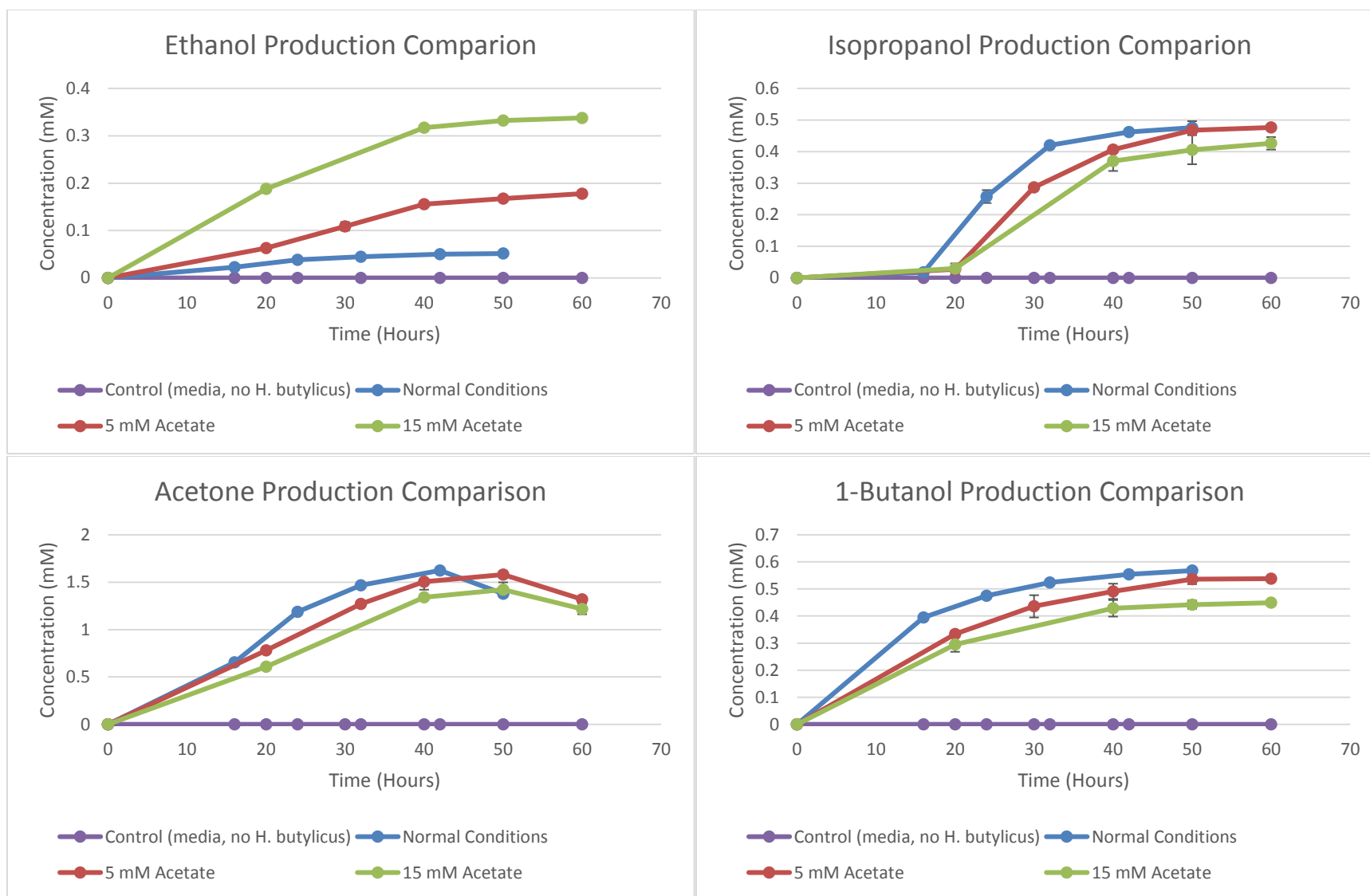


Figure 32. Comparison of solvent production by *H. butylicus* in acetate supplemented media. Cells were grown under the same composition of media and 3.0 atm of H_2 (over-pressurized). GC sample points are from two biological replicates, each an average of duplicate GC samples. Error bars shown as \pm standard deviation.

4.0 Discussion

H. butylicus is one of few hyperthermophiles capable of producing 1-butanol as a fermentation end-product. An alcohol dehydrogenase (Hbut_0414) has recently been found to be responsible for the production of 1-butanol in *H. butylicus* (Tse 2016), however, the pathway for 1-butanol production in this microorganism is unknown. Preliminary results using high performance liquid chromatography have shown acetone, ethanol, and isopropanol were produced as additional end-products in *H. butylicus* (Tse 2016), providing a basis for this study. Throughout this thesis research, solvent production of *H. butylicus* was studied to gain a more thorough understanding of the metabolism of this microorganism.

4.1 Optimal growth conditions for *H. butylicus*

H. butylicus is a hyperthermophilic archaeon that grows optimally between 95°C and 106°C (Zillig et al. 1990). It was determined in this study that a pH of 7.0 provided the highest growth (**Section 3.1.1: Fig. 13**), a maximum cell density of 2.48×10^8 cells/mL which is similar to what was reported previously (2.2×10^8 cells/mL) (Zillig et al. 1990). Growth of *H. butylicus* is reported to be stimulated by the addition of H₂ (Zillig et al. 1990). Molecular H₂ is known to be one of the most energetic substrates found in deep terrestrial subsurface environments (Libert et al. 2011). It is a common energy source for archaea and bacteria that are able to oxidize hydrogen under aerobic or anaerobic conditions, where energy is gained via the fixation of carbon when reacting with H₂ (or CO₂) (Libert et al. 2011). The supplementation of H₂ has shown to enhance growth in the bacterium *Campylobacter jejuni* through the action of a hydrogenase (Weerakoon et al. 2009). The hydrogenases in *H. butylicus* aid in the reduction of sulfur and H₂ to H₂S (Brugger et al. 2007) while concomitantly providing energy to enhance cell growth. The addition of 3.0 atm of H₂ (over-pressurized) resulted in the highest growth (**Section 3.1.1: Fig. 14**) indicating that when more H₂ is added, a higher level of growth is obtained. A H₂ pressure greater than 3.0 atm (over-pressurized) was not tested because of safety and handling concerns, however, 3.0 atm was sufficient in providing a similar maximum cell density, as previously reported. When comparing the cell densities to cultures grown under 3 psi of H₂ (over-pressurized), a 58% lower level of cell density relative to what was observed with the higher level of H₂ (**Section 3.1.1: Fig. 14**), which is similar to previous reports (Zillig et al. 1990, Tse 2016).

The addition of sulfur has also been reported to stimulate the growth of *H. butylicus* (Zillig et al. 1990), a past result which was confirmed in this study (**Section 3.1.1: Fig. 15**). A sulfur concentration of 10.0 g/L resulted in the highest amount of growth and a correlation between growth and sulfur concentration was observed (i.e., higher sulfur concentrations result in a higher cell density) (**Section 3.1.1: Fig. 15**). Previous reports used a continuous flow of H₂ (200 kpa or 1.97 atm) and a high-pressure resistant fermenter during the growth of *H. butylicus* (Zillig et al. 1990). Although no continuous flow or high-pressure fermenter was used, a similar high cell density was achieved in this study. The previous reported generation time of this microorganism was 2.5 hours in the presence of sulfur and H₂ (Zillig et al. 1990), however, a generation time of

4.4 hours was calculated in the present study. The longer generation time may be a result of deviations from the growth conditions previously reported.

Once optimal pH and the best conditions for H₂ pressure and sulfur concentration were determined, *H. butylicus* cultures were grown under the conditions reported herein, a series of replicated tests showed that these conditions were optimal for growth and were replicable. Under these conditions a cell density greater than 1.0 x 10⁸ cells/mL could be achieved, thereby enabling the further study of solvent production by *H. butylicus*.

There is some debate as to whether *H. butylicus* is capable of solvent production (Poehlein et al. 2017). A study by Zimmermann (2013) reports no butanol production was found in *H. butylicus* cultures grown in the laboratory. In the study, HPLC analysis was used to determine solvent production (Zimmermann 2013). The detection limit, however, was unclear resulting in difficulty determining the sensitivity of the method. Additionally, the growth curve produced for *H. butylicus* cultures was significantly lower (maximum of 1.0 x 10⁶ cells/mL) than that reported by Zillig et al. (1990) (maximum of 2.0 x 10⁸ cells/mL). As further discussed in Section 4.3, solvent production in *H. butylicus* appears to be strongly dependent on growth thus, non-optimal growth conditions may have attributed to a much lower production of solvents and would furthermore require a much more sensitive method for their detection. For these reasons, the conclusion that *H. butylicus* does not produce butanol, as reported by Zimmermann (2013) cannot be substantiated.

4.2 Effect of acetate and butyrate on the growth of *H. butylicus*

With cultures of *H. butylicus* reported to produce ethanol, acetone, isopropanol, and 1-butanol as fermentation end-products (Tse 2016), various concentrations of sodium butyrate and sodium acetate were added to the medium to determine their effect on the growth of *H. butylicus*.

Cultures grown in butyrate supplemented media displayed no significant differences in cell density relative to growth under optimal conditions (**Section 3.1.1: Fig. 16**). A similar test was conducted using the acetone-butanol-ethanol (ABE) producer *C. beijerinckii* NCIMB 8052 where growth was observed following the supplementation of 40 mM of butyrate into media (Wang et al. 2013). In the case of *C. beijerinckii* NCIMB 8052, the culture grew rapidly to the exponential phase compared to the culture grown in un-supplemented media where there was an obvious lag phase (Wang et al. 2013). Butyric acid (pKa = 4.91) is considered an organic waste product and reported to be the most prevalent organic waste product of anaerobic digestion by *C. beijerinckii* (Cho et al. 2019). Additionally, studies have shown that supplementing 18 mM of butyrate into culture media prevented strain degeneration (Lee et al. 2008). If *H. butylicus* is able to withstand the presence of this organic acid, this may prove beneficial for waste organic acid consumption.

Cultures grown in acetate supplemented media, however, displayed a more noticeable change. When 5 mM of sodium acetate was supplemented into *H. butylicus* media, a 43% decrease in the maximum cell density was observed compared to cultures grown under optimal conditions (**Section 3.1.2: Fig. 18**). A larger decrease was observed for cultures supplemented with 15 mM sodium acetate, where a 75% decrease in maximum cell density was observed (**Section 3.1.2: Fig. 18**). Sodium acetate has a pKa of 4.54 (Neavyn et al. 2013). The exact reason for why the cell density decreased upon the addition of acetate is unknown. A possibility for the decreased cell density is that the concentration of acetate was debilitating for the culture, however, is unlikely as the same concentration of sodium butyrate was used for the sodium acetate experiment, and the former did not have any noticeable effect on cell growth. Experimental error cannot be excluded and may be a possible reason for the decrease in growth. Culture bottles may have been contaminated with oxygen (possibly) from a leak in the manifold, improper sealing of the bottles, or other similar technical reasons that may have resulted in a decrease in growth as well. Even trace amounts of oxygen are toxic to strictly anaerobic organisms (White 2000) and

would be extremely debilitating to the cell culture. Although a few possibilities were discussed, the definitive reason for a decreased cell density from acetate addition remains unknown. Further experimentation is required to fully understand these results.

4.3 Dependency of solvent production by *H. butylicus* on growth conditions

Optimizing conditions of growth were crucial to obtaining the maximum cell growth and ultimately, maximum solvent production by *H. butylicus*. Prior to optimization, growth was variable and often non-reproducible. This was a result of inconsistencies in methodological and experimental procedures during culturing. Several issues resulted in poor growth including incorrect adjustment of pH, contamination of oxygen into culture samples, and variations in sulfur used. Although sulfur stimulates growth and is not required for growth (Zillig et al. 1990), it was surprising to find how significant the “correct” sulfur used was for the growth of *H. butylicus* in this study. Through a series of trials, precipitated sulfur from Sigma-Aldrich was the only sulfur that sufficiently stimulated growth. The exact reason for this is unknown. Once all conditions were optimized and reproducible high cell growth was achieved, solvent experiments were conducted.

Preliminary HPLC analyses found that acetone, isopropanol, and butyrate were produced by *H. butylicus* (and that their production was growth-dependent) (Tse 2016), in addition to 1-butanol and acetate (Zillig et al. 1990). The present study confirmed these results using GC analyses and additionally, detected ethanol as a fermentation end-product. Similarly, 1-butanol, acetone, and isopropanol production were dependent on cell density where an increase in cell density correspondingly resulted in an increase in solvent production. Cell density-dependent solvent production was also observed for ethanol production. A drop in acetone production was observed following the late-log phase (**Section 3.3.1: Fig. 30**). It is suspected that the reduction of acetone resulted in the production of isopropanol possibly catalyzed by an alcohol dehydrogenase, as was previously observed in *C. beijerinckii* NRRL B593 (Ismail et al. 1993). From these results, it appears that there is an inherent connection between the metabolic activities and growth of *H. butylicus*. Experimental results indicate that a deviation from the optimal conditions affects both cell growth and solvent production. In some solvent producing clostridia, solvent production is dependent upon extracellular pH and has distinct “acidogenic” (resulted in a lower pH) and “solventogenic” (resulted in a higher pH) phases (Patakova et al. 2019). Other organisms require the production of intermediates to begin solvent production indicating that optimal growth conditions (including pH) must be in place (White 2000). An example of this is in butanediol fermentation, where the production of butanediol is favored under slightly acidic conditions as

this limits the decrease in external pH caused by the synthesis of organic acids (White 2000). In one study, the cultivation pH was found to play a significant role in the production of 2,3-butanediol by the bacterial strain *Klebsiella* sp. Zmd30 and that controlling the pH at 6.0 provided optimal solvent production (Wong et al. 2014). It was also found that butanediol production was dependent on growth (Wong et al. 2014), as was observed in *H. butylicus*. To elaborate this aspect, the effect of varying growth conditions (including pH) on the metabolism of *H. butylicus* needs to be investigated through further biochemical and genetic studies.

4.4 Stimulation of *H. butylicus* solvent production in the presence of acetate and butyrate

Acetate and butyrate were previously detected as end-products of *H. butylicus* metabolism (Zillig et al. 1990; Tse 2016). The presence of these organic acids suggests the possibility of them being produced *in vivo*, which may be then converted into the corresponding alcohols (Blamey and Adams 1993; Huber et al. 1995; Nissen and Basen 2019).

Cultures of *H. butylicus* were supplemented with 5- and 15-mM concentrations of sodium butyrate and sodium acetate, respectively, to determine the effect on solvent production. In the butyrate supplemented culture, similar amounts of solvent production were observed for ethanol, acetone, and isopropanol. For production of 1-butanol, a significant increase was observed with 15 mM butyrate resulting in an approximately 167% increase (at maximum concentration) compared to cultures without any butyrate addition (**Section 3.3.2 Fig. 31**). The addition of 5 mM butyrate resulted in an approximately 67% increase (at maximum concentration) (**Section 3.3.2 Fig. 31**). This is an indication that *H. butylicus* may possess mechanisms to allow for the reduction of butyrate to produce 1-butanol. There is a possibility that an aldehyde:oxidoreductase (AOR) is responsible for this conversion, as was observed in *C. beijerinckii* NCIMB 8052 and *P. furiosus* (Wang et al. 2013; Basen et al. 2014) (see: **Section 1.2.3**).

In the acetate supplemented culture, similar levels of production of acetone, isopropanol, and 1-butanol were observed. The production of ethanol however, showed a significant increase from the addition of acetate addition (**Section 3.3.3 Fig. 32**). The addition of 5 mM acetate resulted in an approximately 111% increase in ethanol production while addition of 15 mM acetate resulted in an approximately 148% increase addition (**Section 3.3.3 Fig. 32**). Similar to what was observed in the butyrate supplemented culture, the reduction of acetate to ethanol may have been catalyzed by an AOR (or an AOR-like) enzyme in *H. butylicus*. In this instance, solvent production appeared to start later and reach maximum concentration later than what was observed in cultures grown without acetate, which may be related to the decreased growth rate observed in acetate supplemented cultures.

To explore this possibility, potential homolog genes for AOR were searched for in the *H. butylicus* genome. Four AOR proteins were found in the *P. furiosus* genome and run against the

H. butylicus genome (**Table 10**). The highest AOR identity was found in the Hbut_0737 gene (48.54%), which was identified to be an “aldehyde ferredoxin oxidoreductase family protein”. Although this gene has not been characterized, there is potential for this AOR to play a key role in organic acid conversions in *H. butylicus*.

Table 10. Potential *P. furiosus* AOR homologs in *H. butylicus*

Protein in <i>P. furiosus</i> (Accession number)	Protein in <i>H. butylicus</i> (Accession number)	<i>H. butylicus</i> gene	Percent Identity
Tungsten-containing aldehyde ferredoxin oxidoreductases (Q51739.1)	Aldehyde ferredoxin oxidoreductase family protein (WP_011822166.1)	Hbut_0737	48.54
	Aldehyde ferredoxin oxidoreductase family protein (WP_011822692.1)	Hbut_1553	35.24
	Aldehyde ferredoxin oxidoreductase family protein (WP_011821541.1)	Hbut_0351	34.15
	Aldehyde ferredoxin oxidoreductase family protein (WP_110138747.1)	Hbut_1001	34.82
Aldehyde:ferredoxin oxidoreductase (CAA56170.1)	Aldehyde ferredoxin oxidoreductase family protein (WP_011822166.1)	Hbut_0737	48.54
	Aldehyde ferredoxin oxidoreductase family protein (WP_011822692.1)	Hbut_1553	35.24
	Aldehyde ferredoxin oxidoreductase family protein (WP_011821541.1)	Hbut_0351	34.15
	Aldehyde ferredoxin oxidoreductase family protein (WP_110138747.1)	Hbut_1001	34.82
Aldehyde:ferredoxin oxidoreductase (aor) (AAL80470.1)	Aldehyde ferredoxin oxidoreductase family protein (WP_011822166.1)	Hbut_0737	48.54
	Aldehyde ferredoxin oxidoreductase family protein (WP_011822692.1)	Hbut_1553	35.24
	Aldehyde ferredoxin oxidoreductase family protein (WP_011821541.1)	Hbut_0351	34.15
	Aldehyde ferredoxin oxidoreductase family protein (WP_110138747.1)	Hbut_1001	34.82
Tungsten-containing glyceraldehyde-3- phosphate ferredoxin oxidoreductase (Q8U3K2.1)	Aldehyde ferredoxin oxidoreductase family protein (WP_110138747.1)	Hbut_1001	25.17
	Aldehyde ferredoxin oxidoreductase family protein (WP_011822692.1)	Hbut_1553	25.18
	Aldehyde ferredoxin oxidoreductase family protein (WP_011821541.1)	Hbut_0351	23.90
	Aldehyde ferredoxin oxidoreductase family protein (WP_011822166.1)	Hbut_0737	23.16

Low concentrations of acetate and butyrate have previously been reported in *H. butylicus* (Zillig et al. 1990; Tse 2016), suggesting a possible mechanism may exist for butyrate and acetate conversion in the organism. This pathway may look similar to the pathway proposed by Nissen and Basen (2019) involving and AOR and ADH (**Section 1.2.3: Fig. 5**).

4.5 Proposed pathways and key enzymes involved in solvent production by *H. butylicus*

The vast majority of the butanol production pathway (and enzymes involved) in *H. butylicus* currently remains unknown. In efforts to better understanding this hyperthermophile's metabolism, different pathways for solvent production were explored.

With end-products of *H. butylicus* bearing similarity to those of *C. beijerinckii* (formerly called “*C. butylicum*” and also the reason why the organism was named “*Hyperthermus butylicus*”) (Zillig et al. 1990), it is speculated that there may be a link between the two microorganisms. A search of the genomes of *C. acetobutylicum* ATCC 824 and *H. butylicus*, however, showed no significant homologs for the key enzymes of butanol production (butyryl-CoA dehydrogenase, β -hydroxybutyryl-CoA dehydrogenase, acetoacetyl-Co:acetate:CoA-transferase, acetoacetyl-CoA:butyrate:CoA transferase, and butyraldehyde dehydrogenase). Being from two separate domains, it is not surprising that no homologs were found between *C. acetobutylicum* ATCC 824 and *H. butylicus*. Nevertheless, this is an indication that a novel pathway or enzymes with catalytic functions, but with no or very low sequence similarity for 1-butanol production, is present in *H. butylicus*, warranting further investigation.

Potential enzymes for solvent production in *H. butylicus* were searched using HMMs (Hidden Markov Model) (**Appendix A: Gene Sequence Analysis**). HMM searching summarizes functional information using whole families of proteins as profiles, rather than single queries through BLAST sequence searching. HMM searches against profiles of key enzymes for butanol production in *C. acetobutylicum* ATCC 824, *S. cerevisiae* S288c, and *E. coli* BW25113 (as previously discussed in the Introduction: **Section 1.2.1 – 1.24**) were performed. From the search, percent identity hits (< 60%) were the following: pyruvate:ferredoxin oxidoreductase, acetyl-CoA acetyltransferase, beta-hydroxybutyryl-CoA dehydrogenase, butyraldehyde dehydrogenase, butanol dehydrogenase, 2-isopropylmalate dehydrogenase, 2-ketoacid decarboxylase, glycine oxidase, and pyruvate decarboxylase.

The key enzymes for ABE production in *C. acetobutylicum* ATCC 824, acetoacetyl-CoA:acetate-CoA-transferase and acetoacetyl-CoA:butyrate-CoA-transferase, did not show any significant similarity from the search suggesting that there may be an alternative pathway for

production. The experimental data showed a corresponding increase in ethanol and 1-butanol from the addition of acetate and butyrate thus, it is possible that an AOR-like enzyme is present in *H. butylicus*. The function of AORs in hyperthermophiles is thought to catalyze the reversible oxidation of aldehydes (Basen et al. 2014). The possibility of the enzyme catalyzing the conversion of organic acids to their corresponding aldehyde was previously discussed and demonstrated *in vivo* (Heider et al. 1994; Keller et al. 2017). *H. butylicus* utilizes peptides as a growth substrate (Zillig et al. 1990) indicating the possibility of the keto-acid pathway (found in *S. cerevisiae*) to be present. The pathway involves a pyruvate decarboxylase (PDC), which is essential for the biosynthesis of amino acids to butanol. There is also a possibility of a bifunctional enzyme with both PDC and POR activities present, which may concomitantly catalyze the production of pyruvate to acetaldehyde and acetyl-CoA, respectively (Eram et al. 2014). In combination with research from other butanol producing microorganisms and the data obtained from this study, a hypothetical pathway for solvent production in *H. butylicus* was proposed (**Fig. 33**). Currently, no definite conclusion regarding the pathway for solvent production in *H. butylicus* can be made. However, the potential involvement of an AOR-like enzyme for the conversion of organic acids has been proposed from this study.

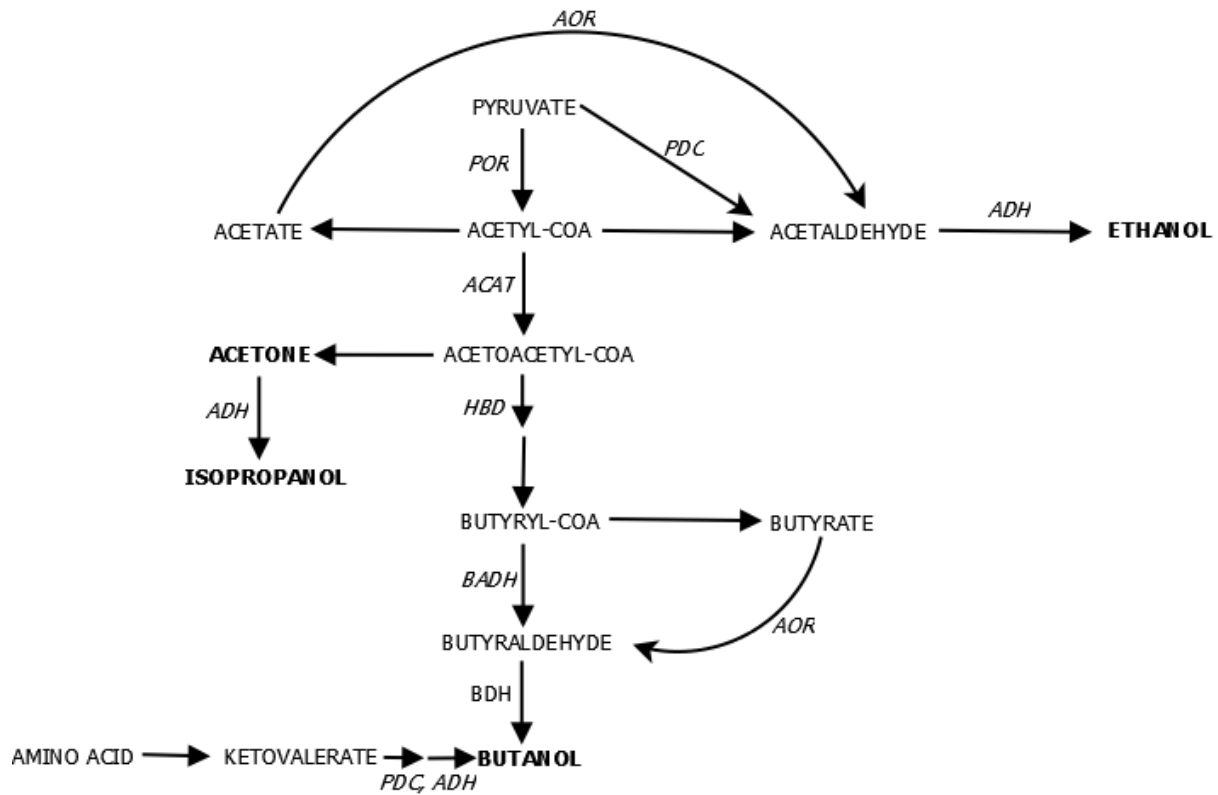


Figure 33. Proposed pathway for solvent production in *H. butylicus*. Detected solvents are indicated in bold (ethanol, acetone, isopropanol, 1-butanol). Italicized enzymes are potentially present (AOR: aldehyde:oxidoreductase; POR: pyruvate:ferredoxin oxidoreductase; PDC: pyruvate decarboxylase; ADH: alcohol dehydrogenase; ACAT: acetyl-CoA acetyltransferase/Thiolase; HBD: beta-hydroxybutyryl-CoA dehydrogenase; BADH: butyraldehyde dehydrogenase; BDH: butanol dehydrogenase); (Adapted from Garcia et al. 2011; Branduardi et al. 2013; Al-Shorgani et al. 2012; Nissen and Basen 2019).

4.6 Conclusions

The aims of this study were to broaden the understanding of the metabolism of *H. butylicus*, and to also contribute to the ongoing efforts in finding an alternative renewable energy source to replace petroleum-based sources. From this study the following conclusions were made:

- 1) Conditions of growth including pH, concentration of sulfur, and H₂ pressure were optimized for *H. butylicus*. Optimal growth conditions were found to be the following: pH 7.0, 10.0 g/L of sulfur, 3.0 atm of H₂.
- 2) 2) Production of acetone, ethanol, isopropanol, and 1-butanol by *H. butylicus* was confirmed using GC analysis. Solvent production was growth-dependent, sharing significant similarity to that in clostridial species, however, no significant homologs for the key enzymes of butanol production were found. This suggests an alternative pathway for solvent production in *H. butylicus* is likely present.
- 3) The addition of organic acids such as sodium acetate and sodium butyrate to the culture media significantly stimulated the production of ethanol and 1-butanol, respectively.
- 4) In combination with existing butanol production pathways and experimental results from this study, potential pathways for *H. butylicus* were proposed. Due to the similarity in end-products to clostridial species, an alternative ABE pathway may be present. Without any significant homologs for acetoacetyl-CoA:acetate-CoA-transferase and acetoacetyl-CoA:butyrate-CoA-transferase present in *H. butylicus*, novel enzymes and/or pathways are likely present. *H. butylicus* utilizing peptides as a growth substrate brings the possibility for the keto-acid pathway to be present involving a PDC-like enzyme, which is essential for the production of 1-butanol from 2-ketovalerate. Lastly, *H. butylicus* possess the ability to utilize the organic acids acetate and butyrate to increase the production of ethanol and 1-butanol, respectively, suggesting a butyraldehyde dehydrogenase and/or an AOR/ADH pathway may be present.

4.7 Future Prospects

The confirmation of solvent production by *H. butylicus* provides a foundation to further explore its metabolic features. The proposed pathways are of significant interest in future research. A few possible areas can be considered for future studies:

- 1) Biochemical determination of key enzymes in various pathways and/or further genome sequencing analysis. As only solvent production was studied in this thesis, biochemical experimentation (measuring catalytic activity from cell-free extract of *H. butylicus*) is required to determine which enzymes are present to be further tested for purification and characterization. From bioinformatic analyses, several predicted enzymes have the potential to be involved in *H. butylicus*' solvent production: pyruvate:ferredoxin oxidoreductase, acetyl-CoA acetyltransferase, beta-hydroxybutyryl-CoA dehydrogenase, butyraldehyde dehydrogenase, butanol dehydrogenase, 2-isopropylmalate dehydrogenase, 2-ketoacid decarboxylase, glycine oxidase, and pyruvate decarboxylase.
- 2) Quantify acetate and butyrate concentration consumed and remaining following supplementation at varying concentrations. From the experimental results, it was determined that the amount of organic acid supplied did not equate to the amount consumed by *H. butylicus*. In this respect, quantifying the amount of organic acid consumed will support the solvent production data. Using GC or HPLC analysis, the extracellular concentration of acetate and butyrate could be detected to determine the amount remaining in the media (unconsumed concentration) then further, the amount consumed by the organism.
- 3) Exploring pH dependency of solvent production with and without the addition of organic acids to verify if there might be “acidogenic” and “solventogenic” phases present in *H. butylicus*.

References

- Abdehagh, N., Tezel, F. H., & Thibault, J. (2014). Separation techniques in butanol production: challenges and developments. *Biomass and Bioenergy*, 60, 222-246.
- Al-Shorgani, N. K. N., Ali, E., Kalil, M. S., & Yusoff, W. M. W. (2012). Bioconversion of butyric acid to butanol by *Clostridium saccharoperbutylacetonicum* N1-4 (ATCC 13564) in a limited nutrient medium. *BioEnergy Research*, 5(2), 287-293.
- Anitha, P.M., Selvam, D.P., & Sadiku, R.E. (2020). Biobutanol: A Promising Alternative Commercial Biofuel. *Handbook of Nanomaterials and Nanocomposites for Energy and Environmental Applications*, 1-19.
- Atalah, J., Cáceres-Moreno, P., Espina, G., & Blamey, J. M. (2019). Thermophiles and the applications of their enzymes as new biocatalysts. *Bioresource Technology*, 280, 478-488.
- Atsumi, S., Cann, A. F., Connor, M. R., Shen, C. R., Smith, K. M., Brynildsen, M. P., Chou, K.J.Y., Hnai, T., & Liao, J.C. (2008). Metabolic engineering of *Escherichia coli* for 1-butanol production. *Metabolic Engineering*, 10(6), 305-311.
- Azhar, S. H. M., Abdulla, R., Jambo, S. A., Marbawi, H., Gansau, J. A., Faik, A. A. M., & Rodrigues, K. F. (2017). Yeasts in sustainable bioethanol production: A review. *Biochemistry and Biophysics Reports*, 10, 52-61.
- Bai, F. W., Anderson, W. A., & Moo-Young, M. (2008). Ethanol fermentation technologies from sugar and starch feedstocks. *Biotechnology Advances*, 26(1), 89-105.
- Balch, W.E., Fox, G.E., Magrum, L.J., Woese, C.R., Wolfe, R.S. (1979). *Methanogens*: reevaluation of a unique biological group. *Microbiological reviews* 43(2): 260.
- Basen, M., Schut, G. J., Nguyen, D. M., Lipscomb, G. L., Benn, R. A., Prybol, C. J., Vaccaro, B.J., Poole, F.L., Kelly, R.M., & Adams, M. W. (2014). Single gene insertion drives bioalcohol production by a thermophilic archaeon. *Proceedings of the National Academy of Sciences*, 111(49), 17618-17623.
- Blamey, J. M., & Adams, M. W. (1993). Purification and characterization of pyruvate ferredoxin oxidoreductase from the hyperthermophilic archaeon *Pyrococcus furiosus*. *Biochimica et Biophysica Acta (BBA)-Protein Structure and Molecular Enzymology*, 1161(1), 19-27.
- Branduardi, P., Longo, V., Berterame, N. M., Rossi, G., & Porro, D. (2013). A novel pathway to produce butanol and isobutanol in *Saccharomyces cerevisiae*. *Biotechnology for Biofuels*, 6(1), 1-12.

Chen, C. K., & Blaschek, H. P. (1999). Effect of acetate on molecular and physiological aspects of *Clostridium beijerinckii* NCIMB 8052 solvent production and strain degeneration. *Applied and environmental microbiology*, 65(2), 499-505.

Chen, X., Schreiber, K., Appel, J., Makowka, A., Fähnrich, B., Roettger, M., et al. (2016). The Entner–Doudoroff pathway is an overlooked glycolytic route in cyanobacteria and plants. *Proceedings of the National Academy of Sciences*, 113(19), 5441-5446.

Cho, S. H., Kim, J., Han, J., Lee, D., Kim, H. J., Kim, Y. T., Cheng, X., Xu, Y., Lee, J.C., & Kwon, E. E. (2019). Bioalcohol production from acidogenic products via a two-step process: A case study of butyric acid to butanol. *Applied Energy*, 252, 113482.

Christensen, H. N. (1990). Role of amino acid transport and countertransport in nutrition and metabolism. *Physiological Reviews*, 70(1), 43-77.

Conway, T. (1992). The entner-doudoroff pathway: History, physiology and molecular biology. *FEMS Microbiology Reviews*, 9(1), 1-27.

de Miguel Bouzas, T., Barros-Velázquez, J., & Gonzalez Villa, T. (2006). Industrial applications of hyperthermophilic enzymes: a review. *Protein and peptide letters*, 13(7), 645-651.

Deutsche Sammlung von Mikroorganismen und Zellkulturen, Germany,
https://www.dsmz.de/microorganisms/medium/pdf/DSMZ_Medium491.pdf

Doran-Peterson, J., Cook, D. M., & Brandon, S. K. (2008). Microbial conversion of sugars from plant biomass to lactic acid or ethanol. *The Plant Journal*, 54(4), 582-592.

Dumorne, K., Cordova, D. C., Astorga-Elo, M., & Renganathan, P. (2017). Extremozymes: a potential source for industrial applications. *Journal of Microbiology and Biotechnology*, 27(4): 649-659.

Durre, P. (1998). New insights and novel developments in clostridial acetone/butanol/isopropanol fermentation. *Applied Microbiology and Biotechnology*, 49(6), 639-648.

Durre, P. (2007). Biobutanol: An attractive biofuel. *Biotechnology Journal: Healthcare Nutrition Technology*, 2(12), 1525-1534.

Ebaid, R., Wang, H., Sha, C., Abomohra, A. E. F., & Shao, W. (2019). Recent trends in hyperthermophilic enzymes production and future perspectives for biofuel industry: A critical review. *Journal of Cleaner Production*, 238, 117925.

Eram, M. S., Oduaran, E., & Ma, K. (2014). The bifunctional pyruvate decarboxylase/pyruvate ferredoxin oxidoreductase from *Thermococcus guaymasensis*. *Archaea*, 2014.

- Fraisse, L., & Simon, H. (1988). Observations on the reduction of non-activated carboxylates by *Clostridium formicoaceticum* with carbon monoxide or formate and the influence of various viologens. *Archives of microbiology*, 150(4), 381-386.
- Garcia, V., Pääkkilä, J., Ojamo, H., Muurinen, E., & Keiski, R. L. (2011). Challenges in biobutanol production: How to improve the efficiency? *Renewable and Sustainable Energy Reviews*, 15(2), 964-980.
- Garcia-Granados, R., Lerma-Escalera, J. A., & Morones-Ramírez, J. R. (2019). Metabolic engineering and synthetic biology: Synergies, future, and challenges. *Frontiers in Bioengineering and Biotechnology*, 7, 36.
- Gheshlaghi, R., Scharer, J. M., Moo-Young, M., & Chou, C. P. (2009). Metabolic pathways of clostridia for producing butanol. *Biotechnology Advances*, 27(6), 764-781.
- Gonzalez-Ramos, D., van den Broek, M., van Maris, A. J., Pronk, J. T., & Daran, J. G. (2013). Genome-scale analyses of butanol tolerance in *saccharomyces cerevisiae* reveal an essential role of protein degradation. *Biotechnology for Biofuels*, 6(1), 48.
- Guo, M., Song, W., & Buhain, J. (2015). Bioenergy and biofuels: History, status, and perspective. *Renewable and Sustainable Energy Reviews*, 42, 712-725.
- Heider, J., Ma, K., & Adams, M. W. (1995). Purification, characterization, and metabolic function of tungsten-containing aldehyde ferredoxin oxidoreductase from the hyperthermophilic and proteolytic archaeon *Thermococcus* strain ES-1. *Journal of Bacteriology*, 177(16), 4757-4764.
- Hoelzle, R. D., Viridis, B., & Batstone, D. J. (2014). Regulation mechanisms in mixed and pure culture microbial fermentation. *Biotechnology and bioengineering*, 111(11), 2139-2154.
- Huber, R., Burggraf, S., Mayer, T., Barns, S. M., Rossnagel, P., & Stetter, K. O. (1995). Isolation of a hyperthermophilic archaeum predicted by in situ RNA analysis. *Nature*, 376(6535), 57-58.
- Huber, C., Skopan, H., Feicht, R., White, H., & Simon, H. (1995). Pterin cofactor, substrate specificity, and observations on the kinetics of the reversible tungsten-containing aldehyde oxidoreductase from *Clostridium thermoaceticum*. *Archives of microbiology*, 164(2), 110-118.
- Ismail, A. A., Zhu, C. X., Colby, G. D., & Chen, J. S. (1993). Purification and characterization of a primary-secondary alcohol dehydrogenase from two strains of *Clostridium beijerinckii*. *Journal of bacteriology*, 175(16), 5097-5105.

- Isom, C. E., Nanny, M. A., & Tanner, R. S. (2015). Improved conversion efficiencies for n-fatty acid reduction to primary alcohols by the solventogenic acetogen “*Clostridium ragsdalei*”. *Journal of Industrial Microbiology and Biotechnology*, 42(1), 29-38.
- Jambunathan, P., & Zhang, K. (2014). Novel pathways and products from 2-keto acids. *Current opinion in biotechnology*, 29, 1-7.
- Jin, C., Yao, M., Liu, H., Chia-fon, F. L., & Ji, J. (2011). Progress in the production and application of n-butanol as a biofuel. *Renewable and Sustainable Energy Reviews*, 15(8), 4080-4106.
- Jones, D. T., & Woods, D. R. (1986). Acetone-butanol fermentation revisited. *Microbiological Reviews*, 50(4), 484.
- Karimi, S., Karri, R. R., Yarak, M. T., & Koduru, J. R. (2021). Processes and separation technologies for the production of fuel-grade bioethanol: a review. *Environmental Chemistry Letters*, 1-18.
- Kashket, E. R., & Cao, Z. Y. (1995). Clostridial strain degeneration. *FEMS microbiology reviews*, 17(3), 307-315.
- Keller, M. W., Lipscomb, G. L., Nguyen, D. M., Crowley, A. T., Schut, G. J., Scott, I., Kelly, R.M., & Adams, M. W. (2017). Ethanol production by the hyperthermophilic archaeon *Pyrococcus furiosus* by expression of bacterial bifunctional alcohol dehydrogenases. *Microbial biotechnology*, 10(6), 1535-1545.
- Kinoshita, S., Udaka, S., & Shimono, M. (1957). Studies on the amino acid fermentation. *The Journal of General and Applied Microbiology*, 3(3), 193-205.
- Knoshaug, E. P., & Zhang, M. (2009). Butanol tolerance in a selection of microorganisms. *Applied Biochemistry and Biotechnology*, 153(1-3), 13-20.
- Koffas, M., Roberge, C., Lee, K., & Stephanopoulos, G. (1999). Metabolic engineering. *Annual Review of Biomedical Engineering*, 1(1), 535-557.
- Lee, S. M., Cho, M. O., Park, C. H., Chung, Y. C., Kim, J. H., Sang, B. I., & Um, Y. (2008). Continuous butanol production using suspended and immobilized *Clostridium beijerinckii* NCIMB 8052 with supplementary butyrate. *Energy & fuels*, 22(5), 3459-3464.
- Lee, S. Y., Park, J. H., Jang, S. H., Nielsen, L. K., Kim, J., & Jung, K. S. (2008). Fermentative butanol production by clostridia. *Biotechnology and Bioengineering*, 101(2), 209-228.

- Liu, X., Gu, Q., Yu, X., & Luo, W. (2012). Enhancement of butanol tolerance and butanol yield in clostridium acetobutylicum mutant NT642 obtained by nitrogen ion beam implantation. *Journal of Microbiology*, 50(6), 1024-1028.
- Ma, K., Loessner, H., Heider, J., Johnson, M. K., & Adams, M. W. (1995). Effects of elemental sulfur on the metabolism of the deep-sea hyperthermophilic archaeon thermococcus strain ES-1: Characterization of a sulfur-regulated, non-heme iron alcohol dehydrogenase. *Journal of Bacteriology*, 177(16), 4748-4756.
- McGovern, P. E., Zhang, J., Tang, J., Zhang, Z., Hall, G. R., Moreau, R. A., et al. (2004). Fermented beverages of pre-and proto-historic china. *Proceedings of the National Academy of Sciences*, 101(51), 17593-17598.
- Mielenz, J. R., Bardsley, J. S., & Wyman, C. E. (2009). Fermentation of soybean hulls to ethanol while preserving protein value. *Bioresource Technology*, 100(14), 3532-3539.
- Mukund, S., & Adams, M.W. (1991). The novel tungsten-iron-sulfur protein of the hyperthermophilic archaeobacterium, *Pyrococcus furiosus*, is an aldehyde ferredoxin oxidoreductase. Evidence for its participation in a unique glycolytic pathway. *Journal of Biological Chemistry*, 266(22), 14208-14216.
- Ndaba, B., Chiyanzu, I., & Marx, S. (2015). N-butanol derived from biochemical and chemical routes: A review. *Biotechnology Reports*, 8, 1-9.
- Neavyn, M. J., Boyer, E. W., Bird, S. B., & Babu, K. M. (2013). Sodium acetate as a replacement for sodium bicarbonate in medical toxicology: a review. *Journal of Medical Toxicology*, 9(3), 250-254.
- Nigam, P. S., & Singh, A. (2011). Production of liquid biofuels from renewable resources. *Progress in Energy and Combustion Science*, 37(1), 52-68.
- Nissen, L.S., & Basen, M. (2019). The emerging role of aldehyde:ferredoxin oxidoreductases in microbially-catalyzed alcohol production. *Journal of biotechnology*, 306, 105-117.
- Obergruber, M., Hönig, V., Procházka, P., Kučerová, V., Kotek, M., Bouček, J., & Mařík, J. (2021). Physicochemical Properties of Biobutanol as an Advanced Biofuel. *Materials*, 14(4), 914.
- Olson, D.G., Sparling, R., & Lynd, L.R. (2015). Ethanol production by engineered thermophiles. *Current Opinion in Biotechnology*, 33, 130-141.
- Pan, M., Tong, C., Qian, W., Lu, F., Yin, J., & Huang, H. (2020). The effect of butanol isomers on diesel engine performance, emission and combustion characteristics under different load conditions. *Fuel*, 277, 118188.

Patakova, P., Branska, B., Sedlar, K., Vasylykivska, M., Jureckova, K., Kolek, J., Koscova, P., & Provaznik, I. (2019). Acidogenesis, solventogenesis, metabolic stress response and life cycle changes in *Clostridium beijerinckii* NRRL B-598 at the transcriptomic level. *Scientific reports*, 9(1), 1-21.

Pley, U., Schipka, J., Gambacorta, A., Jannasch, H. W., Fricke, H., Rachel, R., & Stetter, K.O. (1991). *Pyrodictium abyssi* sp. nov. represents a novel heterotrophic marine archaeal hyperthermophile growing at 110 C. *Systematic and Applied Microbiology*, 14(3), 245-253.

Poehlein, A., Solano, J. D. M., Flitsch, S. K., Krabben, P., Winzer, K., Reid, S. J., Jones, D.T., Green, E., Minton, N.P., Daniel, R., & Dürre, P. (2017). Microbial solvent formation revisited by comparative genome analysis. *Biotechnology for biofuels*, 10(1), 58.

Pugazhendhi, A., Mathimani, T., Varjani, S., Rene, E.R., Kumar, G., Kim, S.H., Ponnusamy, V.K., & Yoon, J.J. (2019). Biobutanol as a promising liquid fuel for the future-recent updates and perspectives. *Fuel*, 253, pp.637-646.

Ranjan, A., & Moholkar, V. S. (2012). Biobutanol: Science, engineering, and economics. *International Journal of Energy Research*, 36(3), 277-323.

Serrano-Ruiz, J. C., Ramos-Fernández, E. V., & Sepúlveda-Escribano, A. (2012). From biodiesel and bioethanol to liquid hydrocarbon fuels: new hydrotreating and advanced microbial technologies. *Energy & Environmental Science*, 5(2), 5638-5652.

Sarathy, S. M., Vranckx, S., Yasunaga, K., Mehl, M., Oßwald, P., Metcalfe, W. K., et al. (2012). A comprehensive chemical kinetic combustion model for the four butanol isomers. *Combustion and Flame*, 159(6), 2028-2055.

Sarmiento, F., Peralta, R., & Blamey, J. M. (2015). Cold and hot extremozymes: Industrial relevance and current trends. *Frontiers in Bioengineering and Biotechnology*, 3, 148.

Si, T., Luo, Y., Xiao, H., & Zhao, H. (2014). Utilizing an endogenous pathway for 1-butanol production in *Saccharomyces cerevisiae*. *Metabolic engineering*, 22, 60-68.

Solomon, K., & Voigt, M. (1986). Bread and beer: The early use of cereals in human diet. *Expedition*, 28(2), 23-34.

Stetter, K. O. (2006). Hyperthermophiles in the history of life. *Philosophical Transactions of the Royal Society B: Biological Sciences*, 361(1474), 1837-1843.

Strobl, G., Feicht, R., White, H., Lottspeich, F., & Simon, H. (1992). The tungsten-containing aldehyde oxidoreductase from *Clostridium thermoaceticum* and its complex with a viologen-accepting NADPH oxidoreductase.

- Swidah, R., Ogunlabi, O., Grant, C. M., & Ashe, M. P. (2018). N-butanol production in *S. cerevisiae*: Co-ordinate use of endogenous and exogenous pathways. *Applied Microbiology and Biotechnology*, 102(22), 9857-9866.
- Tan, K. T., Lee, K. T., & Mohamed, A. R. (2008). Role of energy policy in renewable energy accomplishment: The case of second-generation bioethanol. *Energy Policy*, 36(9), 3360-3365.
- Tanno, K., & Willcox, G. (2012). Distinguishing wild and domestic wheat and barley spikelets from early holocene sites in the near east. *Vegetation History and Archaeobotany*, 21(2), 107-115.
- Tse, Ching. (2016). Characterization of Alcohol Dehydrogenases from *Hyperthermus butylicus*. MSc. Thesis, Department of Biology, University of Waterloo.
- Tse, C, Ibrahim, N.E., & Ma, K. (2017). Characterization of Alcohol Dehydrogenases from *Hyperthermus butylicus*. *Journal of Microbiology and Biochemistry*, 2(1), 1-12.
- Unsworth, L. D., van der Oost, J., & Koutsopoulos, S. (2007). Hyperthermophilic enzymes – stability, activity, and implementation strategies for high temperature applications. *The FEBS Journal*, 274(16), 4044-4056.
- Varol, Y., Oner, C., Oztop, H. F., & Altun, S. (2014). Comparison of methanol, ethanol, or n-butanol blending with unleaded gasoline on exhaust emissions of an SI engine. *Energy Sources, Part A: Recovery, Utilization, and Environmental Effects*, 36(9), 938-948.
- van Wolferen, M., Ajon, M., Driessen, A. J., & Albers, S. V. (2013). How hyperthermophiles adapt to change their lives: DNA exchange in extreme conditions. *Extremophiles*, 17(4), 545-563.
- Vieille, C., & Zeikus, G. J. (2001). Hyperthermophilic enzymes: Sources, uses, and molecular mechanisms for thermostability. *Microbiology and Molecular Biology Reviews*, 65(1), 1-43.
- Wagner, M., Roger, A. J., Flax, J. L., Brusseau, G. A., & Stahl, D. A. (1998). Phylogeny of dissimilatory sulfite reductases supports an early origin of sulfate respiration. *Journal of Bacteriology*, 180(11), 2975-2982.
- Wang, S., Dong, S., Wang, P., Tao, Y., & Wang, Y. (2017). Genome editing in *Clostridium saccharoperbutylacetonicum* N1-4 with the CRISPR-Cas9 system. *Applied and Environmental Microbiology*, 83(10), 1-16.
- Wang, Y., Ho, S. H., Yen, H. W., Nagarajan, D., Ren, N. Q., Li, S., Hu, S., Lee, D.J., Kondo, A., & Chang, J. S. (2017). Current advances on fermentative biobutanol production using third generation feedstock. *Biotechnology advances*, 35(8), 1049-1059.

Wang, Y., Van Le, Q., Yang, H., Lam, S. S., Yang, Y., Gu, H., Sonne, C., & Peng, W. (2021). Progress in microbial biomass conversion into green energy. *Chemosphere*, 130835.

Weerakoon, D. R., Borden, N. J., Goodson, C. M., Grimes, J., & Olson, J. W. (2009). The role of respiratory donor enzymes in *Campylobacter jejuni* host colonization and physiology. *Microbial pathogenesis*, 47(1), 8-15.

White, D. (2000). *Physiology and biochemistry of prokaryotes*. Oxford University Press.

White, H., Strobl, G., Feicht, R., & Simon, H. (1989). Carboxylic acid reductase: a new tungsten enzyme catalyses the reduction of non-activated carboxylic acids to aldehydes. *European journal of biochemistry*, 184(1), 89-96.

Wolfe, A. J. (2015). Glycolysis for the microbiome generation. *Microbiology Spectrum*, 3(3), 1-20.

Wong, C. L., Yen, H. W., Lin, C. L., & Chang, J. S. (2014). Effects of pH and fermentation strategies on 2, 3-butanediol production with an isolated *Klebsiella* sp. Zmd30 strain. *Bioresource technology*, 152, 169-176.

Wu, P., Wang, G., Wang, G., Børresen, B. T., Liu, H., & Zhang, J. (2016). Butanol production under microaerobic conditions with a symbiotic system of *Clostridium acetobutylicum* and *Bacillus cereus*. *Microbial Cell Factories*, 15(1), 1-11.

Xia, J., Yang, Y., Liu, C., Yang, S., & Bai, F. (2019). Engineering *Zymomonas mobilis* for robust cellulosic ethanol production. *Trends in Biotechnology*, 37(9), 960-972.

Zillig, W., Holz, I., Janekovic, D., Klenk, H. P., Imself, E., Trent, J., et al. (1990). *Hyperthermus butylicus*, a hyperthermophilic sulfur-reducing archaeobacterium that ferments peptides. *Journal of Bacteriology*, 172(7), 3959-3965.

Zimmermann, T. (2013). *Untersuchungen zur Butanolbildung von Hyperthermus butylicus und Clostridium acetobutylicum* (Doctoral dissertation, Universität Ulm).

Appendix A

Gene Sequence Analysis

Potential homologs of genes in *H. butylicus* encoding key enzymes involved in butanol production in *C. acetobutylicum* ATCC 824.

Target enzyme	Key Enzyme for butanol production in <i>C. acetobutylicum</i> ATCC 824 (locus tag)	Potential homologous gene in <i>H. butylicus</i> DSM 5456 (old locus tag)	E-value	Percent identity (%)
Pyruvate:ferredoxin oxireductase	CA_C2499	Hbut_0730	8e-38	28.03
Acetyl-CoA acetyltransferase	CA_C2873	Hbut_1528	1e-11	23.33
β -hydroxybutyryl-CoA dehydrogenase	CA_C2708	Hbut_0193	2.8	33.33
Crotonase	CA_C2712	No significant hits	N/A	N/A
3-hydroxybutyryl-CoA dehydrogenase	CA_C2712	Hbut_1001	2.8	17.39
	CA_C2708	Hbut_0914	2.8	25.71
Acetoacetyl-CoA:acetate:CoA-transferase	X	X	X	X
Acetoacetyl-CoA:butyrate:CoA transferase	CA_P0163	No significant hits	N/A	N/A
Acetoacetate decarboxylase	CA_P0165	Hbut_0896	7.9	40.00
Butyraldehyde dehydrogenase	AAD04638.1*	No significant hits	N/A	N/A
Butanol dehydrogenase	CA_C3298	No significant hits	N/A	N/A
	CA_C3299	Hbut_0094	0.47	19.00
	CA_C3392	No significant hits	N/A	N/A

Key enzymes were searched in the *C. acetobutylicum* ATCC 824 genome (Taxonomy ID: 272562) and potential homologs were obtained using BLASTp searches of genes in *H. butylicus* DSM 5456 (Taxonomy ID: 415426). Percent identity obtained using Jalview by performing pairwise alignments on sequences of interest. *locus tag not identified in genome.

Potential homologs of genes in *H. butylicus* encoding key enzymes involved in butanol production in *S. cerevisiae* S288c.

Target enzyme	Key Enzyme for butanol production in <i>S. cerevisiae</i> S288c (locus tag)	Potential homologous gene in <i>H. butylicus</i> (old locus tag)	E-value	Percent identity (%)
Glycine oxidase**	BSU11670	Hbut_0730	1e-12	24.48
Malate synthase	YNL117W	No significant hits	N/A	N/A
3-isopropylmalate dehydrogenase	YCL018W	No significant hits	N/A	N/A
Pyruvate decarboxylase	YLR044C (PDC1)	No significant hits	N/A	N/A
	YLR134W (PDC5)	No significant hits	N/A	N/A

(PDC1, PDCC5, PDC6)	YGR087C (PDC6)	Hbut_0252	4.2	19.05
Butanol dehydrogenase	YMR303C	No significant hits	N/A	N/A

Key enzymes were searched in the *S. cerevisiae* S288c genome (Taxonomy ID: 4932) and potential homologs were obtained using BLASTp searches of genes in *H. butylicus* DSM 5456 (Taxonomy ID: 415426). Percent identity obtained using Jalview by performing pairwise alignments on sequences of interest. **Gene for glycine oxidase is from the *Bacillus subtilis* subsp. *Subtilis* str. 168 genome.

Potential homologs of genes in *H. butylicus* encoding key enzymes involved in butanol production in *E. coli* BW25113.

Target enzyme	Key Enzyme for butanol production in <i>E. coli</i> BW25113 (locus tag)	Potential homologous gene in <i>H. butylicus</i> DSM 5456 (old locus tag)	E-value	Percent identity (%)
Theronin dehydratase	BW25113_0269	No significant hits	N/A	N/A
2-isopropylmalate synthase	BW25113_0074	No significant hits	N/A	N/A
2-isopropylmalate isomerase	BW25113_1180	Hbut_0220	1e-21	27.85
3-isopropylmalate dehydrogenase	BW25113_0073	Hbut_0799	8.4	28.21
2-ketoacid decarboxylase*	AAS49166	No significant hits	N/A	N/A
Alcohol dehydrogenase 2**	YMR303C	Hbut_1602	6.3	23.26

Key enzymes were searched in the *E. coli* BW25113 genome (Taxonomy Id: 679895) and potential homologs were obtained using BLASTp searches of genes in *H. butylicus* DSM 5456 (Taxonomy ID: 415426). Percent identity obtained using Jalview by performing pairwise alignments on sequences of interest. *gene from *L. lactis* inserted into *E. coli* BW25113. **gene from *S. cerevisiae* S288c inserted into *E. coli*.

HMMsearching with whole Pfam domains and archaea-only domains of key enzymes in *C. acetobutylicum* for butanol production.

Key enzyme for butanol production	Pfam Domains	Pfam match	e-value	Percent identity (%)	
Pyruvate:ferredoxin oxio-reductase	PFOR_II	Hbut_0730 ¹	5.6e-27 ¹	50.5 ¹	
		Hbut_0669 ¹	1.6e-24 ¹	47.1 ¹	
	EKR	Hbut_0730 ²	5.8e-139 ²	47.2 ²	
		Hbut_0669 ²	1.8e-132 ²	40.9 ²	
		Hbut_1455 ²	4.8e-18 ²	30.5 ²	
		Hbut_1625 ²	2.2e-13 ²	43.5 ²	
		No hits for query	N/A	N/A	
		Fer4_16	Hbut_0187 ¹	8.4e-07 ¹	45.0 ¹
			Hbut_0668 ¹	1.3e-05 ¹	32.1 ¹
			Hbut_1380 ¹	7.6e-06 ¹	50.0 ¹
Hbut_0731 ¹	1.8e-05 ¹		35.7 ¹		
Hbut_1052 ¹	0.00053 ¹		25.9 ¹		

	TPP_enzyme_C	Hbut_0983 ¹	8.0e-29 ¹	33.8 ¹
		Hbut_1455 ¹	9.7e-26 ¹	32.9 ¹
		Hbut_0670 ¹	6.7e-24 ¹	30.3 ¹
		Hbut_1625 ¹	2.0e-23 ¹	30.9 ¹
		Hbut_0729 ¹	2.1e-19 ¹	23.3 ¹
		Hbut_1625 ²	8.1e-150 ²	43.3 ²
		Hbut_1455 ²	3.4e-143 ²	45.8 ²
		Hbut_0983 ²	7.9e-78 ²	35.3 ²
		Hbut_0729 ²	6.7e-75 ²	36.9 ²
		Hbut_0670 ²	5.0e-72 ²	30.4 ²
		Hbut_0730 ²	9.9e-09 ²	32.6 ²
		Hbut_0669 ²	1.9e-05 ²	26.4 ²
Acetyl-CoA acetyltransferase	N-terminal domain	Hbut_1528 ¹	5.6e-21 ¹	30.3 ¹
		Hbut_1528 ²	1.4e-182 ²	66.1 ²
	C-terminal domain	Hbut_1528 ¹	5.6e-07 ¹	58.3 ¹
		Hbut_1528 ²	1.9e-166 ²	58.2 ²
		Hbut_1527 ²	5.6e-05 ²	24.0 ²
β -hydroxybutyryl-CoA dehydrogenase	NAD binding domain	Hbut_0912 ¹	0.11 ¹	18.8 ¹
		Hbut_1061 ¹	0.59 ¹	40.7 ¹
		Hbut_0193 ¹	0.67 ¹	23.9 ¹
		No significant sequences ²	N/A ²	N/A ²
	C-terminal domain	No significant sequences ¹	N/A ¹	N/A ¹
		No significant sequences ²	N/A ²	N/A ²
Crotonase	Enoyl-CoA hydratase/isomerase domain	No significant sequences ¹	N/A ¹	N/A ¹
		No significant sequences ²	N/A ²	N/A ²
3-hydroxybutyryl-CoA dehydrogenase	Enoyl-CoA hydratase/isomerase domain	No significant sequences ¹	N/A ¹	N/A ¹
		No significant sequences ²	N/A ²	N/A ²
Acetoacetyl-CoA:acetate:CoA-transferase	X	X	X	X
Acetoacetyl-CoA:butyrate:CoA transferase	CoA_trans domain	No significant sequences ¹	N/A ¹	N/A ¹
		No significant sequences ²	N/A ²	N/A ²
Acetoacetate decarboxylase	Acetoacetate decarboxylase	No significant sequences ¹	N/A ¹	N/A ¹
		No significant sequences ²	N/A ²	N/A ²

Butyraldehyde dehydrogenase	Aldehyde dehydrogenase	No significant sequences ¹	N/A ¹	N/A ¹
		No significant sequences ²	N/A ²	N/A ²
	Iron-containing alcohol dehydrogenase	No significant sequences ¹	N/A ¹	N/A ¹
		Hbut_1566 ²	3.8e-09 ²	22.4 ²
Butanol dehydrogenase	Iron-containing alcohol dehydrogenase	Hbut_1566 ¹	4.5e-21	21.6
		No significant sequences ²	N/A ²	N/A ²

¹Found by HMMsearching whole Pfam domain

²Found by HMMsearching Archaea-only domain

E-values and percent identity are reported for key enzymes in C. acetobutylicum butanol production pathway. Raw HMM files from Pam were used for the whole Pfam searching, and sequence alignments for archaea-only domains were performing using the MUSCLE alignment method with Seaview. Rows marked with "X" indicate gene was not annotated in the genome.

HMMsearching with whole Pfam domains and archaea-only domains of key enzymes in *S. cerevisiae* S288c for butanol production.

Key enzyme for butanol production	Pfam Domains	Pfam match	e-value	Percent identity (%)
Glycine oxidase**	FAD dependent oxidoreductase	Hbut_0625 ¹	1.2e-51 ¹	34.2 ¹
		Hbut_0180 ¹	8.9e-07 ¹	37.5 ¹
		Hbut_0802 ¹	3.7e-06 ¹	41.9 ¹
		Hbut_0253 ¹	0.0001 ¹	34.8 ¹
		Hbut_0495 ¹	0.0047 ¹	36.4 ¹
		Hbut_0625 ²	4.1e-95 ²	35.6 ²
		Hbut_0802 ²	3.1e-12 ²	36.1 ²
		Hbut_0180 ²	2.0e-07 ²	48.4 ²
		Hbut_1257 ²	8.1e-07 ²	24.6 ²
		Hbut_0253 ²	2.6e-05 ²	46.5 ²
		Hbut_1061 ²	0.0005 ²	42.9 ²
		Hbut_0495 ²	0.00075 ²	35.3 ²
		Hbut_0016 ²	0.0014 ²	36.8 ²
		Malate synthase	Malate synthase	No significant sequences ¹
No significant sequences ²	N/A ²			N/A ²
β –isopropylmalate dehydrogenase	Isocitrate/isopropylmalate dehydrogenase	No significant sequences ¹	N/A ¹	N/A ¹
		No significant sequences ²	N/A ²	N/A ²
Pyruvate decarboxylase (PDC1, PDC5, PDC6)	Thiamine pyrophosphate enzyme, N-terminal TPP binding domain	Hbut_1625 ¹	0.051 ¹	24.7 ¹
		Hbut_1455 ¹	0.072 ¹	26.8 ¹
		Hbut_1455 ²	6.0e-08 ²	26.7 ²
		Hbut_1625 ²	0.00047 ²	24.3 ²
		Hbut_0983 ²	0.003 ²	25.2 ²
		Hbut_0983 ²	0.003 ²	25.2 ²
	Thiamine pyrophosphate enzyme, central domain	Hbut_1625 ¹	0.051 ¹	24.7 ¹
		Hbut_1455 ¹	0.072 ¹	26.8 ¹
		Hbut_0670 ²	0.47 ²	28.6 ²
	Thiamine pyrophosphate enzyme, C-terminal TPP binding domain	Hbut_0983 ¹	8.0e-29 ¹	33.8 ¹
		Hbut_1455 ¹	9.7e-26 ¹	32.9 ¹
		Hbut_0670 ¹	6.7e-24 ¹	30.3 ¹
		Hbut_1625 ¹	2.0e-23 ¹	30.9 ¹
		Hbut_0729 ¹	2.1e-19 ¹	23.3 ¹
Hbut_1455 ²		2.4e-171 ²	50.7 ²	
Hbut_1625 ²		1.4e-160 ²	46.3 ²	
Hbut_0983 ²	3.8e-83 ²	32.6 ²		
Hbut_0729 ²	1.7e-79 ²	36.3 ²		
Hbut_0670 ²	2.8e-79 ²	31.8 ²		
Hbut_0730 ²	0.00024 ²	36.6 ²		

Butanol dehydrogenase	Alcohol dehydrogenase GroES-like domain	No significant sequences ¹	N/A ¹	N/A ¹
		Hbut_0414 ²	1.3e-09 ²	28.7 ²
		Hbut_0495 ²	4.4e-08 ²	31.1 ²

¹Found by HMMsearching whole Pfam domain

²Found by HMMsearching Archaea-only domain

E-values and percent identity are reported for key enzymes in S. cerevisiae S288c butanol production pathway. Raw HMM files from Pam were used for the whole Pfam searching, and sequence alignments for archaea-only domains were performing using the MUSCLE alignment method with Seaview. Rows marked with "X" indicate gene was not annotated in the genome.

HMMsearching with whole Pfam domains and archaea-only domains of key enzymes in *E. coli* BW25113 for butanol production.

Key enzyme for butanol production	Pfam Domains	Pfam match	e-value	Percent identity (%)	
Theronin dehydratase	Dehydratase	No significant sequences ¹	N/A ¹	N/A ¹	
		No significant sequences ²	N/A ²	N/A ²	
2-isopropylmalate synthase	HMGL-like domain	No significant sequences ¹	N/A ¹	N/A ¹	
		No significant sequences ²	N/A ²	N/A ²	
	LeuA allosteric (dimerisation) domain	No significant sequences ¹	N/A ¹	N/A ¹	
		No significant sequences ²	N/A ²	N/A ²	
2-isopropylmalate isomerase	Fumarylacetoacetate (FAA) hydrolase family	Hbut_0220 ¹	1.3e-50 ¹	40.1 ¹	
		Hbut_0220 ²	4.1e-50 ²	37.8 ²	
3-isopropylmalate dehydrogenase	Isocitrate/isopropylmalate dehydrogenase	No significant sequences ¹	N/A ¹	N/A ¹	
		No significant sequences ²	N/A ²	N/A ²	
2-ketoacid decarboxylase**	Thiamine pyrophosphate enzyme, N-terminal TPP binding domain	Hbut_1625 ¹	0.051 ¹	24.7 ¹	
		Hbut_1455 ¹	0.072 ¹	26.8 ¹	
		Hbut_1455 ²	6.0e-08 ²	26.7 ²	
	Thiamine pyrophosphate enzyme, central domain	Hbut_1625 ¹	0.051 ¹	24.7 ¹	
		Hbut_1455 ¹	0.072 ¹	26.8 ¹	
		Hbut_0670 ²	0.47 ²	28.6 ²	
	Thiamine pyrophosphate enzyme, C-terminal TPP binding domain	Hbut_0983 ¹	8.0e-29 ¹	33.8 ¹	
		Hbut_1455 ¹	9.7e-26 ¹	32.9 ¹	
		Hbut_0670 ¹	6.7e-24 ¹	30.3 ¹	
		Hbut_1625 ¹	2.0e-23 ¹	30.9 ¹	
			Hbut_0729 ¹	2.1e-19 ¹	23.3 ¹
			Hbut_1455 ²	2.4e-171 ²	50.7 ²
			Hbut_1625 ²	1.4e-160 ²	46.3 ²
Hbut_0983 ²			3.8e-83 ²	32.6 ²	
		Hbut_0729 ²	1.7e-79 ²	36.3 ²	

		Hbut_0670 ²	2.8e-79 ²	31.8 ²
		Hbut_0730 ²	0.00024 ²	36.6 ²
Alcohol dehydrogenase 2*	Alcohol dehydrogenase GroES-like domain	No significant sequences ¹	N/A ¹	N/A ¹
		Hbut_0414 ²	1.3e-09 ²	28.7 ²
		Hbut_0495 ²	4.4e-08 ²	31.1 ²

**gene from L. lactis inserted into E. coli BW25113. **gene from S. cerevisiae S288c inserted into E. coli BW25113.*

¹Found by HMMsearching whole Pfam domain

²Found by HMMsearching Archaea-only domain

E-values and percent identity are reported for key enzymes in E. coli BW25113 butanol production pathway. Raw HMM files from Pam were used for the whole Pfam searching, and sequence alignments for archaea-only domains were performing using the MUSCLE alignment method with Seaview. Rows marked with "X" indicate gene was not annotated in the genome

Appendix B

GC Operation Procedure

Operating procedures for the use of Shimadzu GC-14a and PeakSimple software (version 4.51)

Note: Shimadzu GC-14a is a stand-alone and manually operating instrument. Its chromatograph can be recorded either by an integrator using recording paper or using PeakSimple software (version 4.51) that is computer-controlled, which is part of another GC Buck.

I. Turning on the Shimadzu GC-14a and get ready to use the PeakSimple software (version 4.51)

**The GC is equipped with two columns connected to each other. The first column is the DB-5 followed by the DB-624. This combined column is optimal for detecting the following solvents: acetone, ethanol, butanol, isopropanol. The method currently set on the GC is the following:*

Injector temperature: 200 degrees C

Detector temperature: 250 degrees C

Initial temperature: 35 degrees C (hold for 10 min)

Ramp: 3 degrees/min to 40 degrees C, 45 degrees C/min to 150 degrees C (hold for 1 min)

Range: 1 for 10 min, 2 for 10 min, 1 for 10 min

Entire program length: 30 min

**The GC takes ~15-20 min to cool down. Do not inject another sample until the GC has fully cooled down and returned to the initial temperature (the current initial temperature set on the GC is 35 degrees C).*

***within the injector, there is a rubber septum that acts as a filter between the outside of the injection port and the glass column (contains glass wool which acts as an additional filter between the sample and column). This rubber septa must be changed regularly (between 150-200 punctures) to avoid contamination of the glass column.*

1. Open the gas tanks (left to right) and set to the following pressures:



Hydrogen tank
psi = 30

Helium tank
psi = 50

Nitrogen tank
psi = 20

Air tank
psi = 10

2. Turn on the GC Buck by flipping the power switch located on the bottom right side of the machine.



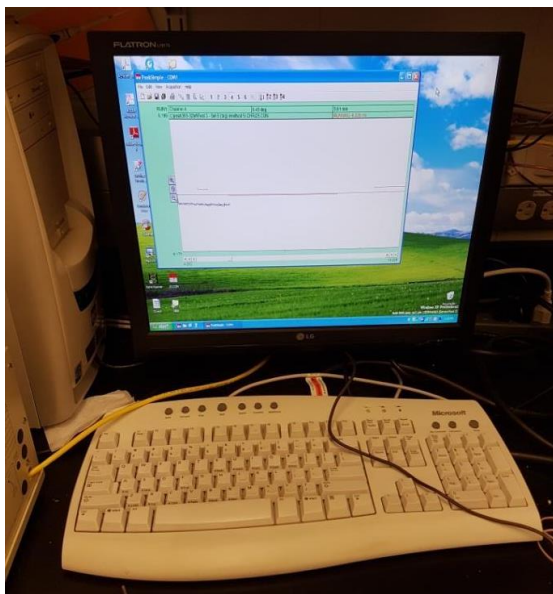
3. Turn on the Shimadzu GC-14a by flipping the white power switch located at the bottom right of the machine. Depress the FID and Heater buttons to turn them on.



4. Ignite the FID using a butane lighter. Place the lighter above the FID port, for a few seconds - and listen for a “pop” sound. Once the sound is heard, use a clean glass slide to check for condensation. If condensation is seen, you have successfully ignited the FID. If not, you need to repeat this step again. Once the FID is successfully ignited, press the red “START” button on the GC so the set temperatures can be achieved (it takes a few minutes for the oven temp, detector temp, injector temp to reach the set temps). You can check to see if they have reached the desired temps by selecting “MONIT”, followed by the desired current temp of each component (ie. COL, INJ, DET-T).



5. Turn on the computer connected to the GC Buck to use the PeakSimple integration software.



6. Once PeakSimple has opened, go to: “File” -> “Control File” -> select “25” located on the Desktop.

7. Once this control file has been initialized, go to: “Edit” -> “Channels” -> Under “Channel 4: Channel 4” -> “Events” -> “Add” -> “Reverse” -> select “OK” -> select “OK”.

8. On the Shimadzu GC 14-a, press the “Range” button, then the number “1”.

9. After the range changes from “4” (least sensitive) to “1” (second most sensitive) and the “Reverse” event has been added, press the spacebar twice (doing this changes the baseline from a negative mV to a positive mV”).

10. The added “Reverse” event can now be removed. Go to: “Edit” -> “Channels” -> Under “Channel 4: Channel 4” -> “Events” -> “Remove” -> “Reverse” -> select “OK” -> select “OK”.

11. Once the Shimadzu GC 14-a has reached the initial temperature, the LED beside “Ready” will turn on, and the GC is ready to be injected with your sample.

12. Using a 10 μ l gas-tight syringe, rinse the syringe with DI water. Obtain 1 μ l of your sample, and carefully inject the needle into the injection port (ensure the needle does not bend). Once the sample has been injected, remove the needle from the injection port, and press the “START” button on the Shimadzu GC 14-a, while quickly pressing the spacebar of the keyboard after (this will start the recording on PeakSimple).

Note: you do not need to press the space bar to stop the recording, as PeakSimple has been set to stop once the program has completed on the GC (To set the program length time, go to: "Edit" -> "Channels" -> Under "Channel 4: Channel 4" -> "Details" -> Under "End time: ", enter length of program (in min) -> select "OK" -> select "OK".)

13. Once the sample has completed its run, save your recording. Go to: "File" -> "Save as" -> [name your file; ensure it is saved as a .CHR file and saved under Channel 4] -> "Save".

14. Steps 11-13 can be repeated for your next sample (ensure the LED light beside "Ready" is on before injecting again).

II. Shutting down the GC Shimadzu GC-14a and close the PeakSimple software (version 4.51)

1. Close PeakSimple software and shut down the computer (as normally done).
2. Once the LED beside "ready" is on on the Shimadzu GC-14a, change the range on the GC from "1" back to "4".
3. Depress the FID and Heater button to turn them off. Flip the white power switch to "off" to turn off the GC.
4. Close all gas tanks (in the order they were opened).
5. Turn off the GC Buck by flipping the power switch to "off".

III. Shimadzu GC-14a Parameter Set up (to set a new program)

To set a new program, input the following:

Set the injector temperature:

1. Press "INJ" -> enter desired injector temperature (in degrees C) using the number pad -> Press "ENT".

Set the detector (FID) temperature:

1. Press "DET-T" -> enter desired detector temperature (in degrees C) using the number pad -> Press "ENT".

Set the initial temperature:

1. Press "COL" -> Press "INIT TEMP" -> enter desired initial temperature (in degrees C) using the number pad -> Press "ENT".
2. If you want the initial temperature to hold for a certain amount of time:
 - a) Press "COL" -> Press "INIT TIME" -> enter desired initial temperature hold time (in min) using the number pad -> Press "ENT".

Set the ramp temperature/min rate:

1. Press “COL” -> Press “PROG RATE” -> enter the first desired temperature/min rate of the program (in degrees C/min) using the number pad -> Press “ENT” -> enter the second desired temperature/min rate of the program (in degrees C/min) using the number pad -> Press “ENT” -> [keep repeating until all the desired temperature/min rate of the program have been entered or stop at the second desired temperature/min rate].

Example: for the current set program, the program ramps at “3 degrees/min to 40 degrees C” then “45 degrees C/min to 150 degrees C”. The following would be entered:

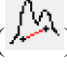
Press “COL” -> Press “PROG RATE” -> enter “3” -> Press “ENT” -> enter “45” -> Press “ENT”.

2. Set the temperature the program rate goes up to: Press “COL” -> Press “FINAL TEMP” -> enter the first desired temperature for the first rate (in degrees C) using the number pad -> Press “ENT” -> enter the second desired temperature for the second rate (in degrees C) using the number pad -> Press “ENT” -> [keep repeating until all the desired temperature for each rate have been entered, or stop at the second desired temperature for the rate].

3. If there are hold times for the desired temperatures (for the rates): Press “COL” -> Press “FINAL TIME” -> enter the first desired hold time for the first rate (in min) using the number pad -> Press “ENT” -> enter the second desired hold time for the second rate (in min) using the number pad -> Press “ENT” -> [keep repeating until all the desired hold times for each rate have been entered, or stop at the second desired hold time for the rate].

Appendix C

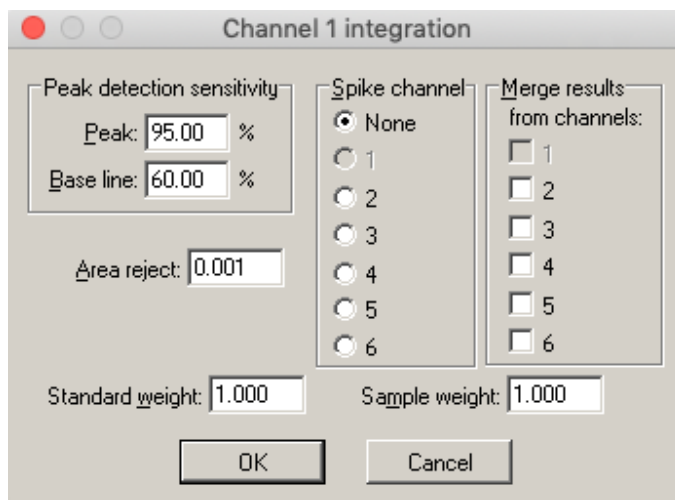
PeakSimple Operation Procedure

When integrating the area of a target peak, a manual baseline can be drawn using the “Rubber Band” tool () in the “Manual Integration” toolbar. Using the “Rubber Band” tool, the user can click at the beginning of the peak and drag the cursor to the end of the peak allowing a manual baseline to be created by the software, where the area above the drawn baseline is the area integrated. Using this method, the software will integrate the area of the peak and provide the data in the “Results” menu. When determining the height of the peak, the cursor is simply placed on top of the peak and a value in the right-hand corner of the software will indicate the height (mV); the value to the left of the height is the corresponding time point.

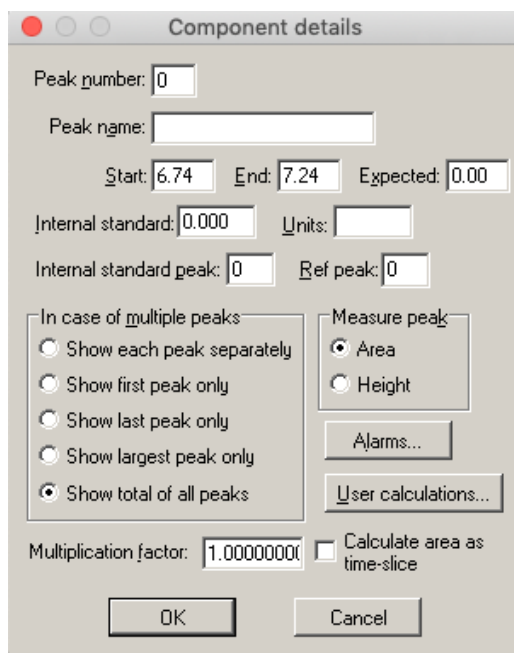


Manual integration toolbar in PeakSimple software (version 4.51) for GC data. The “rubber band” tool for creating a manual baseline can be found in the 9th option down from the top of the toolbar.

To set an area reject value is set to 0.001 (allowing for the detection of smaller peaks), a component is created to allow for the integration of a target peak, with “Show total of all peaks” under the “In case of multiple peaks” option selected; this step is crucial as other options will provide varying results. This option can be found in the “Channels” menu, under “Integration”.

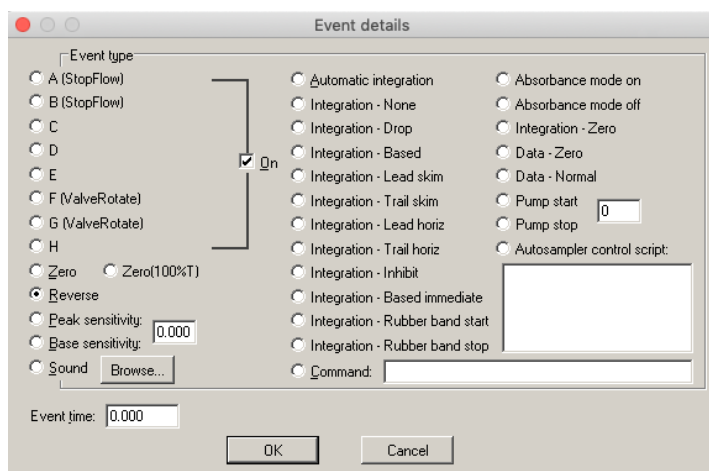


Setting area reject in PeakSimple (version 4.51). Area reject is set to 0.001 for all GC sample runs.

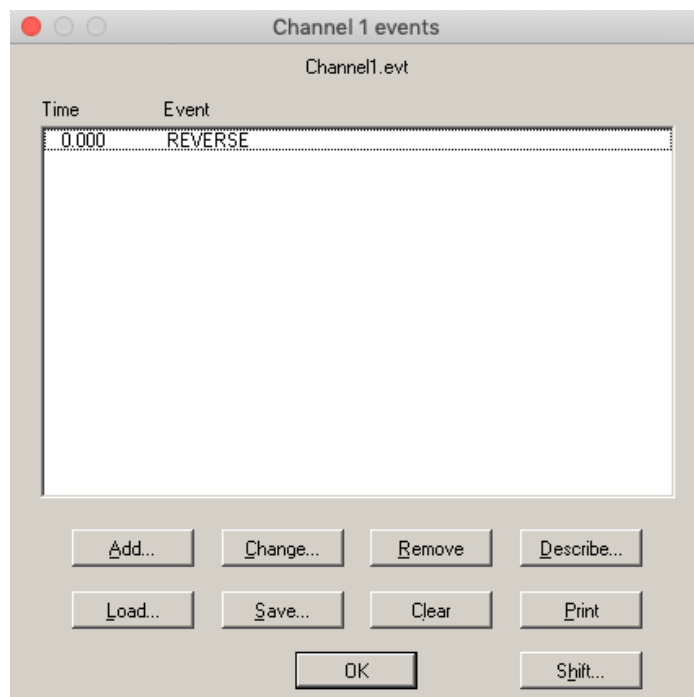


Setting integration parameters in PeakSimple (version 4.51). The option “Show total of all peaks” in the “Components” menu is selected for integration of all GC sample runs.

The voltage of the baseline (mV) must be equalized when the GC Buck is turned on thus, a series of steps must be done to create a positive baseline. Under the “Events” menu, then a “Reverse” event will be added. Once the events are added, the spacebar is pressed to reverse the baseline making it positive. The “Reverse” event is then removed after equalizing the baseline. A positive baseline is required to have peaks appear above the baseline.

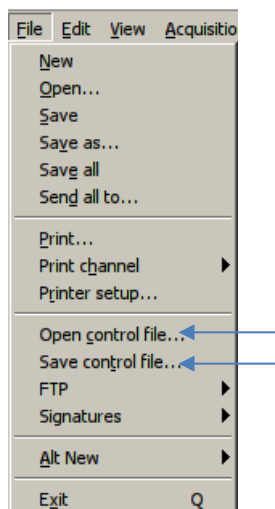


Adding an event in PeakSimple (version 4.51). The “Event details” window can be accessed from the “Channels” menu.



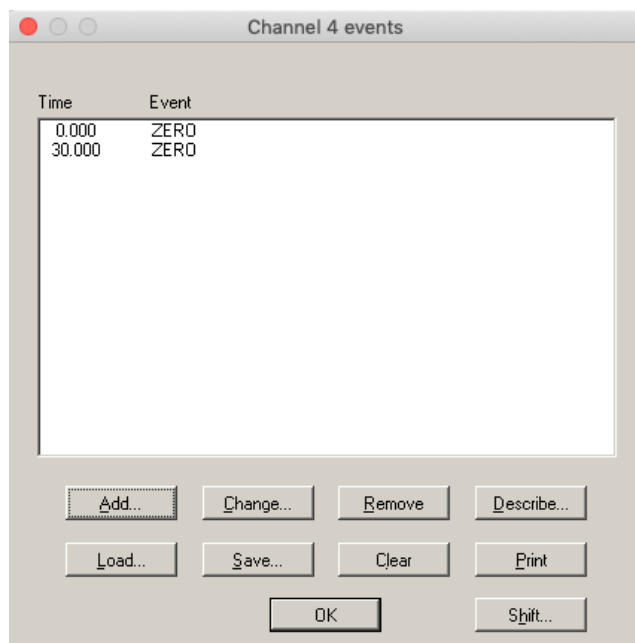
Setting “Reverse” event in PeakSimple (version 4.51). The “reverse” event is required to create a positive (mV) baseline, allowing peaks to show above the baseline.

Once these parameters are set, a control file (.CON) can be created which allows the user to save these settings and use them for future GC runs. Controls files are saved and opened as how a file is typically saved and opened (in the “File” menu).



Accessing Control files in PeakSimple (version 4.51). “Open control file...” allows the user to load a saved control file, while “Save control file...” allows the user to save set parameters.

When a GC run begins the start button (spacebar) must be manually pressed by the user to begin recording. Similar to how the “Reverse” event was added, a stop time can be set in PeakSimple in the “Events” menu which allows the software to end the recording (or the user can again press the spacebar to manually stop the recording); for the method used in this study, a stop time of 30 min is used (**Fig. 19**). A “ZERO” event is added at 0 min to indicate the start of the GC run, and again at 30 min for the end of the run.



Setting a recording stop time in PeakSimple (version 4.51). A “zero” event at 0 min (start of the run) and again at 30 min (end of the run) is added for each GC sample run.

PeakSimple files (.CHR) must manually be saved by the user after each run and can be saved at a destination of the user’s choice (recommended that chromatographs are saved in the same folder for ease of access during post analyses). Files can be accessed from the location where the user originally saved the .CHR file for post-run analyses. PeakSimple files (.CHR) can be saved on a USB drive allowing the user to analyze the chromatographs on a different computer, on which the PeakSimple software is installed. Although post-run analyses can be performed on a different computer other than the GC Buck, the same parameters and software version (4.51) must be used. Additionally, PeakSimple is a Windows exclusive software.

Appendix D

GC Integrator Operation Procedure

Operating Shimadzu GC-14a with Shimadzu CR601 Chromatopac Integrator

*See Appendix B protocol for operation of Shimadzu GC-14a.

1. To operate the Integrator, switch the power button on and wait a few seconds for the machine to power up.
2. To begin recording, the “START/STOP” button on the integrator and “START” button on the Shimadzu GC-14a must be pressed at the same time.
3. The recorder can be preset to stop recording by pressing “STOP.TM” followed by the desired stop time (For example, for a stop time of 30 min, the user would select: “STOP.TM” -> “3” -> “0”).
4. The attenuation of the Integrator can be adjusted which will change the scale of the integration. In general, the larger the number, the more scaled in the integration is (beginning from 0 to 10 where each interval increases the scale by 10). To change the attenuation, press “ATTEN” then the value of attenuation you desire.

Appendix E

Standard Curve Raw Data

1-Butanol standard curve raw data

Product	Individual product													
	mM	mV	mV (avg)	Δ mVa	mV SD	Area	Area Avg	Δ Area	Area (Isob)	Area (Isob Avg)	Ratio	Ratio (avg)	Ratio SD	SD (avg)
1-Butanol	0	0.046 0.049	0.048	0	0.002	3.558 3.192	3.375	0	59.088 60.403	59.745	0.060 0.053	0.056	0	0.259
	0.25	0.365 0.321	0.343	0.296	0.031	132.480 130.761	131.621	128.245	61.433 60.659	61.046	2.157 2.156	2.156	0.001	1.216
	0.5	0.668 0.604	0.636	0.589	0.045	264.958 269.743	267.351	263.975	61.496 61.159	61.328	4.309 4.411	4.359	0.072	3.384
	1	1.259 1.311	1.285	1.238	0.037	543.077 541.830	542.454	539.078	63.987 62.684	63.335	8.487 8.644	8.565	0.111	0.882
	3	2.304 2.353	2.329	2.281	0.035	1626.116 1631.856	1628.986	1625.611	62.965 60.685	61.825	25.826 26.890	26.348	0.753	4.059
	5	4.065 3.828	3.947	3.899	0.168	2707.227 2713.331	2710.279	2706.904	62.645 63.761	63.203	43.215 42.555	42.882	0.467	4.316

Mixed samples													
mV	mV (avg)	Δ mV	mV SD	Area (calc)	Area (avg)	ΔArea	Area (isob)	Area (isob avg)	Ratio	Ratio (avg)	Ratio SD	SD (avg)	Calculated Concentration
0.047 0.440	0.244	0	0.278	2.958 3.105	3.031	0	61.581 60.095	60.838	0.048 0.052	0.050	0	0.104	0.000
0.359 0.337	0.348	0.105	0.016	134.919 136.158	135.539	132.508	60.543 60.882	60.712	2.228 2.236	2.232	0.006	0.876	0.253
0.845 0.917	0.881	0.638	0.051	271.027 270.519	270.773	267.742	60.648 60.833	60.740	4.469 4.447	4.458	0.016	0.359	0.505
1.412 1.583	1.498	1.254	0.121	549.227 556.173	552.700	549.669	61.100 60.610	60.855	8.989 9.176	9.082	0.132	4.912	1.029
2.558 2.547	2.553	2.309	0.008	1635.489 1640.688	1638.089	1635.057	61.584 59.788	60.686	26.557 27.442	26.993	0.626	3.676	3.058
4.341 4.520	4.431	4.187	0.127	2720.038 2724.630	2722.334	2719.303	61.594 62.810	62.202	44.161 43.379	43.766	0.553	3.247	4.959

Ethanol standard curve raw data

Product	Individual product												
	mM	mV	mV (avg)	Δ mVa	mV SD	Area	Area (avg)	ΔArea	Area SD	Area (Isob Avg)	Area Ratio	SD (Peak Ratio)	Peak Ratio (ΔArea/Area(Isob Avg))
Ethanol	0	0.012	0.501	0	0.001	2.059	2.097	0	0.054	64.4545	0.032	0.001	0
		0.011				2.135					0.033		
	0.25	0.99	0.963	0.462	0.039	20.394	20.455	18.358	0.086	65.6975	0.310	0.001	0.279
		0.935				20.515					0.312		
	0.5	2.01	2.023	1.522	0.018	39.64	40.081	37.984	0.624	64.845	0.611	0.010	0.586
		2.035				40.522					0.625		
	1	3.5	3.528	3.027	0.039	82.959	82.217	80.120	1.050	63.7065	1.302	0.016	1.258
		3.555				81.474					1.279		
	3	10.32	10.583	10.082	0.371	247.921	245.485	243.388	3.445	67.584	3.668	0.051	3.601
		10.845				243.0488					3.596		
	5	17.345	17.125	16.625	0.311	410.847	411.758	409.661	1.289	67.6775	6.071	0.019	6.053
		16.905				412.669					6.098		

Mixed samples				Mixed samples (AEI Total)							
mV	mV (avg)	Δ mV	mV SD	Area	Area (avg)	Δ Area	Area SD	Area (Isob Avg)	Individual Peak Ratio	Individual Peak Ratio SD	Peak Ratio Avg (Δ Area/Area(Isob Avg))
0.013 0.011	0.012	0	0.001	2.017 2.359	2.1882	0	0.242	65.792	0.031 0.036	0.004	0
1.08 1.04	1.060	1.048	0.028	151.266 146.013	148.6397	146.451	3.714	64.232	2.355 2.273	0.058	2.280
2.105 2.085	2.095	2.083	0.014	296.509 288.796	292.6528	290.465	5.454	63.827	4.645 4.525	0.085	4.551
3.77 3.74	3.755	3.743	0.021	1341.597 1259.821	1300.7092	1298.521	57.824	66.374	20.213 18.981	0.871	19.564
10.575 10.595	10.585	10.573	0.014	1821.540 1783.947	1802.7436	1800.555	26.582	65.049	28.003 27.425	0.409	27.680
17.695 17.635	17.665	17.653	0.042	3206.360 3129.673	3168.0167	3165.829	54.226	65.417	49.014 47.842	0.829	48.394

Individual AEI combined area vs Mix AEI combined area			Calculated Ethanol Concentration		
Individual AEI (avg)	Mixed AEI (avg)	Difference (%)	Calculated area	Calculated ratio	Calculated concentration
0	0	0	0	0	0
143.073 ± 2.76	146.451 ± 5.05	3.8	25.743	0.401	0.301
288.137 ± 5.64	290.465 ± 1.68	1.5	51.167	0.802	0.603
1186.021 ± 2.40	1298.521 ± 4.44	9.1	91.943	1.385	1.042
1783.454 ± 2.81	1800.555 ± 8.45	1.0	259.715	3.993	3.002
2971.034 ± 7.21	3115.829 ± 8.01	4.7	433.628	6.629	4.985

Isopropanol standard curve raw data

Product	Individual product												
	mM	mV	mV (avg)	Δ mVa	mV SD	Area	Area (avg)	ΔArea	Area SD	Area (Isob avg)	Individual Peak Ratio	Individual Peak Ratio SD	Peak Ratio Avg (ΔArea/Area(Isob Avg))
Isopropanol	0	0 0	0	0	0	2.059 2.135	2.097	0	0.054	60.435	0.034 0.035	0.001	0
	0.25	1.235 1.855	1.545	1.545	0.438	58.441 62.883	60.662	58.565	3.141	62.82	0.930 1.001	0.050	0.932
	0.5	2.78 3.115	2.948	2.948	0.237	120.991 123.102	122.047	119.950	1.493	60.85	1.988 2.023	0.025	1.971
	1	5.175 4.375	4.775	4.775	0.566	245.430 250.312	247.871	245.774	3.453	62.065	3.954 4.033	0.056	3.960
	3	17.505 17.44	17.473	17.473	0.046	728.532 733.883	731.207	729.110	3.784	61.695	11.809 11.895	0.061	11.818
	5	25.49 25.425	25.458	25.458	0.046	1224.194 1236.034	1230.114	1228.017	8.372	58.38	20.969 21.172	0.143	21.035

Mixed samples				Mixed samples (AEI Total)							
mV	mV (avg)	Δ mV	mV SD	Area	Area (avg)	Δ Area	Area SD	Area (Isob Avg)	Area Ratio	SD (Peak Ratio)	Ratio (Δ Area/Area(Isob Avg))
0.013 0.011	0.012	0	0.001	2.017 2.359	2.188	0	0.242	65.792	0.031 0.036	0.004	0
1.42 1.58	1.500	1.488	0.113	151.266 146.013	148.640	146.451	3.714	64.232	2.355 2.273	0.058	2.280
3.32 2.48	2.900	2.888	0.594	296.509 288.796	292.653	290.465	5.454	63.827	4.645 4.525	0.085	4.551
5.56 5.525	5.543	5.531	0.025	1341.597 1259.821	1300.709	1298.521	57.824	66.374	20.213 18.981	0.871	19.564
18.715 18.625	18.670	18.658	0.064	1821.540 1783.947	1802.744	1800.555	26.582	65.049	28.003 27.425	0.409	27.680
28.045 27.99	28.018	28.006	0.039	3206.360 3029.673	3118.017	3115.829	124.936	65.417	49.014 46.313	1.910	47.630

Individual AEI combined area vs Mix AEI combined area			Calculated Isopropanol Concentration		
Individual AEI (avg)	Mixed AEI (avg)	Difference (%)	Calculated area	Calculated ratio	Calculated concentration
0	0	0	0	0	0
143.073 ± 2.76	146.451 ± 5.05	3.8	68.758	1.070	0.259
288.137 ± 5.64	290.465 ± 1.68	1.5	133.449	2.091	0.506
1186.021 ± 2.40	1298.521 ± 4.44	9.1	255.553	3.850	0.932
1783.454 ± 2.81	1800.555 ± 8.45	1.0	862.149	13.254	3.210
2971.034 ± 7.21	3115.829 ± 8.01	4.7	1294.078	19.782	4.791

Acetone standard curve raw data

Product	Individual product												
	mM	mV1	mV1 (avg)	Δ mVa	SD	Area	Area (avg)	ΔArea	Area SD	Area (Isob avg)	Individual Peak Ratio	Individual Peak Ratio SD	Peak Ratio Avg (ΔArea/Area(Isob Avg))
Acetone	0	0 0	0	0	0	2.059 2.135	2.097	0	0.054	58.19	0.035 0.037	0.001	0
	0.25	1.555 1.55	1.553	1.553	0.004	70.481 62.020	66.250	64.153	5.983	57.900	1.217 1.071	0.103	1.108
	0.5	3.675 3.67	3.673	3.673	0.004	129.810 134.790	132.300	130.203	3.521	58.795	2.208 2.293	0.060	2.215
	1	7.02 6.985	7.003	7.003	0.025	270.323 263.535	266.929	264.832	4.800	60.990	4.432 4.321	0.079	4.342
	3	21.03 21.075	21.053	21.053	0.032	809.212 812.700	810.956	808.859	2.466	59.850	13.521 13.579	0.041	13.515
	5	34.925 34.45	34.688	34.688	0.336	1335.092 1331.619	1333.356	1331.259	2.455	61.044	21.871 21.814	0.040	21.808

Mixed samples				Mixed samples (AEI Total)							
mV1	mV1 (avg)	Δ mV1	SD	Area	Area (avg)	Δ Area	Area SD	Area (Isob Avg)	Area Ratio	SD (Peak Ratio)	Peak Ratio (Δ Area/Area(Isob Avg))
0	0	0	0	2.017	2.188	0	0.242	65.792	0.031	0.004	0
0				2.359					0.036		
2.692	2.676	2.676	0.023	151.266	148.640	146.451	3.714	64.232	2.355	0.058	2.280
2.66				146.013					2.273		
5.545	5.563	5.563	0.025	296.509	292.653	290.465	5.454	63.827	4.645	0.085	4.551
5.581				288.796					4.525		
11.285	11.368	11.368	0.117	1341.597	1300.709	1298.521	57.824	66.374	20.213	0.871	19.564
11.45				1259.821					18.981		
36.165	35.653	35.653	0.725	1821.540	1802.744	1800.555	26.582	65.049	28.003	0.409	27.680
35.14				1783.947					27.425		
56.525	55.380	55.380	1.619	3206.360	3118.017	3115.829	124.936	65.417	49.014	1.910	47.630
54.235				3029.673					46.313		

Individual AEI combined area vs Mix AEI combined area			Calculated Acetone Concentration			
Individual AEI (avg)	Mixed AEI (avg)	Difference (%)	Acetone mV (mv1 - [Δ ethanol mixed mV + isopropanol interference])	Calculated area	Calculated ratio	Calculated concentration
0 ± 2.76	0	0	0	0	0	0
143.073 ± 2.76	146.451 ± 5.05	3.8	1.581	60.628	0.944	0.215
288.137 ± 5.64	290.465 ± 1.68	1.5	3.418	131.073	2.054	0.467
1186.021 ± 2.40	1298.521 ± 4.44	9.1	7.563	290.007	4.369	0.993
1783.454 ± 2.81	1800.555 ± 8.45	1.0	25.018	959.371	14.748	3.353
2971.034 ± 7.21	3115.829 ± 8.01	4.7	37.710	1446.103	22.106	5.026

Appendix F

Solvent Production Raw Data

H. butylicus optimal conditions solvent data

						area per mV 24.564				ratio per mM 1.3298
Product	Ethanol									
	Time	mV	mV (avg)	Δ mVa	mV SD	Calculated Area	Isobutanol Peak Area (Avg)	Calculated Ratio	Calculated Concentration (mM)	
Hb (normal conditions)	0	0.080 0.081	0.081	0	0.001	0	60.938	0	0	
	16	0.156 0.154	0.155	0.075	0.001	1.830	60.693	0.030	0.023	
	24	0.204 0.21	0.207	0.127	0.004	3.107	62.756	0.050	0.037	
	32	0.226 0.229	0.228	0.147	0.002	3.611	61.108	0.059	0.044	
	42	0.249 0.246	0.248	0.167	0.002	4.102	61.488	0.067	0.050	
	50	0.250 0.253	0.252	0.171	0.002	4.200	61.250	0.069	0.052	

						area per mV 46.208				ratio per mM 4.129
Product	Isopropanol									
	Time	mV	mV (avg)	Δ mVa	mV SD	Calculated Area	Isobutanol Peak Area (Avg)	Calculated Ratio	Calculated Concentration (mM)	
Hb (normal conditions)	0	0 0	0	0	0	0	60.938	0	0	
	16	0.096 0.095	0.096	0.096	0.001	4.413	60.693	0.073	0.018	
	24	1.355 1.358	1.357	1.357	0.021	62.681	62.756	0.999	0.242	
	32	2.2 2.193	2.197	2.197	0.004	101.496	61.108	1.661	0.402	
	42	2.442 2.437	2.440	2.440	0.004	112.724	61.488	1.833	0.444	
	50	2.503 2.532	2.518	2.518	0.021	116.329	61.250	1.899	0.460	

						area per mV 38.355				ratio per mM 4.3982
Product	Acetone									
	Time	mV1	mV1 (avg)	Δ mVa1	mV SD	Acetone mV (Δ mva1 - [Δ ethanol mixed mV + isopropanol interference])	Isobutanol Peak Area (Avg)	Calculated area	Calculated ratio	Calculated concentration
Hb (normal conditions)	0	0 0	0	0	0	0	60.938	0	0	0
	16	4.514	4.582	4.582	0.095	4.532	60.693	173.806	2.864	0.651
		4.649								
	24	8.22	8.270	8.270	0.070	8.220	62.756	315.259	5.024	1.142
		8.319								
	32	10.194	10.148	10.148	0.065	10.098	61.108	387.309	6.338	1.441
		10.102								
	42	11.391	11.349	11.349	0.060	11.299	61.488	433.354	7.048	1.602
		11.306								
	50	9.988	9.920	9.920	0.097	9.699	61.250	371.986	6.073	1.381
		9.851								

ratio per mM
8.8263

Product	Butanol									
	Time	Area	Area (avg)	ΔArea	Area (Isob avg)	Individual Ratio	Individual Ratio SD	Ratio (avg)	Area SD	Calculated Concentration (mM)
Hb (normal conditions)	0	3.146	3.341	0	60.938	0.052	0.005	0	0.276	0
		3.536				0.058				
	16	221.125	218.366	215.025	60.693	3.643	0.064	3.543	3.902	0.401
		215.607				3.552				
	24	258.488	262.040	258.699	62.756	4.119	0.080	4.122	5.023	0.467
		265.592				4.232				
32	285.71	286.508	283.167	61.108	4.676	0.018	4.634	1.129	0.525	
	287.306				4.702					
42	304.168	306.120	302.779	61.488	4.947	0.045	4.924	2.761	0.558	
	308.072				5.010					
50	315.317	314.052	310.711	61.250	5.148	0.029	5.073	1.790	0.575	
	312.786				5.107					

Product	Total AEI Area						Difference (%)
	Time	Mix Area	Mix Area SD	Mix Area (avg)	ΔMix Area (avg)	Calculated AEI Total	
Hb (normal conditions)	0	2.921	0.106	2.996	0.000	0.000	0.000
		3.071					
	16	176.630	6.479	172.049	169.052	180.049	6.300
		167.467					
	24	348.582	29.609	369.519	366.523	381.047	3.886
		390.456					
	32	473.179	12.918	482.313	479.317	492.416	2.696
		491.448					
	42	555.867	4.488	559.040	556.044	550.181	-1.060
		562.214					
	50	472.943	15.800	484.115	481.119	492.515	2.341
		495.287					

H. butylicus with 5 mM butyrate solvent data

						area per mV 24.564				ratio per mM 1.3298
Product	Ethanol									
	Time	mV	mV (avg)	Δ mVa	SD	Calculated Area	Isobutanol Peak Area (Avg)	Calculated Ratio	Calculated Concentration	
Hb w/ 5 mM Butyrate	0	0.050 0.050	0.050	0	0.000	0	61.285	0	0	
	20	0.154 0.149	0.152	0.102	0.004	2.493	61.090	0.0408	0.031	
	30	0.202 0.208	0.205	0.155	0.004	3.807	62.395	0.0610	0.046	
	40	0.221 0.229	0.225	0.175	0.006	4.299	64.610	0.0665	0.050	
	50	0.236 0.24	0.238	0.188	0.003	4.618	65.210	0.0708	0.053	
	60	0.239 0.242	0.241	0.191	0.002	4.679	66.460	0.0704	0.053	
	70	0.243 0.239	0.241	0.191	0.003	4.692	65.090	0.0721	0.054	
	80	0.235 0.24	0.238	0.188	0.004	4.606	63.890	0.0721	0.054	

						area per mV 46.208				ratio per mM 4.129
Product	Isopropanol									
	Time	mV	mV (avg)	Δ mVa	SD	Calculated Area	Isobutanol Peak Area (Avg)	Calculated Ratio	Calculated Concentration	
Hb w/ 5 mM Butyrate	0	0 0	0	0	0	0	61.285	0	0	
	20	0.988 1.053	1.021	1.021	0.046	47.155	61.090	0.7719	0.187	
	30	2.547 2.566	2.557	2.557	0.013	118.131	62.395	1.8933	0.459	
	40	2.743 2.694	2.719	2.719	0.035	125.616	64.610	1.9442	0.471	
	50	2.711 2.809	2.760	2.760	0.069	127.534	65.210	1.9557	0.474	
	60	2.784 2.801	2.793	2.793	0.012	129.036	66.460	1.9416	0.470	
	70	2.637 2.711	2.674	2.674	0.052	123.560	65.090	1.8983	0.460	
	80	2.67 2.682	2.676	2.676	0	123.653	63.890	1.9354	0.469	

						area per mV 38.355				ratio per mM 4.3982
Product	Acetone									
	Time	mV1	mV1 (avg)	Δ mVa1	mV1 SD	Acetone mV (Δmva1 - [Ethanol mixed mV + isopropanol interference])	Isobutanol Peak Area (Avg)	Calculated area	Calculated ratio	Calculated concentration
Hb w/ 5 mM Butyrate	0	0 0	0	0	0	0	61.285	0	0	0
	20	6.585 6.355	6.470	6.470	0.162	6.319	61.090	242.354	3.967	0.902
	30	9.8325 10.193	10.013	10.013	0.255	9.808	62.395	376.198	6.029	1.371
	40	11.792 11.516	11.654	11.654	0.195	11.429	64.610	438.377	6.785	1.543
	50	12.355 12.073	12.214	12.214	0.199	11.976	65.210	459.357	7.044	1.602
	60	10.706 10.454	10.580	10.580	0.178	10.340	66.460	396.586	5.967	1.357
	70	8.928 9.108	9.018	9.018	0.127	8.777	65.090	336.659	5.172	1.176
	80	7.881 8.241	8.061	8.061	0.255	7.824	63.890	300.086	4.697	1.068

										ratio per mM
										8.8263
Butanol										
Product	Time	Area	Area (avg)	ΔArea	Area (Isob avg)	Individual Ratio	Individual Ratio SD	Ratio	Area SD	Calculated Concentration (mM)
Hb w/ 5 mM Butyrate	0	3.198	3.085	0	61.285	0.052	0.002	0	0.121	0
		3.027				0.049				
	20	328.685	332.339	329.254	61.090	5.380	0.085	5.390	5.167	0.611
		335.992				5.500				
	30	398.126	402.862	399.777	62.395	6.381	0.107	6.407	6.698	0.726
		407.598				6.533				
	40	519.422	526.138	523.053	64.610	8.039	0.147	8.096	9.497	0.917
		532.853				8.247				
	50	599.063	605.501	602.416	65.210	9.187	0.140	9.238	9.104	1.047
		611.938				9.384				
	60	633.867	628.354	625.269	66.460	9.538	0.117	9.408	7.797	1.066
		622.84				9.372				
	70	628.646	631.687	628.602	65.090	9.658	0.066	9.657	4.300	1.094
		634.727				9.752				
	80	626.115	627.407	624.322	63.890	9.800	0.029	9.772	1.827	1.107
		628.699				9.840				

Product	Total AEI Area						
	Time	Mix Area	Mix Area SD	Mix Area (avg)	ΔMix Area (avg)	Calculated AEI Total	Difference (%)
Hb w/ 5 mM Butyrate	0	3.018 2.539	0.339	2.779	0.000	0.000	0.000
	20	271.111 284.254	9.293	277.682	274.904	292.003	6.032
	30	490.544 496.004	3.861	493.274	490.495	498.136	1.546
	40	569.352 575.497	4.346	572.425	569.646	568.292	-0.238
	50	597.738 591.516	4.399	594.627	591.848	591.509	-0.057
	60	538.001 526.898	7.852	532.449	529.671	530.301	-0.119
	70	477.360 473.222	2.926	475.291	472.512	464.911	-1.622
	80	431.980 436.284	3.044	434.132	431.354	428.344	-0.700

***H. butylicus* with 15 mM butyrate solvent data**

						area per mV				ratio per mM
						24.564				1.3298
Product	Ethanol									
	Time	mV	mV (avg)	Δ mVa	mV SD	Calculated Area	Isobutanol Peak Area (Avg)	Calculated Ratio	Calculated Concentration (mM)	
Hb w/ 15 mM Butyrate	0	0.048	0.049	0.000	0.001	0	64.770	0	0	
		0.050								
	20	0.151	0.154	0.105	0.004	2.588	64.150	0.040	0.030	
		0.158								
	40	0.251	0.253	0.204	0.003	5.009	66.735	0.075	0.056	
		0.255								
50	0.255	0.258	0.209	0.004	5.133	65.180	0.079	0.059		
	0.261									
60	0.262	0.263	0.214	0.001	5.248	66.065	0.079	0.060		
	0.264									

						area per mV				ratio per mM
						46.208				4.129
Product	Isopropanol									
	Time	mV	mV (avg)	Δ mVa	mV SD	Calculated Area	Isobutanol Peak Area (Avg)	Calculated Ratio	Calculated Concentration (mM)	
Hb w/ 15 mM Butyrate	0	0	0	0	0	0	64.770	0	0	
		0								
	20	1.003	0.999	0.999	0.006	46.139	64.150	0.719	0.174	
		0.994								
	40	2.823	2.808	2.808	0.022	129.729	66.735	1.944	0.471	
2.792										
50	2.832	2.837	2.837	0.006	131.069	65.180	2.011	0.487		
	2.841									
60	2.917	2.924	2.924	0.009	135.089	66.065	2.045	0.495		
	2.93									

						area per mV				ratio per mM	
						38.355				4.3982	
Product	Acetone										
	Time	mV1	mV1 (avg)	Δ mVa1	mVa1 SD	Acetone mV1 (Δ mva1 - [Δ ethanol mixed mV + isopropanol interference])	Isobutanol Peak Area (Avg)	Calculated area	Calculated ratio	Calculated concentration	
Hb w/ 15 mM Butyrate	0	0.000	0	0	0	0	64.770	0	0	0	
		0.000									
	20	7.986	7.838	7.838	0.210	7.788	64.150	298.690	4.656	1.059	
		7.689									
	40	12.096	12.250	12.250	0.218	12.200	66.735	467.916	7.012	1.594	
12.404											
50	12.779	12.595	12.595	0.260	12.545	65.180	481.163	7.382	1.678		
	12.411										
60	11.297	11.060	11.060	0.335	11.010	66.065	422.287	6.392	1.453		
	10.823										

ratio per mM
8.8263

Product	Butanol									
	Time	Area	Area (avg)	ΔArea	Area (Isob avg)	Individual Ratio	Individual Ratio SD	Ratio (avg)	Area SD	Concentration mM (calc)
Hb w/ 15 mM Acetate	0	2.980 3.141	3.085	0	64.770	0.046 0.048	0.002	0	0.114	0
	20	2271.503 2349.330	2310.416	2307.331	64.150	35.409 36.622	0.858	35.968	55.032	4.075
	40	3318.398 3380.630	3349.514	3346.429	66.735	49.725 50.658	0.659	50.145	44.005	5.681
	50	3407.545 3358.367	3382.956	3379.871	65.180	52.279 51.525	0.534	51.854	34.774	5.875
	60	3505.483 3476.028	3490.756	3487.671	66.065	53.061 52.615	0.315	52.792	20.828	5.981

Product	Total AEI Area						
	Time	Mix Area	Mix Area SD	Mix Area (avg)	ΔMix Area (avg)	Calculated AEI Total	Difference (%)
Hb w/ 15 mM Butyrate	0	3.504 4.636	0.801	4.070	0.000	0.000	0.000
	20	329.709 335.072	3.792	332.391	328.321	347.416	5.652
	40	596.143 573.322	16.137	584.732	580.662	602.653	3.717
	50	612.273 584.700	19.498	598.487	594.417	617.365	3.788
	60	543.174 575.918	23.154	559.546	555.476	562.624	1.279

***H. butylicus* with butyrate solvent comparison data**

Product	Time	CONTROL (media)	Hb (normal conditions)		5 mM Butyrate		15 mM Butyrate	
		Concentration mM (calc)	Concentration mM (calc)	SD	Concentration mM (calc)	SD	Concentration mM (calc)	SD
Ethanol	0	0.000	0.000	0.001	0.000	0.001	0.000	0.001
	16	0.000	0.023	0.001				
	20	0.000			0.031	0.004	0.032	0.004
	24	0.000	0.038	0.004				
	32	0.000	0.045	0.002	0.047	0.006		
	42	0.000	0.050	0.002	0.052	0.003	0.061	0.003
	50	0.000	0.051	0.002	0.056	0.003	0.063	0.004
	60	0.000			0.058	0.002	0.064	0.006

Product	Time	CONTROL (media)	Hb (normal conditions)		5 mM Butyrate		15 mM Butyrate	
		Concentration mM (calc)	Concentration mM (calc)	SD	Concentration mM (calc)	SD	Concentration mM (calc)	SD
Isopropanol	0	0.000	0.000	0.000	0.000	0.000	0.000	0.000
	16	0.000	0.018	0.001				
	20	0.000			0.193	0.046	0.190	0.006
	24	0.000	0.258	0.021				
	32	0.000	0.420	0.004	0.486	0.013		
	42	0.000	0.462	0.004	0.512	0.035	0.532	0.022
	50	0.000	0.476	0.021	0.520	0.069	0.539	0.006
	60	0.000			0.531	0.012	0.554	0.009

Product	Time	CONTROL (media)	Hb (normal conditions)		5 mM Butyrate		15 mM Butyrate	
		Concentration mM (calc)	Concentration mM (calc)	SD	Concentration mM (calc)	SD	Concentration mM (calc)	SD
Acetone	0	0.000	0	0	0	0	0	0
	16	0.000	0.654	0.004				
	20	0.000			0.907	0.095	1.126	0.191
	24	0.000	1.1861	0.001				
	32	0.000	1.467	0.008	1.417	0.070		
	42	0.000	1.624	0.011	1.635	0.065	1.755	0.198
	50	0.000	1.378	0.009	1.716	0.060	1.812	0.146
	60	0.000			1.493	0.045	1.585	0.022

Product	Time	CONTROL (media)	Hb (normal conditions)		5 mM Butyrate		15 mM Butyrate	
		Concentration mM (calc)	Concentration mM (calc)	SD	Concentration mM (calc)	SD	Concentration mM (calc)	SD
1-Butanol	0	0.000	0	0.005	0	0.001	0	0.001
	16	0.000	0.395	0.033				
	20	0.000			0.601	0.041	4.245	0.441
	24	0.000	0.475	0.020				
	32	0.000	0.523	0.014	0.735	0.054		
	42	0.000	0.554	0.001	0.953	0.075	6.127	0.351
	50	0.000	0.568	0.008	1.098	0.072	6.214	0.278
	60	0.000			1.149	0.062	6.391	0.166

***H. butylicus* with 5 mM acetate solvent data**

						area per mV			ratio per mM
						24.564			1.3298
Product	Ethanol								
	Time	mV	mV (avg)	Δ mVa	mV SD	Calculated Area	Isobutanol Peak Area (Avg)	Calculated Ratio	Calculated Concentration
Hb w/ 5 mM Acetate	0	0.048	0.0495	0	0.002	0	61.115	0	0
		0.051							
	20	0.257	0.259	0.210	0.003	5.146	63.000	0.0817	0.061
		0.261							
	30	0.416	0.410	0.360	0.009	8.843	61.440	0.1439	0.108
		0.403							
	40	0.562	0.565	0.515	0.004	12.650	60.575	0.2088	0.157
		0.567							
	50	0.611	0.607	0.558	0.006	13.694	62.385	0.2195	0.165
		0.603							
	60	0.642	0.637	0.588	0.007	14.431	62.285	0.2317	0.174
		0.632							
	70	0.653	0.650	0.600	0.005	14.738	61.610	0.2392	0.180
		0.646							
80	0.652	0.654	0.604	0.002	14.837	62.430	0.2377	0.179	
	0.655								

						area per mV			ratio per mM
						46.208			4.129
Product	Isopropanol								
	Time	mV	mV (avg)	Δ mVa	mV SD	Calculated Area	Isobutanol Peak Area (Avg)	Calculated Ratio	Calculated Concentration
Hb w/ 5 mM Acetate	0	0	0	0	0	0	61.115	0	0
		0							
	20	0.158	0.145	0.145	0.018	6.700	63.000	0.1064	0.026
		0.132							
	30	1.516	1.509	1.509	0.010	69.728	61.440	1.1349	0.275
		1.502							
	40	2.134	2.141	2.141	0.010	98.931	60.575	1.6332	0.396
		2.148							
	50	2.473	2.476	2.476	0.004	114.411	62.385	1.8340	0.444
		2.479							
	60	2.511	2.504	2.504	0.010	115.705	62.285	1.8577	0.450
		2.497							
	70	2.55	2.556	2.556	0.008	118.108	61.610	1.9170	0.464
		2.562							
80	2.58	2.572	2.572	0.021	118.847	62.430	1.9037	0.461	
	2.564								

		area per mV 38.355					ratio per mM 4.3982			
Product	Acetone									
	Time	mV1	mV1 (avg)	ΔmVa1	mV1 SD	Acetone mV (Δmva1 - [Δethanol mixed mV + isopropanol interference])	Isobutanol Peak Area (Avg)	Calculated area	Calculated ratio	Calculated concentration
Hb w/ 5 mM Acetate	0	0 0	0	0	0	0	61.115	0	0	0
	20	5.712 5.690	5.701	5.701	0.016	5.442	63.000	208.709	3.313	0.753
	30	9.205 9.190	9.198	9.198	0.011	8.788	61.440	337.046	5.486	1.247
	40	10.943 11.061	11.002	11.002	0.083	10.437	60.575	400.311	6.609	1.503
	50	11.656 11.605	11.631	11.631	0.036	11.023	62.385	422.787	6.777	1.541
	60	9.772 9.783	9.778	9.778	0.008	9.140	62.285	350.565	5.628	1.280
	70	8.463 8.470	8.467	8.467	0.005	7.817	61.610	299.802	4.866	1.106
	80	8.152 8.107	8.130	8.130	0.032	7.476	62.430	286.723	4.593	1.044

							ratio per mM 8.8263			
Product	Butanol									
	Time	Area	Area (avg)	ΔArea	Area (Isob avg)	Individual Ratio	Individual Ratio SD	Ratio	Area SD	Concentration mM (calc)
Hb w/ 5 mM Acetate	0	3.0748	3.085	0	61.115	0.050	0.003	0.000	105.916	0
		3.3115				0.054				
	20	186.645	185.609	182.524	63.000	2.963	0.023	2.897	33.706	0.328
		184.572				2.930				
	30	243.961	240.327	237.242	61.440	3.971	0.084	3.861	16.587	0.437
		236.692				3.852				
	40	268.358	270.859	267.774	60.575	4.430	0.058	4.421	16.037	0.501
		273.358				4.513				
	50	298.296	296.689	293.604	62.385	4.782	0.036	4.706	1.939	0.533
		295.081				4.730				
	60	294.808	295.514	292.429	62.285	4.733	0.016	4.695	1.195	0.532
		296.218				4.756				
	70	297.186	294.180	291.095	61.610	4.824	0.069	4.725	3.354	0.535
		291.173				4.726				
	80	296.756	295.388	292.303	62.430	4.753	0.031	4.682	1.935	0.530
		294.019				4.710				

Product	Total AEI Area						Difference (%)
	Time	Mix Area	Mix Area SD	Mix Area (avg)	ΔMix Area (avg)	Calculated AEI Total	
Hb w/ 5 mM Acetate	0	2.348 2.139	0.148	2.244	0.000	0.000	0.000
	20	220.001 224.460	3.153	222.231	219.987	220.555	0.258
	30	405.816 420.912	10.674	413.364	411.121	415.617	1.088
	40	507.679 512.287	3.258	509.983	507.740	511.893	0.815
	50	551.015 546.998	2.840	549.007	546.763	550.893	0.752
	60	449.339 487.493	26.979	468.416	466.173	480.701	3.069
	70	421.511 415.667	4.132	418.589	416.346	432.648	3.840
	80	407.444 415.107	5.419	411.276	409.032	420.406	2.743

***H. butylicus* with 15 mM acetate solvent data**

		area per mV				ratio per mM			
		24.564				1.3298			
Product	Ethanol								
	Time	mV	mV (avg)	Δ mVa	mV SD	Calculated Area	Isobutanol Peak Area (Avg)	Calculated Ratio	Calculated Concentration (mM)
Hb w/ 15 mM Acetate	0	0.051 0.052	0.0515	0	0.001	0	65.895	0	0
	20	0.677 0.661	0.6690	0.6175	0.011	15.168	61.895	0.245	0.184
	40	1.106 1.092	1.0990	1.0475	0.010	25.731	61.895	0.416	0.313
	50	1.155 1.162	1.1585	1.1070	0.005	27.192	61.660	0.441	0.332
	60	1.189 1.163	1.1760	1.1245	0.018	27.622	63.435	0.435	0.327

		area per mV				ratio per mM			
		46.208				4.129			
Product	Isopropanol								
	Time	mV	mV (avg)	Δ mVa	mV SD	Calculated Area	Isobutanol Peak Area (Avg)	Calculated Ratio	Calculated Concentration (mM)
Hb w/ 15 mM Acetate	0	0 0	0	0	0	0	65.895	0	0
	20	0.162 0.155	0.159	0.159	0.005	7.324	61.895	0.118	0.029
	40	1.923 1.967	1.945	1.945	0.031	89.875	61.895	1.452	0.352
	50	2.184 2.119	2.152	2.152	0.046	99.417	61.660	1.612	0.390
	60	2.245 2.273	2.259	2.259	0.020	104.384	63.435	1.646	0.399

		area per mV				ratio per mM				
		38.355				4.3982				
Product	Acetone									
	Time	mV1	mV1 (avg)	Δ mVa1	mV1 SD	Acetone mV (Δmva1 - [Δethanol mixed mV + isopropanol interference])	Isobutanol Peak Area (Avg)	Calculated area	Calculated ratio	Calculated concentration
Hb w/ 15 mM Acetate	0	0 0	0	0	0	0	65.895	0	0	0
	20	4.321 4.305	4.313	4.313	0.011	4.198	61.895	161.014	2.601	0.591
	40	9.428 9.396	9.412	9.412	0.023	9.281	61.895	355.973	5.751	1.308
	50	10.111 10.002	10.057	10.057	0.077	9.920	61.660	380.462	6.170	1.403
	60	8.673 8.594	8.634	8.634	0.056	8.496	63.435	325.845	5.137	1.168

ratio per mM 8.8263

Product	Butanol									
	Time	Area	Area (avg)	ΔArea	Area (Isob avg)	Individual Ratio	Individual Ratio SD	Ratio	Area SD	Concentration mM (calc)
Hb w/ 15 mM Acetate	0	3.052 3.497	3.2745	0	65.895	0.046 0.053	0.005	0	0.315	0
	20	160.468 165.197	162.833	159.558	61.895	2.593 2.669	0.054	2.578	3.344	0.292
	40	233.729 239.126	236.428	233.153	61.895	3.776 3.863	0.062	3.767	3.816	0.427
	50	244.282 247.059	245.671	242.396	61.660	3.962 4.007	0.032	3.931	1.964	0.445
	60	248.451 250.506	249.479	246.204	63.435	3.917 3.949	0.023	3.881	1.453	0.440

Product	Total AEI Area						
	Time	Mix Area	Mix Area SD	Mix Area (avg)	ΔMix Area (avg)	Calculated AEI Total	Difference (%)
Hb w/ 15 mM Acetate	0	3.124 3.011	0.080	3.068	0.000	0.000	0.000
	20	179.437 186.625	5.083	183.031	179.963	183.507	1.950
	40	466.376 472.622	4.417	469.499	466.432	471.578	1.097
	50	516.118 508.683	5.257	512.401	509.333	507.071	-0.445
	60	472.486 461.319	7.896	466.903	463.835	457.851	-1.299

***H. butylicus* with acetate solvent comparison data**

Product	Time	CONTROL (media)			5 mM Acetate		15 mM Acetate	
		Hb (normal conditions)			Concentration mM (calc)	SD	Concentration mM (calc)	SD
		Concentration mM (calc)	Concentration mM (calc)	SD				
Ethanol	0	0.000	0.000	0.001	0	0.002	0	0.001
	16	0.000	0.023	0.003				
	20	0.000			0.063	0.003	0.188	0.011
	24	0.000	0.038	0.004				
	30				0.109	0.009		
	32	0.000	0.045	0.002				
	40				0.156	0.004	0.317	0.010
	42	0.000	0.050	0.002				
	50	0.000	0.051	0.002	0.167	0.006	0.332	0.005
60	0.000			0.178	0.007	0.338	0.018	

Product	Time	CONTROL (media)			5 mM Acetate		15 mM Acetate	
		Hb (normal conditions)			Concentration mM (calc)	SD	Concentration mM (calc)	SD
		Concentration mM (calc)	Concentration mM (calc)	SD				
Isopropanol	0	0.000	0.000	0.000	0	0	0	0
	16	0.000	0.018	0.001				
	20	0.000			0.027	0.018	0.030	0.005
	24	0.000	0.258	0.021				
	30	0.000			0.287	0.004		
	32	0.000	0.420	0.004				
	40	0.000			0.406	0.010	0.370	0.031
	42	0.000	0.462	0.004				
	50	0.000	0.476	0.021	0.467	0.004	0.406	0.046
60	0.000			0.476	0.010	0.426	0.020	

Product	Time	CONTROL (media)			5 mM Acetate		15 mM Acetate	
		Hb (normal conditions)			Concentration mM (calc)	SD	Concentration mM (calc)	SD
		Concentration mM (calc)	Concentration mM (calc)	SD				
Acetone	0	0.000	0	0	0	0	0	0
	16	0.000	0.654	0.004				
	20	0.000			0.782	0.016	0.610	0.011
	24	0.000	1.1861	0.001				
	30	0.000						
	32	0.000	1.467	0.008	1.269	0.011		
	40	0.000			1.504	0.083	1.340	0.023
	42	0.000	1.624	0.011				
	50	0.000	1.378	0.009	1.580	0.036	1.421	0.077
60	0.000			1.320	0.008	1.217	0.056	

Product	Time	CONTROL (media)			5 mM Acetate		15 mM Acetate	
		Concentration mM (calc)	Concentration mM (calc)	SD	Concentration mM (calc)	SD	Concentration mM (calc)	SD
1-Butanol	0	0.000	0	0.005	0	0.001	0	0.002
	16	0.000	0.395	0.033				
	20	0.000			0.334	0.012	0.2949	0.027
	24	0.000	0.475	0.020				
	30	0.000			0.436	0.041		
	32	0.000	0.523	0.014				
	40	0.000		0.001	0.491	0.028	0.429	0.031
	42	0.000	0.554	0.001				
	50	0.000	0.568	0.008	0.536	0.018	0.442	0.016
	60	0.000			0.538	0.008	0.449	0.012